The role of mitochondria in innate immunity

by

Karine Doiron

Integrated Program in Neuroscience, McGill University, Montreal

August 2018

A thesis submitted to McGill University in partial fulfillment of the requirements of the degree of doctor of philosophy in science

Table of Contents

Abstract 5

Résumé 7

List of Figures 9

List of Tables 9

List of Abbreviations 10

Acknowledgements 14

Contribution to Original Knowledge 16

Contributions of Authors 17

Chapter 1: Introduction 19

1.1 The bacterial ancestor 20

1.2 The Mitochondria 21

1.3 Innate immunity and mitochondria - a double-edged sword 22

1.4 Mitochondrial surface –a platform integrating various innate immune signals 23

1.4.1 Toll-like receptor signaling 23

1.4.2 Inflammasome signaling 23

1.4.3 The RIG-I/MAVS pathway 24

1.5 Post-translational modifications (PTMs) 26

1.6 Mitochondrial-anchored protein ligase (MAPL) 30

1.7 Mitochondria –a danger-associated molecular pattern (DAMP) 31

1.8 Mitochondrial DNA –a potential DAMP 32

1.9 Evidence for mtDNA release 33

1.9.1 Extrinsic mtDNA release 33

1.9.2 Intrinsic mtDNA release 35

1.10 Mitochondria-derived vesicles (MDVs) 38

Chapter 2: Rationale and objectives 41

2.1 Rationale 42

2.2 Hypotheses and specific aims 44

Chapter 3: Materials and Methods **45**

3.1 Antibodies and Reagents *46*

3.2 Buffers *47*

3.2.1 Native buffer for IRF3 dimerization assay 47

3.2.2 RIPA lysis buffer for BirA assay 47

3.2.3 Guanidine lysis buffer for NTA pulldown 47

3.2.4 Mitochondrial Isolation Buffer (MIB) 47

3.2.5 Galactose media composition 47

3.2.6 Laemmli buffer 2X 48

3.3 Mapl$^{-/-}$ mouse model *48*

3.4 Primary skin fibroblast isolation and immortalization *48*

3.5 Cytokine and chemokine detection by enzyme-linked immunosorbent assay (ELISA) *49*

3.6 In vivo activation of antiviral signaling *49*

3.7 IRF3 dimerization assay *49*

3.8 RNA isolation and quantitative RT-PCR (qPCR) *49*

3.9 Biotin Identification assay (BioID) *51*

3.10 Ni-NTA pulldown *53*

3.11 SUMOylation assay *53*

3.12 IFNβ- and ISRE-luciferase reporter assays *54*

3.13 Isolation of mitochondria derived vesicles (MDVs) *54*

3.14 Sucrose gradient fractionation *55*

3.15 Denaturing and Native PAGE *55*

3.16 Polymerase Chain Reactions (PCR) *55*

3.17 Gene silencing with siRNA *56*

3.18 Immunofluorescence staining and Imaging *57*

3.19 Statistical analysis *58*

Chapter 4: Results **59**

4.1 Hypothesis 1: MAPL is the SUMO E3 ligase for RIG-I, and is required for the antiviral response. *60*

4.1.1 Antiviral response to dsRNA virus in absence of MAPL 60

4.1.2 *In vivo* requirement of MAPL in the antiviral RIG-I/MAVS pathway 60

4.1.3 Impairment of the transcriptional response to Sendai virus in absence of MAPL 62

4.1.4 Molecular events occurring during Sendai virus without MAPL 64
4.1.5 Biotin identification (BioID) of MAPL interactome 66
4.1.6 Validation of the BioID data 69
4.1.7 MAPL-dependent SUMOylation of RIG-I 69
4.1.8 *In vitro* SUMOylation of RIG-I by MAPL E3 ligase 70
4.1.9 SUMOylation of RIG-I does not increase its stability 72
4.1.10 MAPL-dependent SUMOylation of RIG-I is required for RIG-I activation 72
4.2 Hypothesis 2: mtDNA is released as a MDV cargo under certain conditions, and may drive an innate immune response. *74*
4.2.1 Visualization of mtDNA by immunofluorescence 74
4.2.2 mtDNA-positive vesicle-like structures are independent of DRP1 76
4.2.3 Floatation of MDVs 80
4.2.4 Detection of mtDNA in the cytosol by PCR 82
4.2.5 Innate immune activation upon UV is dependent on SNX9 and mtDNA 83
4.2.6 cGAS is activated by UV exposure 86
Chapter 5: Discussion and Future Directions **88**
5.1 MAPL is the SUMO E3 ligase for RIG-I and is required for the antiviral response to dsRNA virus *89*
5.1.1 BioID for the investigation of the functional role of MAPL in antiviral response 90
5.1.2 MAPL SUMOylation of RIG-I 92
5.2 mtDNA is released via MDVs. *95*
5.2.1 UV exposure-induced DNA damage leads to mtDNA release via MDVs. 95
5.2.2 UV exposure and the immune response 96
5.2.3 A mechanism for the release of mtDNA from MDVs. 97
5.3 Conclusion *100*
Bibliography **101**

Abstract

Mitochondria are dynamic cellular organelles known for their role in energy production, regulation of metabolism, calcium homeostasis and apoptosis. Recent findings emphasize the emerging role of mitochondria as critical intracellular regulators of innate immune responses to both pathogens and cell stress. Mitochondria are essential for the innate immune signaling in response to various bacterial and viral insults, by providing a platform for the assembly and subsequent initiation of immune responses. In addition, due to their bacterial origin, mitochondria present with the potential to launch an immune response by releasing immunogenic components in the form of formylated peptides and mitochondrial DNA (mtDNA). In fact, in the past few years it has been shown that mtDNA released from the mitochondrial matrix into the cytosol launches an inflammatory response through activation of the DNA receptor cGAS (cyclic guanosine monophosphate–adenosine monophosphate synthase). The objectives of this thesis strive for further understanding these two distinct contributions of mitochondria to innate immunity; as a signaling platform for antiviral signaling, and as a direct activator of the cytosolic DNA sensing machinery. The first part of this thesis examines the role of mitochondrial SUMOylation by a membrane anchored ligase called MAPL in mediating the antiviral response to dsRNA virus infection. MAPL has been previously implicated in the innate immune response to Sendai virus infection, therefore the viral-induced MAPL interactome was mapped using the proximity-dependent biotinylation screening method, termed BioID. The data reveals a requirement for SUMOylation of the dsRNA sensor RIG-I to induce a conformational change that allows RIG-I to interact with its mitochondrial antiviral signaling adaptor (MAVS) and launch the innate immune response. This work in combination with *in vitro* and *in vivo* experiments in a MAPL knockout mouse model allows us to highlight a critical role for MAPL and mitochondrial SUMOylation in

regulating antiviral signaling. Additionally, with these groundbreaking data, we set the stage for a systematic analysis of the interaction landscape, providing important insights into the dynamic events occurring at the surface of mitochondria during antiviral response.

A second critical contribution of mitochondria to innate immunity is the potential for released mtDNA or formylated peptides to activate the immune signaling. However, our understanding of the mechanisms that may result in the release of mtDNA into the cytosol has been limited. To address this, we adopted a cell model where exposure to ultraviolet light leads to the activation of innate immune signaling. In this system, mtDNA is observed to exit mitochondria within cargo-selected mitochondrial derived vesicles (MDV). Using a gene silencing approach and immunofluorescence, we demonstrate that mtDNA release requires core proteins previously identified for the generation of vesicles, and that this ultimately drives the innate immune response through cGAS activation. This is the first report of mtDNA as a cargo of MDVs and highlights the importance of this pathway as a direct activator of the cytosolic DNA sensing machinery. Together with the characterization of the role of SUMOylation in generating a signaling platform during viral infection, this thesis provides new insights into multiple mechanisms by which mitochondria contribute to innate immunity.

Résumé

Les mitochondries sont des organites cellulaires dynamiques, connues pour leur rôle dans la production d'énergie, la régulation du métabolisme, l'homéostasie du calcium et l'apoptose. Des découvertes récentes soulignent le rôle émergent des mitochondries en tant que régulateurs intracellulaires critiques des réponses immunitaires innées aux pathogènes et au stress cellulaire. Les mitochondries sont essentielles pour la signalisation immunitaire innée en réponse à diverses agressions bactériennes et virales, en fournissant une plateforme pour l'assemblage et l'initiation subséquente des réponses immunitaires. En outre, en raison de leur origine bactérienne, les mitochondries présentent la capacité de déclencher une réponse immunitaire en libérant des composants immunogènes sous forme de peptides formylés et d'ADN mitochondrial (ADNmt). En effet, au cours des dernières années, il a été montré que l'ADNmt libéré de la matrice mitochondriale dans le cytosol déclenche une réponse inflammatoire via l'activation du récepteur d'ADN cGAS (guanosine monophosphate cyclique-adénosine monophosphate synthase). Les objectifs de cette thèse visent à mieux comprendre ces deux contributions distinctes des mitochondries à l'immunité innée; en tant que plateforme de signalisation pour la signalisation antivirale, et en tant qu'activateur direct de la machinerie de détection de l'ADN cytosolique. La première partie de cette thèse examine le rôle de la SUMOylation mitochondriale par une ligase membranaire appelée MAPL dans la médiation de la réponse antivirale suite à une infection par un virus à ARNdb. MAPL a déjà été impliqué dans la réponse immunitaire innée à l'infection par le virus Sendai, par conséquent l'interactome MAPL induit par le virus a été cartographié en utilisant la méthode de criblage de biotinylation dépendant de la proximité, appelée BioID. Les données révèlent une exigence pour la SUMOylation du récepteur d'ARNdb RIG-I afin d'induire un changement de conformation qui permet à RIG-I d'interagir avec son adaptateur MAVS

(mitochondrial antiviral signaling) et de lancer la réponse immunitaire innée. Ce travail en combinaison avec des expériences *in vitro* et *in vivo* dans un modèle de souris 'knockout' pour MAPL nous permet de mettre en évidence un rôle critique pour MAPL et la SUMOylation mitochondriale dans la régulation de la signalisation antivirale. De plus, avec ces données révolutionnaires, nous ouvrons la voie à une analyse intéractomique systématique, fournissant des informations importantes sur les événements se produisant à la surface des mitochondries au cours de la réponse antivirale.

Une deuxième contribution cruciale des mitochondries à l'immunité innée est le potentiel qu'ont l'ADNmt et les peptides formylés d'activer la signalisation immunitaire. Cependant, notre compréhension des mécanismes qui peuvent entraîner la libération d'ADNmt dans le cytosol est encore très limitée. Pour y remédier, nous avons adopté un modèle cellulaire dans lequel l'exposition à la lumière ultraviolette entraîne l'activation de la signalisation immunitaire innée. Dans ce système, on observe que l'ADN mitochondrial est sélectionné comme cargaison des vésicules dérivées des mitochondries (MDV) et ainsi quitte les mitochondries. En utilisant une approche de silençage génique et l'immunofluorescence, nous démontrons que la libération d'ADNmt nécessite des protéines de base précédemment identifiées pour la génération de vésicules, et que cela conduit à une réponse immunitaire innée par l'activation de cGAS. Pour la première fois l'ADN mitochondrial est identifié comme cargaison des MDVs, ce qui souligne l'importance de cette voie en tant qu'activateur direct de la machinerie de détection de l'ADN cytosolique. Combinée à la caractérisation du rôle de SUMOylation dans la génération d'une plateforme de signalisation pendant l'infection virale, cette thèse apporte de nouvelles perspectives sur les multiples mécanismes par lesquels les mitochondries contribuent à l'immunité innée.

List of Figures

Chapter 1

Figure 1.1. Mitochondria as platforms integrating innate immune signaling. **26**

Figure 1.2. The SUMOylation reaction. **28**

Figure 1.3. Mitochondrial DNA activation of innate immune response. **35**

Chapter 3

Figure 3.1. A test of the knock-down efficiency by Western blot analysis. **57**

Chapter 4

Figure 4.1. Defective innate immune response in vitro and in vivo in the absence of MAPL. **61**

Figure 4.2. Impaired transcriptional response to viral infection with the loss of MAPL. **63**

Figure 4.3. Earlier PARP cleavage in Mapl$^{-/-}$ following SeV infection. **64**

Figure 4.4. MAPL is required for early steps of immune response to Sendai virus infection. **65**

Figure 4.5. Biotin-labeled interaction landscape identifies RIG-I as a MAPL substrate upon SeV infection. **68**

Figure 4.6. MAPL-dependent SUMOylation of RIG-I during Sendai virus infection. **70**

Figure 4.7. MAPL-dependent SUMOylation of RIG-I. **71**

Figure 4.8. MAPL SUMOylation of RIG-I is required for RIG-I activation **73**

Figure 4.9. UV induces the release of vesicle-like structures in 143B and human fibroblasts cells. **76**

Figure 4.10. UV-induced vesicles are independent of DRP1 **78**

Figure 4.11. SNX9 is part of the machinery for UV-induced mtDNA containing MDVs **79**

Figure 4.12. Numerous types of vesicles released upon UV exposure **81**

Figure 4.13. mtDNA detection by PCR **83**

Figure 4.14. UV-induced immune response in human fibroblasts **85**

Figure 4.15. hIL6 release is dependent on mtDNA **86**

Figure 4.16. The UV-induced immune response is dependent on cGAS activation **87**

Chapter 5

Figure 5.1 Model for RIG-I SUMOylation by MAPL and signaling at mitochondria. **93**

Figure 5.2 Model for the release of mtDNA from MDVs. **98**

List of Tables

Chapter 3

Table 3.1. Primers used for qRT-PCR **51**

Table 3.2. mtDNA PCR primers **56**

List of Abbreviations

8-oxoG	8-oxo-7,8-dihydroguanine
ADP	Adenosine Diphosphate
AIM2	Absent in Melanoma 2
AKAP1	A-Kinase Anchor Protein 1
ASC	Apoptosis-Associated Speck-Like Protein Containing CARD
ATP	Adenosine Triphosphate
BAK	Bcl2 homologous Antagonist Killer
BAX	Bcl2-Associated X protein
BER	Base Excision Repair
BioID	Biotin identification
CARD	Caspase Recruitment Domain
cGAMP	Cyclic Guanosine monophosphate–Adenosine Monophosphate
cGAS	Cyclic GMP-AMP Synthase
CHC	Clathrin Heavy Chain
CL	Cardiolipin
CLR	C-type Lectin Receptor
CMV	Cytomegalovirus
CPD	Cyclobutane Pyrimidine Dimers
CTD	Carboxy-Terminal Domain
Cytb	Cytochrome b
DAMP	Danger-Associated Molecular Pattern
DENV	Dengue Virus
DNA	Deoxyribonucleic acid
DNM1L	Dynamin 1-like
DRP1	Dynamin-Related Protein 1
DSB	Double-strand break
dsDNA	Double-Stranded Deoxyribonucleic Acid
dsRNA	Double-Stranded Ribonucleic Acid
ECSIT	Evolutionarily Conserved Signaling Intermediate In Toll Pathway

ELISA	Enzyme-Linked Immunosorbent Assay
ER	Endoplasmic Reticulum
FPR	Formyl Peptide Receptor
Grp75	Glucose-Regulated Protein 75
GTPase	Guanosine TriPhosphatase
HAU	Hemagglutinin Unit
HERC5	HECT And RLD Domain Containing E3 Ubiquitin Protein Ligase
HSP60	Heat Shock Protein 60
HSV-1	Herpes Simplex Virus
IF	ImmunoFluorescence
IFIT	Interferon-Induced Protein with Tetratricopeptide Repeats
IFN	Interferon
IKK	Inhibitor of nuclear factor Kappa-B Kinase
IL18	Interleukin 18
IL1β	Interleukin 1β
IL6	Interleukin 6
INF2	Informin 2
IRF3	Interferon Regulatory Factor 3
ISG	Interferon Stimulated Gene
LAMP1	Lysosomal-Associated Membrane Protein 1
LPS	Lipopolysaccharide
MAPL	Mitochondria-Anchored Protein Ligase
MAVS	Mitochondrial Antiviral Signaling
MDA5	Melanoma Differentiation-Associated protein 5
MDV	Mitochondria-Derived Vesicle
MEF	Mouse Embryonic Fibroblast
Mff	Mitochondrial fission factor
MHC-I	Major Histocompatibility Complex I
MitAP	Mitochondrial Antigen Presentation
MLKL	Mixed Lineage Kinase domain-like protein
mtDNA	Mitochondrial DNA

mtROS	Mitochondrial ROS
MUL1	Mitochondrial Ubiquitin Ligase 1
MULAN	Mitochondrial Ubiquitin Ligase Activator of NF-κB
ND4	NADH dehydrogenase subunit 4
NDUFA9	NADH dehydrogenase [ubiquinone] 1 alpha subcomplex subunit 9
NF-κB	Nuclear Factor kappa-light-chain-enhancer of activated B cells
NLR	Nucleotide-binding oligomerization domain-Like Receptors
NLRP3	NACHT, LRR and PYD domains-containing Protein 3
NT	Non-Targeting
OASL	Oligoadenylate Synthetase-Like protein
ODN	Oligodeoxynucleotides
OGDH	Oxoglutarate Dehydrogenase
OPA1	Optic Atrophy 1
OXPHOS	Oxidative Phosphorylation
PAMP	Pathogen-Associated Molecular Pattern
PARP	Poly (ADP-ribose) polymerase
PDH	Pyruvate Dehydrogenase
PINK1	PTEN-Induced putative Kinase 1
PRR	Pathogen Recognition Receptor
PTM	Post Translational Modification
RANTES	Regulated on Activation, Normal T cell Expressed and Secreted
RIG-I	Retinoic acid-Inducible Gene I
RING	Really Interesting New Gene
RIP3	Receptor-Interacting Protein 3
RLR	Retinoic acid-inducible gene-I-Like Receptors
ROS	Reactive Oxygen Species
rRNA	Ribosomal Ribonucleic Acid
SAE1/2	SUMO-activating enzyme subunit 1/2
SenP	Sentrin Protease
SeV	Sendai Virus
SeV PP	Sendia Virus Protein P

siRNA	Silencing Ribonucleic Acid
SLE	Systemic Lupus Erythematous
SNX9	Sorting Nexin 9
ssRNA	Single-stranded ribonucleic acid
STAT1	Signal transducer and activator of transcription 1
STING	Stimulator of Interferon Genes
STUbL	SUMO-Targeted Ubiquitin Ligase
SUMO	Small Ubiquitin-like Modifier
TBK1	TANK-binding kinase 1
TFAM	Transcription Factor Activator Mitochondrial
TLR	Toll-Like Receptor
TOM20	Translocase of Outer Mitochondrial membrane 20
TRAF6	TNF Receptor-Associated Factor 6
tRNA	Transfer ribonucleic acid
Ubc9	Ubiquitin-conjugating enzyme 9
UV	ultraviolet
VPS35	Vacuolar Protein Sorting-associated protein 35

Acknowledgements

I would like to thank Dr. Heidi McBride for taking me on as a PhD student and for giving me total freedom on my projects. Thank you for your trust, mentorship, and generosity. The 6 years in your lab has been a great experience.

I would like to acknowledge the members of my thesis advisory committee for their time, effort and guidance; Dr. Amit Bar-Or and Dr. Joachim Madrenas, who were present during the first years of my PhD, and Dr. Eric Shoubridge and Dr. Rongtuan Lin, who accepted to take over for the last two years.

I would also like to thank the members of the lab Rodolfo Zunino, Dr. Mai Nguyen, Dr. Vanessa Goyon, Dr. Tim Konig and Sevan Mattie for helping me with experiments or for being there when I needed you. Thank you, Tim, for your help in reviewing this thesis. To Akihiro Yamashita, Yiyang Chen, Dr. Maxime Jacoupy, Dr. Michiel Krols and Dr. Julie Schwartz, it was a pleasure to work and discuss science with you. Thanks to past members Dr. Julien Prudent, Dr. Ayumu Sugiura and Andrew Dixon. Thank you all for the discussions about research and for your thoughtful insights and guidance on my projects.

A special thank you to Dr. Hana Antonicka, for all the times I needed input on my projects, for reviewing all my presentations and my thesis, for your friendship, and especially for all the coffee breaks and the discussions on anything and everything.

To Sevan Mattie, thank you for cheering us up with your amazing pies in the morning. Thanks for all those amazing and interesting conversations we had about food, religion, history, travel, etc.

Thank you to all the members of the Brais lab, Armstrong lab and Shoubridge lab, it was great to get to know you and work with you all those years. I will also remember the great parties

we had on the 6th floor MNI.

Thank you to my husband Serge and to my sons Christophe and Adam, this thesis was a team effort. Thank you for your love, your encouragements, your patience and your never-ending support. The completion of this thesis would not have been possible without your support.

I would like to thank my parents, for making me who I am today. You always made me feel like I could accomplish anything in life. Thank you for your eternal love and support.

Finally, I am thankful to the le *Fonds de Recherche du Québec- Santé* (FRQS) for the financial support for my project, and to the Integrated Program in Neuroscience (IPN)- MNI for the travel awards.

Contribution to Original Knowledge

1- Characterization of the molecular contribution of MAPL-mediated SUMOylation in the antiviral response, as an essential protein that drives the innate immune response to dsRNA virus, *in vitro* and *in vivo*.

2- Identification of a number of novel MAPL partners specific to Sendai virus infection including MAVS and RIG-I, a number of interferon-inducible proteins, and others.

3- Finding that MAPL SUMOylation of RIG-I induces a conformational change required to bind MAVS and initiate the signaling complex.

4- Discovery that mtDNA can be released from mitochondria upon UV stress; a process that is DRP1-independent and SNX9-dependent.

5- The finding that innate immune response following UV treatment is dependent upon SNX9, mtDNA and cGAS, suggesting that MDVs act as an intermediate in the ultimate release of mtDNA into the cytosol where it is recognized by cGAS.

6- The direct detection of mtDNA within cytosol is challenging, as PCR appears to pick up signal from broken mitochondria. Visualization within MDVs provides hints towards a mechanism of mtDNA release into the cytosol, however the final mechanism remains elusive.

Contributions of Authors

This thesis is presented in the standard format, in agreement with the guidelines for thesis preparation. A comprehensive review of the relevant literature is presented in Chapter 1, followed by a description of the rationale and objectives of the thesis in Chapter 2. Chapter 3 comprises the detailed experimental procedures used in order to achieve the specific objectives of the thesis. The results are described in Chapter 4 and appear in the following articles:

Doiron K., Goyon V., Coyaud E., Rajapakse S., Raught B. and McBride H.M., The dynamic interacting landscape of MAPL reveals essential functions for SUMOylation in innate immunity. Scientific Reports, 7: 107, 2017

Doiron K. and McBride H.M., Mitochondrial DNA released through MDVs activates the cGAS pathway. In preparation.

Chapter 5 subsequently presents a general discussion of the thesis topics and results, followed by a final conclusion and summary as well as a bibliography. Under supervision of Dr. McBride, and under advisement from the members of my thesis advisory committee Dr. Madrenas, Dr. Bar-Or, Dr. Shoubridge and Dr. Lin, I planned and executed the experiments. Concerning the first part of this thesis, I would like to acknowledge our collaborators Dr. Raught and Dr. Coyaud from Princess Margaret Cancer Center in Toronto for proceeding with the BioID and subsequent analyses. I recognize the contribution of Dr. Goyon for the production of the MAPL mouse model and the derived mouse embryonic fibroblasts as well as for performing the luciferase assays; Dr. Mai Nguyen for the derivation of the SUMO-6His-stable cell lines and Sanjeeva Rajapakse, an

honor student under my supervision during the second year of my PhD, for helping with the ELISA experiments. The qPCR was performed by the IRIC genomic platform (Université de Montréal).

Chapter 1: Introduction

This thesis will focus on the role of mitochondria in innate immune signaling. While this has perhaps been a surprising emerging function of mitochondria, looking back into evolution can provide insights into how this essential mitochondrial function may have evolved.

1.1 The bacterial ancestor

According to the endosymbiont theory of mitochondria, about 2 billion years ago a proteobacterium using oxygen to convert organic molecules to energy, was captured within a primitive archeabacterium. While the proteobacterium gained a nutrient-rich and safe environment, the archeabacterium gained a ready source of ATP. The mutual benefit which arose from this endosymbiosis led to the eukaryotic cell, where the proteobacterium became the organelle we know as the mitochondrion (Sagan 1967; McInerney et al. 2015). Until very recently, it was thought that this ancestor of mitochondria was an alpha-proteobacterium. However, new phylogenomic analyses have revealed that the mitochondria evolved from a proteobacterial lineage which branched off much earlier, before the diversification of all currently known alpha-proteobacteria (Martijn et al. 2018).

Since this endosymbiotic event, in order to keep the new organelle, the organisms had to develop a tolerance mechanism to prevent recognition of the mitochondria as non-self. In addition, throughout evolution, the multicellular organisms had to develop other mechanisms to control any spillage from the mitochondria in the cytosol where it had the potential to launch an immune response. Indeed, mitochondria have retained characteristic signature elements from their bacterial ancestor, including their autonomous replication (Archibald 2015) and unique phospholipids only found in mitochondria and other prokaryotes (Osman et al. 2011; Rongvaux 2018). Additionally, mitochondria have kept their own circular DNA genome with hypomethylated CpG motifs, and as

in bacteria, mitochondrial protein translation leads to a formylated methionine at the N-terminus of the proteins encoded by their genome (Taanman 1999; Dahlgren et al. 2016), two features with high potential of activating an immune response if released into the cytosol or in the extracellular environment. Present-day mitochondria can therefore be seen as *vestigial bacteria* living in the cytosol of eukaryotic cells and with critical implications for the immune surveillance system (Rongvaux 2018).

Strikingly, the host cell developed mechanisms to control the immune activation potential of mitochondria, and the bacterial ancestor which had to escape host defense at some point and developed endosymbiosis, now contributes to informing the immune system of present eukaryotic cell against insults such as infection by pathogens (West et al. 2011; Rongvaux 2018).

This dual requirement of the cell in establishing a tolerance mechanism toward mitochondria, and at the same time providing other mechanisms to control leakage into the cytosol probably explains why mitochondria are at the center of innate immunity, the first line of defense against pathogens.

1.2 The Mitochondria

Mitochondria are double membrane organelles historically known to act as the energy powerhouses of the cell. They are highly dynamic organelles constantly fusing and dividing in order to maintain cellular function (Braschi & McBride 2010). In addition to generating high amount of adenosine triphosphate (ATP) through cellular respiration, mitochondria are also important for the formation of iron-sulfur clusters (Stehling et al. 2014), metabolism (Vakifahmetoglu-Norberg et al. 2017; Forrester et al. 2018), apoptosis (Vakifahmetoglu-Norberg et al. 2017), calcium homeostasis (Granatiero et al. 2017) and more. Furthermore, over the past

few years, compelling evidence has positioned mitochondria at the center of innate immunity (Rongvaux 2018).

1.3 Innate immunity and mitochondria - a double-edged sword

Innate immunity is the first line of defense of the host against invading pathogens. The host cell recognizes structures named pathogen-associated molecular patterns (PAMPs) and danger-associated molecular patterns (DAMPs) through specialized pathogen recognition receptors (PRRs) that specifically recognize either bacterial bioactive molecules, dsRNA, DNA, or other foreign particles (Kawai & Akira 2009). The term PAMP refers to conserved motifs that are usually essential for the pathogen's life cycle, while DAMP typically refers to cellular products generated in response to cell stress. There are different classes of PRRs: the transmembrane Toll-like receptors (TLRs), Formyl peptide receptors (FPRs) and C-type lectin receptors (CLRs), and the cytosolic nucleotide-binding oligomerization domain-like receptors (NLRs), absent in melanoma 2 (AIM2) and retinoic acid-inducible gene-I-like receptors (RLRs) (Akira et al. 2006; Takeuchi & Akira 2010; Schroder & Tschopp 2010). Acknowledging the bacterial ancestry of mitochondria, it is very interesting to see how they became an integral part of several of these innate immune signaling pathways.

The following sections enumerate the innate immune pathways known to involve mitochondria.

1.4 Mitochondrial surface –a platform integrating various innate immune signals

1.4.1 Toll-like receptor signaling

TLRs are transmembrane receptors located at the cell surface that recycle through endosomal compartments, and they are responsible for the recognition of bacterial components (Takeda & Akira 2004). For example, TLR9 has been shown to bind to unmethylated CpG DNA motifs which are present in bacterial genomes as well as mitochondrial genome (Hemmi et al. 2000). TLR1 specifically recognizes diacylated and triacylated lipopeptides, TLR2 recognizes numerous microbial molecules from broad groups of species (i.e. Gram-negative and Gram-positive bacteria) and TLR4 recognizes lipopolysaccharide (LPS), a component of Gram-negative bacteria cell wall. Engagement of TLR1, TLR2 and TLR4 lead to recruitment of tumor necrosis factor receptor-associated factor 6 (TRAF6) to mitochondria where it has been shown to bind evolutionarily conserved signaling intermediate in Toll pathways (ECSIT) (**Fig. 1.1**), resulting in increased production of mitochondrial reactive oxygen species (mtROS) (West et al. 2011). With these data, West and colleagues uncovered a new pathway linking innate immunity and mitochondria, highlighting a novel role for mtROS as an important component of the antibacterial response (West et al. 2011).

1.4.2 Inflammasome signaling

Inflammasomes are multiprotein complexes, which can differ in their subunit composition, thus responding to different stimuli within the cell. For example, the NLR family member NLRP3 usually assembles into a multiprotein complex with the apoptosis-associated speck like protein containing a caspase recruitment domain (ASC) adaptor protein and the cysteine protease caspase-1 to form what is known as the NLRP3 inflammasome (Agostini et al. 2004). The inflammasome

activation is a two-step process requiring "priming", by a non-activating stimulus promoting transcriptional expression of key components, and a "second hit" promoting functional activation of the inflammasome ultimately leading to production of IL1β and IL18 (Patel et al. 2017). Numerous triggers have been shown to activate the NLRP3 inflammasome. In 2013 Iyer and colleagues demonstrated that cardiolipin (CL), a lipid exclusively synthesized in the inner mitochondrial membrane, is required for NLRP3 inflammasome activation. They suggested a dual role for the binding of CL to NLRP3, in providing a docking platform for the inflammasome assembly at the mitochondria and in the direct activation of the inflammasome itself (Iyer et al. 2013). Supporting this idea, very recently it was shown that both NLRP3 and caspase-1 independently bind CL in the priming step of the inflammasome activation and in response to ROS. A second signal is then needed to activate the NLRP3 inflammasome and the subsequent immune response (Elliott et al. 2018), reinforcing the role of mitochondria again as platforms for the assembly of supramolecular immune complexes (**Fig. 1.1**).

1.4.3 The RIG-I/MAVS pathway

While TLRs sense the presence of bacteria or viruses in the extracellular environment, other receptors like RLRs are specialized for sensing intruders within the cell. Retinoic-acid inducible gene I (RIG-I), along with melanoma-differentiation association gene 5 (MDA5), are essential innate immune cytosolic double-stranded RNA (dsRNA) receptors from the RLR family (Wu & Chen 2014).

In the cytosol, RIG-I remains in a closed conformation, auto-repressed by the interaction of its helicase and caspase-recruitment domains (CARD). Binding of dsRNA to RIG-I C-terminal domain (CTD) and helicase domain, along with ATP hydrolysis by the helicase domain, are

required to expose the CARD domains for downstream signaling (Kowalinski et al. 2011). Following recognition of dsRNA, RIG-I dimerizes and changes its helicase domains conformation to expose the N-terminal CARD domains (Zhu et al. 2014) which are required to bind MAVS at the surface of the mitochondria. MAVS (also called CARDIF, VISA or IPS-1) (Kawai et al. 2005; Xu et al. 2005; Meylan et al. 2005; Seth et al. 2005) is anchored within mitochondria and peroxisomes, and induces a biphasic innate immune antiviral response from both organelles (Dixit et al. 2010). At the mitochondria, MAVS assembles into prion-like aggregates (Hou et al. 2011) and recruits signaling complexes like I kappa B kinase (IKK) and TANK-binding kinase 1 (TBK1) which will lead to activation of transcription factors IRF3/7 and NF-κB (Goubau et al. 2013; Ramos & Gale 2011). Consequently, activated phosphorylated IRF3/7 will translocate to nucleus leading to generation of type I interferons. In addition, inhibitor of κB (IκB) is phosphorylated, leading to its ubiquitination and ensuing proteasome degradation. This releases NF-κB, which can now translocate to the nucleus and drive the production of cytokines (Unterholzner & Bowie 2008) (**Fig. 1.1**). The RIG-I/MAVS signaling pathway therefore establishes mitochondria again as hubs for innate immune signaling.

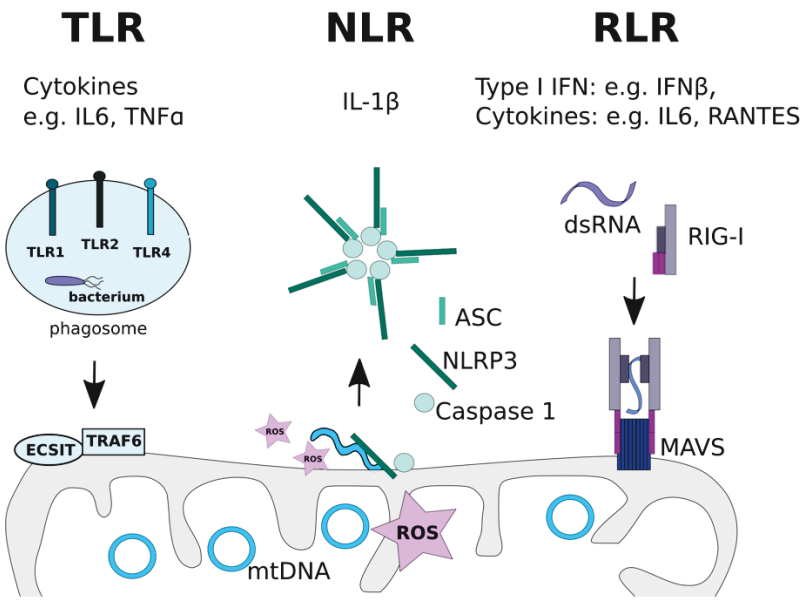

Figure 1.1. Mitochondria as platforms integrating innate immune signaling.

TLR: TLR1/2/4 are recruited at mitochondria where they bind ECSIT and TRAF6 in order to signal to NF-κB for the production of cytokines. **NLR**: The NLRP3 inflammasome requires the release of mtDNA and ROS to be activated and is thought to assemble at mitochondria, subsequently leading to the production of IL1β. **RLR**: The activation of cytosolic RIG-I leads to its recruitment at mitochondria where it binds to MAVS and signals to NF-κB and type I IFN gene expression.

1.5 Post-translational modifications (PTMs)

As the number of pathogens and immunogens increased throughout evolution, the innate immune response acquired increased specificity and complexity through use of post-translational modifications. These modifications allowed precision in how innate signals were restricted in space and time. PTMs play an important role in this regulation of immune signal transduction by allowing fine tuning and dynamic control over protein function through modification of the protein

product itself. Through the addition of modifying chemical groups to the amino acid chains of proteins, PTMs alter the properties of the proteins, thereby greatly expanding their function. PTMs are involved in numerous physiological activities, and are crucial in regulating the innate immune homeostasis and antiviral response. Moreover, they control immune responses via regulation of conformation, activation, stability/turnover, localization and interaction with other molecules (J. Liu et al. 2016; Deribe et al. 2010).

Phosphorylation and ubiquitination are the most studied PTMs. RIG-I is very tightly regulated by the crosstalk between phosphorylation and ubiquitination, and this is important to prevent aberrant signaling. In its inactive conformation, RIG-I is phosphorylated by casein kinase II (CK2) (Z. Sun et al. 2011), as well as conventional protein kinase C-α (PKC-α) and PKC-β (Maharaj et al. 2012). The sensing of dsRNA leads to RIG-I activation by rapid dephosphorylation by phosphatase PP1 (Wies et al. 2013), which is thought to be required for binding and activating of the E3 ubiquitin ligases TRIM25 and Riplet (Baker et al. 2017). Numerous downstream effectors of this signaling pathway, for example MAVS and IRF3, are also regulated through PTMs.

Other PTMs such as SUMOylation, the conjugation of SUMO (Small ubiquitin like modifier), as well as acetylation, methylation, ADP-ribosylation and glutamylation are also increasingly implicated in antiviral innate immunity, via reversible modifications of virus sensors as well as downstream signaling molecules (J. Liu et al. 2016; Mowen & David 2014).

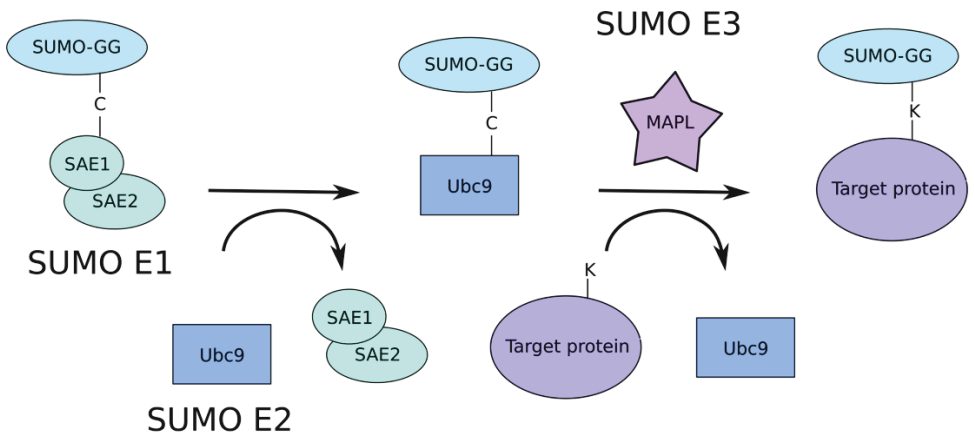

Figure 1.2. The SUMOylation reaction.

SUMO proteins are activated by conjugation to the E1 heterodimer SAE1/SAE2, followed by the SUMO transfer to the E2 enzyme Ubc9. Finally, SUMO is ligated to substrate proteins by an isopeptide bond between terminal glycine on SUMO and the ε-amino group of a lysine in the substrate. The efficiency of the ligation reaction is assisted by SUMO E3 ligase (MAPL) which directly interacts with both target proteins and the E2 enzyme. GG: diglycine, C: cysteine, K: lysine.

In addition to the roles of phosphorylation and ubiquitination in the RIG-I/MAVS antiviral signaling cascade, SUMOylation has also been suggested to be important (Kubota et al. 2008; Mi et al. 2010; Fu et al. 2011; Ran et al. 2011; Jenkins et al. 2013; Hu et al. 2017). Similar to ubiquitination, SUMOylation is the conjugation of SUMO to acceptor lysine residues on substrate proteins. An E1 heterodimer (SAE1/SAE2) first charges the free SUMO and transfers it to an E2 ligase enzyme (Ubc9), that leads to catalytic conjugation of SUMO to the acceptor lysine (Flotho & Melchior 2013) (**Fig. 1.2**). Three major SUMO proteins, SUMO1-3, are encoded by different genes and can form complex SUMO chains as well as mixed SUMO-ubiquitin chains (Lamoliatte et al. 2013; Lamoliatte et al. 2014; Srikumar et al. 2013; Bruderer et al. 2011). Really interesting

new gene- (RING-) finger containing SUMO E3 ligases assist the SUMOylation reaction by acting as scaffolds increasing efficiency and specificity of the conjugation reaction. SUMOylation of a substrate culminates in diverse functional consequences including complex assembly or disassembly, or stabilization of the protein against ubiquitin proteasome degradation (Hay 2013). SUMOylation of IRF3 was shown to be required for its stabilization during viral infection (Ran et al. 2011). Moreover, the cytosolic receptor RIG-I has been shown to be SUMOylated and this was suggested to enhance the type I interferon induction (Mi et al. 2010). In contrast, another study suggested that SUMOylation of RIG-I during infection by the SUMO E3 ligase MAPL (also named MULAN, MUL1, GIDE, HADES) has an inhibitory function during antiviral signaling (Jenkins et al. 2013). Consequently, it is unclear whether SUMOylation of RIG-I leads to activation or inhibition of the antiviral innate response. SUMOylation reactions can be reversed through the action of six different Sentrin proteases (SenP) (Hickey et al. 2012). SenP2 has been shown to deSUMOylate RIG-I (Hu et al. 2017) and IRF3 (Ran et al. 2011), therefore negatively regulating the antiviral response.

Recent studies have demonstrated that different PTMs can mutually interact, increasing the complexity of the PTMs regulatory network responsible for antiviral innate immune signaling (Hunter 2007; Beltrao et al. 2013). In addition, other studies clearly demonstrate the existence of SUMO-ubiquitin mixed chains, yet little is known about the ligases and mechanisms used to generate these novel linkages. Some may be generated by the actions of SUMO-targeted ubiquitin ligases (STUbL), that will bring a ubiquitin ligase to a SUMOylated target, however the SUMOylation of ubiquitin, and the choice of linkage sites remains mostly enigmatic. Ultimately, the presence of mixed ubiquitin/SUMO chains will generate unique signals that may lead to recruitment of protein complexes including both SUMO and ubiquitin interaction motifs (Nie &

Boddy 2016; Lamoliatte et al. 2017; McManus et al. 2017). This is an emerging and complex aspect of PTMs in signaling.

1.6 Mitochondrial-anchored protein ligase (MAPL)

MAPL is an evolutionary conserved protein, composed of two transmembrane domains that resides in the outer membrane of mitochondria and peroxisomes with both C- and N- termini facing the cytosol. MAPL harbors a RING-finger domain at its C-terminus, which confers a E3 ligase activity (Braschi et al. 2009). MAPL was first identified in 2003 from a screen of open reading frames within a cDNA library that activated NF-κB (Matsuda et al. 2003). The McBride lab later identified MAPL as a mitochondrial outer membrane protein that was transported to peroxisomes in vesicular carriers, and whose expression drove mitochondrial fragmentation through the SUMOylation of the fission GTPase Dynamin-related protein 1 (DRP1/DNM1L) (Neuspiel et al. 2008; Braschi et al. 2009). Also in 2008, another group identified MAPL from a bioinformatics approach analyzing all RING-finger proteins within the genome, and they demonstrated ubiquitin E3 ligase activity *in vitro*, localizing the protein to mitochondria where it altered mitochondrial morphology (W. Li et al. 2008).

Although MAPL shows an auto-ubiquitination activity under high micromolar concentrations of E1, E2 and RING-finger domain *in vitro*, much lower, nanomolar concentrations are required for MAPL to sustain a strong SUMOylation activity (Braschi et al. 2009). This led to conclusion that even though MAPL is capable of ubiquitin conjugation *in vitro*, it preferentially acts as a SUMO E3 ligase under physiological conditions, and potentially has the capacity to generate mixed SUMO/ubiquitin chains. DRP1 was identified as the only known substrate of MAPL and observed SUMOylation of DRP1 stabilized the oligomeric ring and promoted

mitochondrial fission (Braschi et al. 2009). Further studies by the McBride lab led to the finding that MAPL is required to SUMOylate DRP1 at mitochondria-endoplasmic reticulum (ER) contact sites during apoptosis, and this is important for the stabilization of the apoptosis signaling platform (Prudent et al. 2015). However, biochemical analysis reveals numerous SUMOylated proteins present on isolated mitochondria, hinting that MAPL may act as a molecular switch for multiple signaling complexes. This thesis defines a new mechanistic role for MAPL as a regulator of innate immunity, something that had been predicted from its earliest identity as an activator of NF-κB in 2003.

1.7 Mitochondria –a danger-associated molecular pattern (DAMP)

Mitochondria are at the center stage of innate immunity as signaling platforms for several PRR assemblies and their subsequent signaling. However, mitochondria are also highly immunogenic and research from the past few years has shown that they can trigger an immune response through activation of the exact same sensors used to recognize bacterial and viral infections (Krysko et al. 2011; Grazioli & Pugin 2018). Cells have developed diverse prevention systems to avoid the leak of pro-inflammatory mitochondrial DAMPs into the cytosol or extracellular space. Autophagy for instance, enables cells to recycle damaged mitochondria in order to prevent leakage of mitochondrial content. Nevertheless, during a major cellular stress or tissue injury, the system can become overwhelmed and mitochondrial DAMPs are released into the cytosol or extracellular space where they trigger an immune response (Deretic & Levine 2018). The mitochondrial peptides with a formylated methionine at their N-terminus, similar to the ones of bacteria, are recognized by formyl peptide receptors (FPRs), leading to production of cytokines and recruitment of phagocytic cells (Dahlgren et al. 2016). Additionally, mtDNA is also detected

as a danger signal because of its unmethylated CpG motifs, and can activate the innate immune response through diverse sensors (Zhang et al. 2010; Grazioli & Pugin 2018).

1.8 Mitochondrial DNA –a potential DAMP

Mitochondria possess their own circular genome, an element they kept from the bacterial ancestor. Although most of the genes were transferred to the nucleus throughout evolution, the 16,6kb double-stranded multicopy human mitochondrial genome consists of 37 genes, 13 of which encode core protein subunits of oxidative phosphorylation (OXPHOS) complexes I, III, IV and V, two rRNAs and 22 tRNAs (Aanen et al. 2014; Shadel & Clayton 1997). Human mtDNA contains no introns, is very compact and is packaged into nucleoid structures distributed within the mitochondrial network (Taanman 1999; Gilkerson 2009)). mtDNA is not associated with histones as nuclear DNA, and nucleoid structures consist of proteins essential for mtDNA packaging as well as transcription and replication. One of the core components of mitochondrial nucleoids is mitochondrial transcription factor A (TFAM), which is known to be involved in the packaging of mtDNA (Kukat & Larsson 2013). TFAM is very abundant and entirely covers mtDNA (Ekstrand 2004; Takamatsu et al. 2002), is essential for DNA maintenance (Larsson et al. 1998) and is also a crucial constituent of the mammalian mtDNA transcription initiation complex (Y. Shi et al. 2012). While low levels of TFAM create a loosely packed nucleoid state favorable for mtDNA transcription, higher levels generate a compact nucleoid with inhibited transcription (Kukat et al. 2015). Moreover, the levels of TFAM have been shown to directly correlate with mtDNA copy number (Kukat et al. 2015; Ekstrand 2004; Ikeda et al. 2015; Chakrabarty et al. 2014).

The maintenance of mtDNA is very important as point mutations, deletions and depletion of mtDNA cause a wide range of mitochondrial diseases (Liang et al. 2014), and were found

associated with cancers (McCrow et al. 2015), and neurodegenerative diseases (Cha et al. 2015). The mitochondrial oxidative phosphorylation process is the main source of ROS in the cell, hence mtDNA is thought to undergo oxidative damage because of its close proximity (Georgieva et al. 2017). Moreover, DNA breaks have been shown to occur during mtDNA replication or mtDNA repair (Alexeyev et al. 2013). mtDNA is therefore emerging as an extremely sensitive gauge of cellular stress.

The repair of mtDNA oxidative damage by base excision repair (BER) is controversial, and it is still unclear if double-strand breaks (DSBs) are repaired in mammalian cells, and which mechanism would be responsible for that. Using a human inducible cell system of mitochondria-targeted restriction enzymes to produce DSBs in the mitochondrial genome, Moretton and colleagues were unable to find DSB repair in mtDNA. None of the five known mitochondrial nucleases was responsible for the loss of mtDNA they observed, nor was mitophagy, autophagy or apoptosis. Thus, they suggested the presence of an additional unknown mechanism in mitochondria, by which damaged mtDNA which underwent DSBs is removed and degraded (Moretton et al. 2017). Interestingly, a recent study showed that linear mtDNA was degraded by components of the replication machinery (Peeva et al. 2018).

1.9 Evidence for mtDNA release

1.9.1 Extrinsic mtDNA release

The presence of freely circulating mtDNA in plasma and serum is very well documented and is detected in various cases of human diseases (Boyapati et al. 2017). This circulating mtDNA occurs through release from ruptured cells in conditions of acute tissue injury, for example after acute myocardial infarction, trauma or during sepsis. Consequently, mtDNA is then recognized by

the receptor TLR9 on the cell surface or within endosomes, which triggers an innate immune response through activation of the NF-κB pathway and the resulting pro-inflammatory cytokines (Wei et al. 2015; Zhang et al. 2010) (**Fig. 1.3**).

Neutrophils have been shown to release mtDNA-protein complexes in their cytosol at steady-state (Caielli et al. 2016). In this process, mtDNA bound to TFAM gets oxidized, dissociates from TFAM and is sent, via mitochondria-derived vesicles, directly for lysosomal degradation. In the pathology of human systemic lupus erythematosus (SLE), TFAM does not dissociate from oxidized mtDNA, and this leads to retention and accumulation of the oxidized mtDNA-TFAM complexes in the mitochondria. The oxidized nucleoids are eventually released as complexes with high interferogenic potential, inducing the production of type I interferons, and ultimately leading to the development of autoantibodies against oxidized mtDNA, which exacerbate the pathology (Caielli et al. 2016).

Ingelsson and colleagues showed very recently that lymphocytes as well as monocytes and neutrophils are able to rapidly release mtDNA in the form of long elastic filaments in response to CpG- and non-CpG oligodeoxynucleotides (ODNs), both known inducers of the immune response (Landrigan et al. 2011; Ingelsson et al. 2018). These mtDNA web-like structures are released in the extracellular space where they act as rapid messengers, priming the activation of type I interferons (Ingelsson et al. 2018).

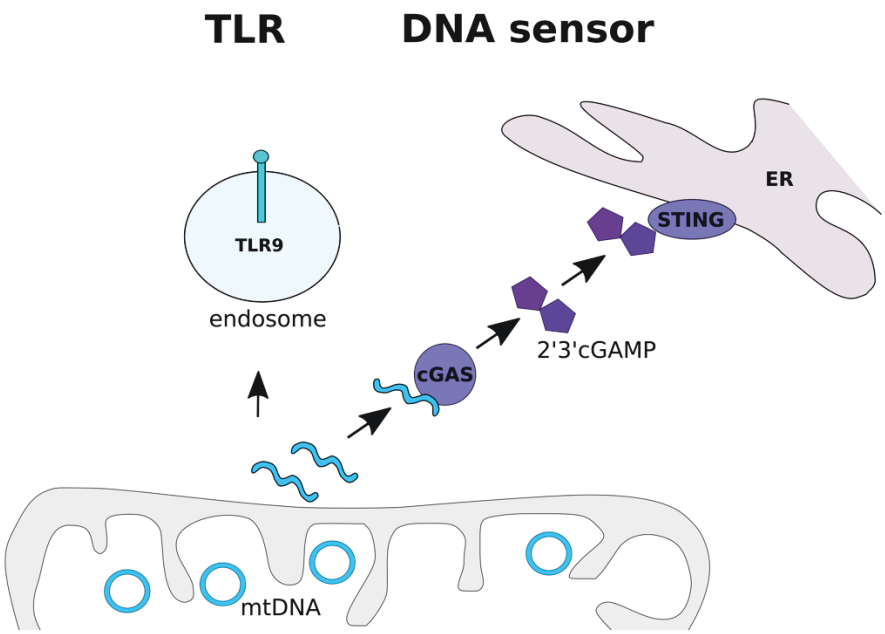

Figure 1.3. Mitochondrial DNA activation of innate immune response.

TLR: mtDNA is recognized by TLR9 in endosomes, leading to activation of NF-κB and cytokine production. **DNA sensor**: mtDNA also binds the cytosolic DNA receptor cGAS, leading to activation of STING at the ER and the subsequent transcription of NF-κB and type I IFN gene expression.

1.9.2 Intrinsic mtDNA release

In contrast to extrinsic mtDNA release into the extracellular space, in 2012 Shimada and colleagues showed that oxidized mitochondrial DNA gets released in the cytosol of macrophages in response to danger signals. The released mtDNA binds to and activates NLRP3 inflammasome as a consequence of mitochondria-dependent apoptotic cascade initiation, leading to activation of caspase-1 and processing of pro-IL1β into its active IL1β form (Shimada et al. 2012; Nakahira et al. 2010) (Z. Zhong et al. 2018) (**Fig. 1.1**).

Additionally, in the past few years, numerous publications clearly identified contexts in which mtDNA is released in the cytosol and activates an innate immune response through the cytosolic DNA sensor cGAS (West et al. 2015; Rongvaux et al. 2014; White et al. 2014; Z. Zhong et al. 2016), promoting type I interferons. Activated cGAS catalyses the synthesis of cGAMP (cyclic guanosine monophosphate–adenosine monophosphate), which acts as second messenger to activate STING (stimulator of interferon genes) at the ER, leading to activation of IRF3 gene expression and production of type I interferons (L. Sun et al. 2013) (**Fig. 1.3**).

Essentially, mitochondria have the capacity to release the intrinsic interferon inducer mtDNA which activates the cGAS-STING pathway, yet the release of cytochrome c and assembly of the apoptosome have been shown to simultaneously block this type I interferon response in a caspase-dependent manner (White et al. 2014; Rongvaux et al. 2014). Those results indicate that the apoptotic caspase cascade is required in order to render mitochondrial apoptosis immunologically silent (White et al. 2014; Rongvaux et al. 2014), therefore establishing a dual role of mitochondria in determining whether apoptosis triggers an inflammatory response or not.

In other situations, like viral infection for example, mtDNA release plays a positive role in priming the immune system to counter the pathogen. Mouse embryonic fibroblasts (MEFs) heterozygous for mitochondrial TFAM are characterized by a reduced oxidative mtDNA damage repair capacity, as well as altered mtDNA packaging, organization and distribution (Woo et al. 2012; West et al. 2015). Using this model of moderate mtDNA stress, West and colleagues show that mtDNA is released into the cytosol where it activates the cGAS/STING pathway via cytosolic DNA sensor cGAS. This process could prime the cells, by increasing the expression of interferon stimulated genes (ISGs) and potentiating the type I interferon production, rendering the cells more resistant for future viral infections. In addition, they demonstrate that herpesvirus simplex (HSV-

1), a DNA virus, also induces mtDNA stress leading to an enhanced type I interferons production, suggesting monitoring of mtDNA homeostasis as another mechanism of antiviral innate immunity (West et al. 2015).

Activation of the DNA sensor cGAS has not only been seen in infections with DNA viruses, but it was also observed during infections with RNA viruses (Schoggins et al. 2014; Aguirre & Fernandez-Sesma 2017). How do RNA viruses activate the cytosolic DNA sensor cGAS? One can imagine that a RNA virus that signals to the mitochondria through the RIG-I-MAVS pathway has the potential to induce a mtDNA stress similar to the one reported by West and colleagues in the TFAM heterozygous mouse (West et al. 2015). Sun and colleagues shed light on this matter using a positive single-stranded RNA (+ssRNA) virus (Dengue virus, DENV). They demonstrated that infection with RNA virus DENV indirectly activates the cGAS pathway through the release of mtDNA in the cytosol, although their results also show that this could happen through mitochondrial damage upon infection (B. Sun et al. 2017). Nonetheless, their finding, together with the observation that *cGAS*$^{-/-}$ mice are more susceptible to infection with +ssRNA West Nile virus (Schoggins et al. 2014), further demonstrate that RNA viruses also activate the cytosolic DNA sensor cGAS.

The mechanism for the release of mtDNA from mitochondria remains unknown. In the apoptotic paradigm, mtDNA release is strictly dependent upon BAK/BAX, and further investigation showed that the pores formed by BAX and BAK in the outer membrane of the mitochondria lead to herniation of the inner mitochondrial membrane and ultimately to the release of the matrix content containing mtDNA in some sort of vesicular structure that appears to become permeabilized (McArthur et al. 2018; Riley et al. 2018). Since the apoptotic program involves the release of cytochrome c, which happens prior to herniation and mtDNA release according to

McArthur, plus the activation of the caspase cascade, it is unclear whether BAX and BAK would be responsible for mtDNA release in the context of immune signaling. For example, a recent study postulates that newly synthesized mtDNA is oxidized and released via membrane pores, and this is crucial for NLRP3 activation (Z. Zhong et al. 2018), yet it is totally unknown how mtDNA is released in contexts where BAX is not active.

1.10 Mitochondria-derived vesicles (MDVs)

One possibility for mtDNA to escape mitochondria would be through the mitochondria-derived vesicle (MDV) pathway. MDVs were discovered by the McBride lab several years ago as a new pathway for mitochondrial quality control, and another mean of inter-organellar communication (Neuspiel et al. 2008; Soubannier, McLelland, et al. 2012; Soubannier, Rippstein, et al. 2012; Sugiura et al. 2017; Sugiura et al. 2014). MDVs incorporate selective cargoes that consist of outer membrane components exclusively or which can include outer membrane, inner membrane and matrix components. Another characteristic of MDV generation is the independence for the mitochondrial fission GTPase DRP1. Their size may vary, depending on their cargo, between 70 and 150 nm (Neuspiel et al. 2008; Soubannier, McLelland, et al. 2012; Soubannier, Rippstein, et al. 2012). While the first MDVs published were targeted for delivery of their cargo to a subpopulation of peroxisomes (Neuspiel et al. 2008), other subtypes were identified; one subtype carrying oxidized cargoes to be delivered to late endosome/multivesicular body for degradation (Soubannier, Rippstein, et al. 2012) and another subtype involved in the presentation of mitochondrial antigens on MHC-I (major histocompatibility complex class I) proteins at the cell surface (Matheoud et al. 2016). Interestingly, a recent publication from Sugiura demonstrated that MDVs are also involved in *the novo* biogenesis of peroxisomes (Sugiura et al. 2017).

How cargoes are selected is still unclear and appears to be cell-type and highly context specific. However, we know that Sorting nexin 9 (SNX9), a protein involved in cellular trafficking and essential for the formation of the narrow neck of the vesicle (Lundmark & Carlsson 2009), is one of the core components of the machinery responsible for the formation of PDH- (pyruvate dehydrogenase) and OGDH- (oxoglutarate dehydrogenase) positive MDVs. Accordingly, silencing of *SNX9* by siRNA leads to accumulation of trapped budding MDVs at the mitochondria (Matheoud et al. 2016). VPS35, a component of the retromer complex which is essential for the endosomal protein sorting machinery (Seaman et al. 1998), has also been shown to mediate MDV transport to peroxisomes (Braschi et al. 2010). It was also suggested that VPS35 interacts with DRP1, mediating removal of DRP1 complexes from mitochondria via MDVs, and their subsequent lysosomal degradation (W. Wang et al. 2016).

A recent study highlights a newly discovered mitochondrial antigen presentation (MitAP) process through the release and trafficking of MDVs, in response to inflammatory conditions. This pathway, independent of mitophagy/autophagy is repressed by Parkinson's disease linked PINK1 and PARKIN, whose requirement have previously been reported for the formation of MDVs in the context of oxidative stress (McLelland et al. 2016). Additionally, the formation of MDVs linked to MitAP were shown to require both SNX9, and Rab9, another protein involved in vesicular trafficking (Matheoud et al. 2016). This study linked the formation of MDVs with the adaptive immune response and a possible autoimmune mechanism likely involved in Parkinson's disease.

In the cell's perspective, the use of MDVs as a vehicle to remove mtDNA from mitochondria would provide regulation and specificity, and would also provide means of release

that would not compromise the integrity of mitochondria by opening pores or channels. On the other hand, the problem remains as to how mtDNA would get out of the MDVs. Perhaps mtDNA containing MDVs would be delivered into a late endosome/multivesicular body which offers the possibility of back-fusion (Abrami et al. 2004; Nour & Modis 2014), or perhaps pore-forming proteins would be involved in the release of mtDNA from MDVs.

Undoubtedly, recent evidences demonstrate how mitochondria lie at the center of immunity. This thesis explores two aspects of the role of mitochondria in innate immunity: the mitochondrial outer membrane as a platform for signaling molecules, and the release of mtDNA as a DAMP with the potential to trigger an immune response.

Chapter 2: Rationale and objectives

2.1 Rationale

This thesis is presented in two parts. The first part is the study of the role of MAPL in the antiviral signaling, and the second part concerns mtDNA release and the following immune consequences.

The McBride lab identified MAPL, the only known mitochondrial SUMO E3 ligase to date (Neuspiel et al. 2008). Although numerous unidentified mitochondrial SUMO targets were observed in a study by Braschi and colleagues, suggesting a global role for SUMOylation in mitochondrial functions, until very recently the only known substrate for MAPL was DRP1 (Braschi et al. 2009). Later, Prudent and colleagues showed that MAPL SUMOylation of DRP1 at mitochondria-ER contact sites is required during cell death in order to stabilize a signaling platform for mitochondrial constriction, calcium flux, cristae remodeling, and proper cytochrome c release (Prudent et al. 2015).

A study published in 2013 proposed that MAPL (MUL1) was involved in antiviral signaling (Jenkins et al. 2013). They showed that MAPL interacts with MAVS at mitochondria, suggesting that MAPL affects the SUMOylation and activation state of RIG-I. In addition, using a silencing RNA (siRNA) approach, they proposed that MAPL is a negative regulator of antiviral signaling (Jenkins et al. 2013).

In order to study the role of MAPL and further our understanding on its roles as a mitochondrial SUMO E3 ligase, a conditional knockout mouse model was generated in the lab. In addition, immortalized mouse embryonic fibroblasts (MEFs) were generated from the *Mapl*$^{-/-}$ and the littermate control *Mapl*$^{fl/fl}$ mice.

Considering the role for MAPL SUMOylation of DRP1 in stabilizing a platform at mitochondria during apoptosis (Prudent et al. 2015), and the fact that it was suggested as the SUMO E3 ligase for RIG-I by Jenkins (Jenkins et al. 2013), it was of great interest to further investigate its function during the antiviral immune signaling.

As mentioned earlier, the second part of this thesis involves the role of mitochondria as potential activator of the immune system via the release of mtDNA.

At the same time MAPL was identified, a new intracellular transport route between mitochondria and peroxisomes via MDVs was also discovered (Neuspiel et al. 2008). Since then, MDVs were shown to be released upon a variety of stressors and triggers, including heat shock and oxidative stress (Soubannier, Rippstein, et al. 2012; Matheoud et al. 2016). In addition, cell-free budding assays and high-resolution immunofluorescence imaging led to the identification of a wide variety of MDV cargoes, depending on the tissue and the stimulus (Soubannier, McLelland, et al. 2012; McLelland et al. 2014; Sugiura et al. 2014; Matheoud et al. 2016). However, in each condition tested, there appeared to be no mtDNA incorporated within MDVs. This suggested that mtDNA was generally excluded as an MDV cargo, although the incorporation of mtDNA may be highly specific to a trigger or signal that had not yet been discovered.

Since then, there has been a groundswell of emerging evidence showing mtDNA release into both the extracellular environment and in the cytosol where it activates the innate immune system. However, no mechanism or regulation of this process has been documented in the case of immune signaling. Having in hands the tools and expertise to study MDVs, it was an exciting challenge to investigate whether mtDNA can be a cargo for MDVs under certain conditions, and if this can be linked to the activation of an innate immune response.

2.2 Hypotheses and specific aims

Hypothesis 1

MAPL is the SUMO E3 ligase for RIG-I, and is required for the antiviral response.

Specific Aims

1- To clarify the role of MAPL in the antiviral response using *Mapl*$^{-/-}$ knock-out cells and a *Mapl*$^{-/-}$ knock-out mouse model.

2- To identify and characterize new substrates of MAPL, specific to the antiviral immune response.

3- To investigate the consequences of MAPL SUMOylation during the antiviral response.

Hypothesis 2

mtDNA is released as a MDV cargo under certain conditions, and may drive an innate immune response.

Specific Aims

1- To identify triggers under which mtDNA is released and figure out a way to track mtDNA release into the cytosol.

2- To test whether mtDNA is released via MDVs, as well as a potential mechanism.

3- To assess the immune consequences of mtDNA release.

Chapter 3: Materials and Methods

3.1 Antibodies and Reagents

ELISA paired antibodies for IL6 (DY406) and RANTES (DY478) are from R&D Systems and the Verikine IFNβ (42400-1) ELISA kit is from PBL. Antibodies against MAPL (HPA017681), βactin (A2228), FLAG (A8592), Vinculin (V4505) and TOM20 (HPA011562) are from Sigma, RIG-I (3743), IRF3 (4302), phospho-IRF3 (4947), MAVS rodent specific (4983), IκBα (4812), phospho-IκBα (2859), GST (2624), Ubiquitin (3936) and TFAM (D5C8) (8076S) are from Cell Signaling, MAVS human (AB1871) is from Enzo lifesciences, IFIT2 (NBP2-15180) from Novus Biologicals, Hsp60 (sc-136291) and LAMP1(H5G11) (sc-18821) from Santa Cruz, biotin (200-002-211) from Jackson ImmunoResearch, Grp75 (ab2799), PDH (ab110333), NDUFA9 (20C11) (ab14713) and TOM22 (ab57523) are from Abcam, OPA1 (612607) from BD Biosciences, DNA (CBL186) from Millipore, and finally antibody against Clathrin Heavy Chain (CHC) was a gift from Tim Kennedy (MNI, McGill University). Goat anti-mouse IgM cross-absorbed secondary Alexa Fluor 488 (A21042), goat anti-rabbit IgG secondary Alexa Fluor 594 (A11012), goat anti-mouse IgG2a cross-absorbed secondary Alexa Fluor 647 (A21241) are from Invitrogen. Streptavidin-HRP (N100) and DAPI (D1306) are from ThermoFisher Scientific, Sendai virus Cantell strain from Charles River; recombinant RIG-I from Novus Biologicals, PolyI:C/LyoVec from Invivogen and MG132 (C2211) from Sigma. siRNA for human *MUL1* (L-007062-00-0010), *DRP1* (L-012092-00-0005), *SNX9* (L-017335-00-0005), *VPS35* (J-010894-05-0020), *MAVS* (L-024237-00-0005) and *cGAS* (L-015607-02-0005) and non-targeting (D-001810-10-20) are from Dharmacon.

3.2 Buffers

3.2.1 Native buffer for IRF3 dimerization assay

20mM Tris-HCl pH 7.5, 150mM NaCl, 10% Glycerol, 0.5% NP-40, 1mM sodium orthovanadate and 0.5% sodium deoxycholate, supplemented with protease inhibitor cocktail

3.2.2 RIPA lysis buffer for BirA assay

50 mM Tris-HCl, 150 mM NaCl, 1 mM EDTA, 1 mM EGTA, 1% Triton X-100, 0.1% SDS, 1:500 protease inhibitor cocktail, 250U Turbonuclease, pH 7.5

3.2.3 Guanidine lysis buffer for NTA pulldown

6M Guanidine, 0.1M NaH2PO4, 10mM imidazole, 10mM Tris-HCl pH 8.0, 20mM 2-chloroacetamide and 10mM β-mercaptoethanol

3.2.4 Mitochondrial Isolation Buffer (MIB)

220 mM mannitol, 68 mM sucrose, 80 mM KCl, 0.5 mM EGTA, 2 mM magnesium acetate, 20 mM Hepes pH 7.4

3.2.5 Galactose media composition

DMEM base (Invitrogen), 10 mM Galactose, 10% dialyzed FBS (Gibco), supplemented with L-glutamine, Na^{2+}-pyruvate and non-essential amino acids (NEAA)

3.2.6 Laemmli buffer 2X

4% SDS, 20% glycerol, 10% β-mercaptoethanol, 0.004% bromophenol blue and 0.125mM Tris-HCl pH 6.8.

3.3 *Mapl*$^{-/-}$ mouse model

The *Mapl*$^{-/-}$ conditional knockout mouse model was generated on C57BL/6 background. The mouse was created by flanking exon 2 of the MAPL gene with flox alleles. Exon 2 was then excised by crossing that mouse with a ubiquitous CMV-Cre mouse strain, generating a germline *Mapl*$^{-/-}$ mouse. The *Mapl*$^{-/-}$ mice are viable. *Mapl*$^{fl/fl}$ are used as wild-type littermate controls.

3.4 Primary skin fibroblast isolation and immortalization

Mapl$^{fl/fl}$ and *Mapl*$^{-/-}$ mouse embryonic fibroblasts (MEFs) were isolated from the skin of embryos at embryonic day E13-E14. Skin cells were collected in sterile ice-cold PBS and digested with Trypsin (Sigma) in 500µL Dulbecco Modified Eagle Medium (DMEM #11965167). The trypsin reaction was then stopped by the addition of 0.57 mg/ml trypsin inhibitors (Roche) and 0.7 mg/ml DNAse I (Roche) to the DMEM. This was followed by a centrifugation at 3000 rpm for 5 minutes at room temperature, resuspension of the cell pellets in 500µL of the same DMEM solution, and one last centrifugation under the same conditions. The samples were finally resuspended in 1 ml of DMEM and plated on 10cm dishes. MEFs were immortalized with a retrovirus expressing the E7 gene of type 16 human papilloma virus and a retroviral vector expressing the protein component (hTert) of human telomerase (Lochmuller et al. 1999). *Mapl*$^{fl/fl}$ and *Mapl*$^{-/-}$MEFs are cultured in high glucose DMEM supplemented with 10% fetal bovine serum.

3.5 Cytokine and chemokine detection by enzyme-linked immunosorbent assay (ELISA)

Mapl$^{fl/fl}$ and *Mapl*$^{-/-}$ MEFs were plated in 96 well plates and left untreated or infected with Sendai virus (SeV) at a concentration of 150 HAU/mL. Supernatants were collected at the times indicated, and ELISA were performed according to manufacturer's protocol to measure the concentration of each cytokine or chemokine. ELISA experiments were repeated three times (n=3).

3.6 *In vivo* activation of antiviral signaling

Wild-type (n=7) and *Mapl*$^{-/-}$ mice (n=5) were injected intravenously with 200µg PolyI:C/LyoVec LMW (Invivogen) or saline. Blood was collected prior to injection as time 0, at 2 hours and 4 hours post-injection. Serum was isolated and levels of IL6, RANTES and IFNβ were measured by ELISA.

3.7 IRF3 dimerization assay

Mapl$^{fl/fl}$ and *Mapl*$^{-/-}$ MEFs were infected with SeV (150HAU/mL) for the times indicated and the cells were lysed in native buffer. Protein concentrations were measured and 25µg protein was run on 9% native gel, transferred to nitrocellulose and immunoblotted with the antibody against mouse IRF3.

3.8 RNA isolation and quantitative RT-PCR (qPCR)

Mapl$^{fl/fl}$ and *Mapl*$^{-/-}$ MEFs were left untreated or infected with SeV (150 HAU/mL) for the times indicated. RNA samples were prepared using the RNeasy Plus RNA isolation kit (QIAGEN). The qPCR experiments were performed by the IRIC Genomics platform. Briefly, total RNA was

treated with DNAse (New England Biolabs), then reverse transcribed (RT) with random primers using the High Capacity cDNA Reverse Transcription Kit (Life Technologies) as described by the manufacturer. RT samples were firstly diluted 1:5. Gene expression was determined using assays designed with the Universal Probe Library (UPL) from Roche (www.universalprobelibrary.com). A standard curve was performed for each of the qPCR assays, to ensure an efficiency between 90% and 110%. 5-25 ng of cDNA samples were used per qPCR reaction, with TaqMan Advanced Fast Universal PCR Master Mix (Life Technologies) and 2 μM of each primer (**Table 1**). The Viia7 qPCR instrument (Life Technologies) was used to detect amplification levels, with an initial step of 3 minutes at 95˚C, followed by 40 cycles of: 5 sec. at 95˚C and 30 sec. at 60˚C. All reactions were run in triplicate and the average values of Ct were used for quantification.

The raw data were used to analyze the results obtained. The relative quantification of target genes was determined using the ΔΔCT method. Briefly, the Ct (threshold cycle) values of target genes were normalized to endogenous control genes *TBP* and *Ywhaz* ($\Delta CT = Ct_{target} - Ct_{CTRL}$) and compared with a calibrator ($\Delta\Delta CT = \Delta Ct_{Sample} - \Delta Ct_{Calibrator}$). Relative expression (RQ) was calculated using the formula is $RQ = 2^{-\Delta\Delta CT}$.

Table 1. Primers used for qPCR

Gene	Reverse primer	Forward primer
Rig-I	5'-gcagaactggaacaggtcgt-3'	5'-tgttcgaagtccgggatg-3'
Ifnα1	5'-acccagcagatcctgaacat-3'	5'-aatgagtctaggagggttgtattcc-3'
Mda5	5'-ctattaaccgtgttcaaaacatgaa-3'	5'-ggatactttgcacctgcaattc-3'
Ifit1	5'-tctaaacagggccttgcag-3'	5'-gcagagccctttttgataatgt-3'
Ifit2	5'-caatgcttaggggaagctga-3'	5'-tgatttctacttggtcaggatgc-3'
Il6	5'-gctaccaaactggatataatcagga-3'	5'-ccaggtagctatggtactccagaa-3'
Ifnβ1	5'-ctggcttccatcatgaacaa-3'	5'-agagggctgtggtggagaa-3'
Nfκb1	5'-cactgctcaggtccactgtc-3'	5'-ctgtcactatcccggagttca-3'
SeV PP protein	5'-tgttatcggattcctcgacgcagtc-3'	5'-tactctcctcacctgatcgattatc-3'
TBP	5'-gggttatcttcacacaccatga-3'	5'-cggtcgcgtcattttctc-3'
Ywhaz	5'- gggtttcctccaatcactagc-3'	5'-cttcctgcagccagaagc-3'

3.9 Biotin Identification assay (BioID)

BioID was performed as described previously (Coyaud et al. 2015). Briefly, the full-length human MAPL (BC014010) coding sequence was amplified by PCR using the following primers:

MAPL-AscI_Fwd: tataGGCGCGCCaATGGAGAGCGGAGGGCGGCCCTCG

MAPL-NotI_Rev: ttaaGCGGCCGCGCTGTTGTACAGGGGTATCACCCG

and cloned into a pcDNA5 FRT/TO BirA-FLAG expression vector. Using the Flp-In system (Invitrogen), 293 T-REx Flp-In cells stably expressing MAPL-BirA-Flag were generated (constructs were generated by collaborators in Toronto). 10 x 15 cm^2 plates of subconfluent (60%)

cells were incubated for 9 hrs in complete media supplemented with 1 μg/ml tetracycline to induce MAPL-BirA-Flag, then 50 μM biotin was added and cells were left untreated or infected with SeV for 15 hours, totalizing 24 hours. Cells were collected and pelleted (2000 rpm, 3 min), washed twice with PBS, and dried pellets were snap frozen. The following BioID experiment as well as analyses were performed by our collaborators in Dr. Brian Raught's lab in Toronto. Pellets were lysed in 10 ml of modified RIPA lysis buffer (50 mM Tris-HCl, 150 mM NaCl, 1 mM EDTA, 1 mM EGTA, 1% Triton X-100, 0.1% SDS, 1:500 protease inhibitor cocktail, 250U Turbonuclease, pH 7.5) at 4ºC for 1 hr, then sonicated to disrupt visible aggregates. The lysates were centrifuged at 35,000 g for 30 min. Clarified supernatants were incubated with 30 μl packed, pre-equilibrated Streptavidin-sepharose beads at 4ºC for 3 hours. Beads were collected by centrifugation, washed 6 times with 50 mM ammonium bicarbonate pH 8.3, and treated with TPCK-trypsin (16 hrs at 37ºC). The supernatant containing the tryptic peptides was collected and lyophilized. Peptides were resuspended in 0.1% formic acid and $1/6^{th}$ of the sample was analyzed per MS run. High performance liquid chromatography was conducted using a pre-column (Acclaim PepMap 50 mm x 100 μm inner diameter pre-column) and Acclaim PepMap (500 mm x 75 μm diameter; C18; 2 μm;100 Å) RSLC (Rapid Separation Liquid Chromatography) column (Thermo Fisher Scientific, Waltham, MA), running a 120 minutes reversed-phase buffer gradient at 250 nl/min on a Proxeon EASY-nLC 1000 pump in-line with a Thermo Q-Exactive HF quadrupole-Orbitrap mass spectrometer. A parent ion scan was performed using a resolving power of 60 000, then up to the twenty most intense peaks were selected for MS/MS (minimum ion count of 1000 for activation), using higher energy collision induced dissociation (HCD) fragmentation. Dynamic exclusion was activated such that MS/MS of the same *m/z* (within a range of 10 ppm; exclusion list size = 500) detected twice within 5 s was excluded from analysis for 15 s. For protein identification, Thermo

.RAW files were converted to .mzXML format using Proteowizard [55] then searched using X!Tandem [56] against the human Human RefSeq Version 45 database (containing 36,113 entries). Search parameters specified a parent ion mass tolerance of 10 ppm, and a MS/MS fragment ion tolerance of 0.4 Da, with up to 2 missed cleavages allowed for trypsin. Variable modification +16@M and W, +32@M and W, +42@N-terminus, +1@N and Q were allowed. Proteins identified with a ProteinProphet cut-off of 0.85 (corresponding to ≤1% FDR) were analyzed with SAINT Express v.3.3. Sixteen control runs were used for comparative purposes, comprising 8 runs of BioID conducted on untransfected 293 T-REx cells and 8 runs of BioID conducted on 293 T-REx cells expressing FlagBirA* only.

3.10 Ni-NTA pulldown

Stable SUMO1-His6-*Mapl*$^{fl/fl}$ and SUMO1-His6-*Mapl*$^{-/-}$ mouse embryonic fibroblasts were generated. Cells were left untreated or infected with Sendai virus (150 HAU/mL) for 18 hours. Cells were lysed in Guanidine lysis buffer and sonicated. 1mg proteins were incubated with 50µL of pre-equilibrated Ni-NTA beads at 4ºC for 4 hours, spun down and washed once with 6M Guanidine buffer then with 8M Urea. Proteins were eluted directly in 2X Laemmli buffer, ran on SDS-PAGE and immunoblotted.

3.11 SUMOylation assay

The SUMO conjugation assay was performed using 50nM SUMO E1, 250nM Ubc9, 10µM His6-SUMO1, 20µM of a consensus biotinylated peptide, an ATP-regenerating system (2.5U creatine kinase, 125nM creatine phosphate, 5mM ATP) and 200ng of recombinant RIG-I. The conjugation reactions were incubated at 30ºC for 90 minutes, then incubated with pre-equilibrated Ni-NTA

beads overnight at 4ºC, washed once in Guanidine buffer then with 8M Urea. Proteins were eluted directly in 2X Laemmli buffer, ran on SDS-PAGE and immunoblotted.

3.12 IFNβ- and ISRE-luciferase reporter assays

U2OS cells were transfected with siRNA for NT (non-targeting), MAVS or MAPL for 48 hours, then with pIFNβ-luc or pISRE-luc reporter plasmid and pE-CFP (1μg each, a gift from Dr. Rongtuan Lin, Lady Davis Institute, McGill University) together with 1μg empty vector (control) or myc-ΔRIG-I (constitutively active form of RIG-I, also a gift from Rongtuan Lin, McGill University). Conditions were done in triplicates each time (n=2). Measures of luciferase activity were performed using Promega Luciferase assay system (E2820) 21 hours after transfection.

3.13 Isolation of mitochondria derived vesicles (MDVs)

4 confluent 15cm dishes of 143B cells grown on galactose were either treated with 400J/m2 ultraviolet-C (UVC) (Hoefer ultraviolet crosslinker) or left untreated and then incubated at 37ºC for 1 hour. Cells were scraped and washed in Mitochondrial Isolation Buffer, then spun at 400g for 5 minutes at 4ºC. Cells were resuspended with 2 times the pellet volume of MIB in presence of protease inhibitor cocktail (Roche Diagnostics) and *broken* by homogenization *using a Dounce homogenizer.* The lysates were centrifuged 800g at 4ºC for 10 minutes to remove nuclei and unbroken cells. The supernatants were then centrifuged 8000g at 4ºC for 10 minutes to remove mitochondria, and another time 21 000g at 4ºC for 15 minutes to remove remaining intracellular organelles. The supernatants containing MDVs were then submitted to sucrose gradient fractionation.

3.14 Sucrose gradient fractionation

All steps were carried out at 4ºC. The supernatants obtained above were adjusted to 50% sucrose in MIB and loaded on the bottom of a discontinuous sucrose gradient with steps at 50%, 40%, 30%, 20%, and buffer. Samples were subjected to centrifugation at 150 000g for 6 hours and fractions were collected for immunoblotting or PCR analyses as indicated.

3.15 Denaturing and Native PAGE

SDS-PAGE (Tris-glycine) was used to separate extracts using 12% polyacrylamide gels. Native PAGE was used to separate IRF3 dimers from monomers in the IRF3 dimerization assay as described previously (Iwamura et al. 2001). Separated proteins were transferred to a nitrocellulose membrane and immunoblot analysis was performed with the indicated antibodies.

3.16 Polymerase Chain Reactions (PCR)

DNA was isolated from sucrose gradient fractions using QIAGEN DNA extraction kit and PCR was carried out using Quick load Taq 2X master mix (NEB) and primers from **Table 2**, where *Dloop1* and *Dloop2* represent two different regions of the mitochondrial D-loop.

Table 2. mtDNA PCR primer list

Gene	Reverse primer	Forward primer
Cytb	5'-ggtgattcctaggggttgt-3'	5'-tatccgccatcccatacatt-3'
Nd4	5'-atcgggtgatgatagccaag-3'	5'-cctgactcctacccctcaca-3'
Dloop1	5'-gggaacgtgtgggctattta-3'	5'-ctcagataggggtcccttga-3'
Dloop2	5'-gcactcttgtgcgggatatt-3'	5'-acaagcaagtacagcaatcaac-3'

3.17 Gene silencing with siRNA

Immortalized human fibroblasts, a kind gift from Dr. Eric Shoubridge, were transfected with siRNA for non-targeting (*NT*), *DRP1*, *SNX9*, *VPS35*, *MAVS*, or *cGAS* (SMARTpool, Dharmacon) for 3 days. Cells were trypsinized and plated in 96 well plate for ELISA or on coverslips for immunofluorescence (IF). Cells were left untreated or treated with 400 J/m^2 UV and left to recover at 37ºC for indicated times. Supernatants were collected at the times indicated for the ELISA analyses, and the cells on coverslips were fixed with paraformaldehyde for further IF staining. Efficiency of siRNA were tested by SDS-PAGE (**Fig. 3.1**)

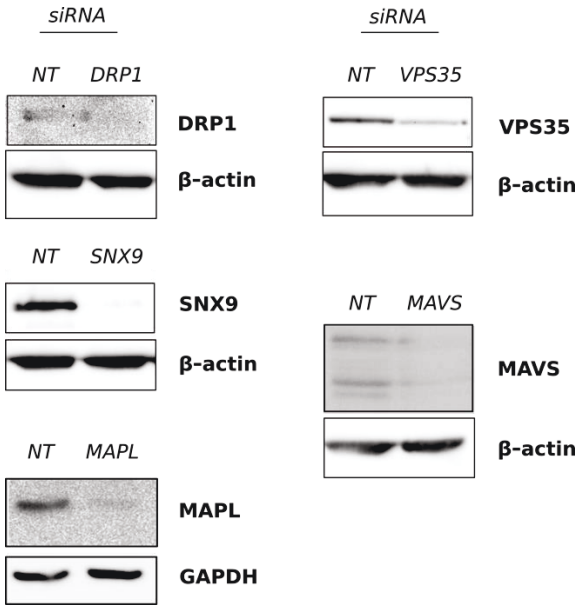

Figure 3.1. A test of the knock-down efficiency by Western blot analysis.

Human fibroblasts were treated twice with siRNAs for *DRP1*, *SNX9*, *MAVS*, *VPS35* and *MAPL* for 3 days and the efficiency of knockdown was verified by SDS-PAGE. β-actin or GAPDH was used as control. These siRNAs were used in experiments for Figures 4.9, 4.10, 4.13 and 4.15 in results chapter 4. Knockdown of cGAS could not be verified due to the lack of appropriate antibody, but the same siRNA was used previously(Gringhuis et al. 2017).

3.18 Immunofluorescence staining and Imaging

Cells were plated on coverslips and fixed 15 minutes at 37°C with 5% paraformaldehyde (PFA), washed 3 times with phosphate-buffered saline (PBS), then PFA was quenched by incubating in 50 mM NH_4Cl/PBS (ammonium chloride) for 10 minutes at room temperature, and washed 3 times with PBS. Cells were permeabilized with 1% Triton-X100/PBS for 10 minutes, washed 3 times with PBS and blocked with 10% FBS-PBS for 30 minutes. Primary antibodies were added in 5% FBS-PBS for 1 hour, then washed 3 times with 5% FBS-PBS. Secondary antibodies were added

in 5% FBS-PBS for 1 hour, then washed 3 times with PBS. When DAPI was used, it was added in the first PBS wash after secondary antibodies. Coverslips were mounted on microscope slide using fluorescent mounting medium (Dako). Cells were observed with spinning confocal microscopy (Olympus IX81 with Andor/Yokogawa spinning disk system (CSU-X), sCMOS camera and 100× or 60× objective lenses (NA1.4)), and image files were analyzed using Fiji, the open source image processing package based on ImageJ.

3.19 Statistical analysis

All values are expressed as mean ± SD. Unless stated otherwise statistical significance was tested by the unpaired two-tailed Student's *t* test. *P* values less than 0.05 were considered to represent statistically significant differences.

Chapter 4: Results

4.1 Hypothesis 1: MAPL is the SUMO E3 ligase for RIG-I, and is required for the antiviral response.

The innate immune consequences of MAPL SUMOylation during the antiviral response were investigated using *Mapl*$^{-/-}$ knock-out cells and a *Mapl*$^{-/-}$ knock-out mouse model. In addition, the BioID approach identifies new substrates of MAPL, specific to the antiviral immune response.

4.1.1 Antiviral response to dsRNA virus in absence of MAPL

In order to investigate the function of MAPL in the response to a dsRNA virus, we infected mouse embryonic fibroblasts (MEFs) derived from *Mapl*$^{fl/fl}$ and *Mapl*$^{-/-}$ mice with the dsRNA Sendai Virus (SeV), and quantified cellular immune response through the release of IL6, RANTES and IFNβ over a period of 24 hours (**Fig. 4.1A**). We observed a complete impairment of *Mapl*$^{-/-}$ MEFs to secrete IL6, as well as a significant reduction of IFNβ and RANTES secretion compared to the control *Mapl*$^{fl/fl}$ cells, indicating a necessity for MAPL in the establishment of a proper innate immune response to dsRNA virus SeV.

4.1.2 *In vivo* requirement of MAPL in the antiviral RIG-I/MAVS pathway

To test whether MAPL is required for the antiviral innate response *in vivo*, we injected *Mapl*$^{-/-}$ and wild-type mice intravenously with Poly(I:C), a synthetic dsRNA polymer, complexed with the transfection reagent LyoVec, and assessed the serum cytokine/chemokine content at time 0 as well as 2 and 4 hours post injection (**Fig. 4.1B**). Unlike naked Poly(I:C) which is recognized by TLR3, complexed Poly(I:C) is recognized by RIG-I (and MDA5), in a cell-type specific manner (Kato et al. 2005). Consistent with the data from MEFs, we observed that secretion of RANTES and IFNβ are significantly decreased in the *Mapl*$^{-/-}$ mice sera relative to wild-types. However, IL6

production is unaffected compared to wild-type mice. This may be explained by the fact that RIG-I responds in a cell type specific manner to dsRNA viruses or transfected Poly(I:C). For example, a subset of dendritic cells (DCs): plasmacytoid DCs (pDCs) uses the TLR system rather than RIG-I to induce type I IFN and IL6 (Kato et al. 2005). Nonetheless, our data clearly show a requirement for MAPL in the activation of the antiviral innate immune response to Poly(I:C) *in vivo*.

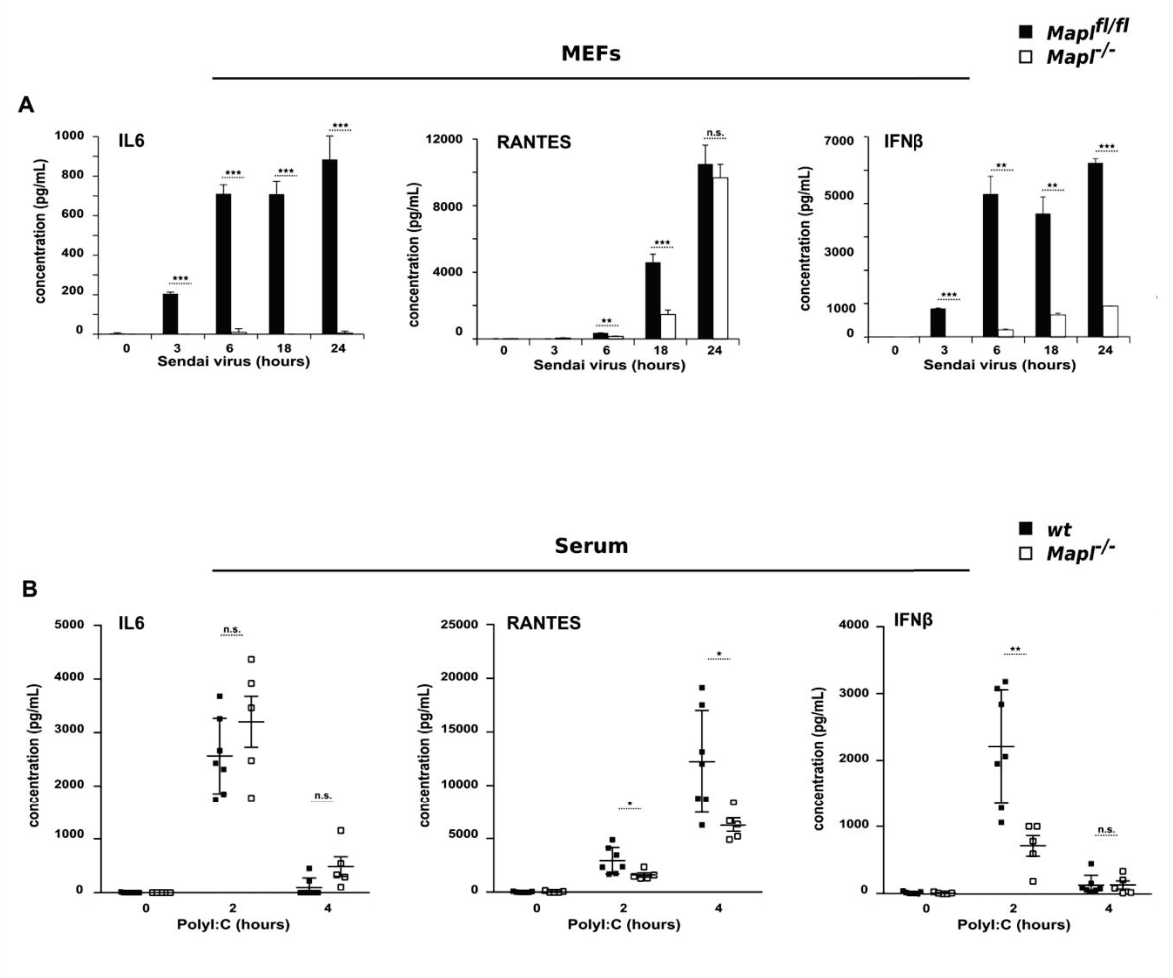

Figure 4.1. Defective innate immune response in vitro and in vivo in the absence of MAPL. **(A)** *Mapl*$^{fl/fl}$ and *Mapl*$^{-/-}$ MEFs were left untreated or infected with Sendai virus (150 HAU/mL) over a time course of 24 hours. IL6, RANTES and IFNβ were measured in supernatants by ELISA. (n=3). **(B)** Wild-type (WT) (n=7) and *Mapl*$^{-/-}$ (n=5) mice were injected intravenously with saline or complexed PolyI:C for 2hrs and 4hrs. Serum IL6, RANTES and IFNβ were measured by

ELISA. Results are expressed as the mean induction, comparing *Mapl*$^{-/-}$ to *Mapl*$^{fl/fl}$ or WT. *P<0.05, **P<0.01 and ***P<0.001, n.s., nonsignificant.

4.1.3 Impairment of the transcriptional response to Sendai virus in absence of MAPL

To better understand the effect of the loss of MAPL during the viral infection we looked at the transcriptional response very early on after SeV infection in MEFs. As revealed by qRT-PCR, we observe an upstream block in transcription as early as 3 hours post-infection, for a number of transcriptionally activated genes including NF-κB, IL6, IFNα, IFNβ, RIG-I, MDA5, IFIT1(ISG56) and IFIT2 (ISG54) (**Fig. 4.2A**) (Schneider et al. 2014). Since one important function of these interferon-stimulated genes (ISG) is to block virus translation, we tested whether *Mapl*$^{-/-}$ MEFs showed an increased viral load. Indeed, and confirming the requirement of MAPL in the transcriptional response, there is as ~6-fold increase in Sendai Protein P (SeV PP) specific mRNA by 36 hours post infection in *Mapl*$^{-/-}$ MEFs, thus reflecting the cellular viral load (**Fig. 4.2B**). This increase in viral load led to the apoptotic cleavage of PARP (Poly (ADP-ribose) polymerase) in *Mapl*$^{-/-}$ MEFs after 18 hours of SeV infection (**Fig. 4.3**). Altogether, these data demonstrate a necessity for MAPL in the dsRNA antiviral innate response, possibly participating in the early signaling events.

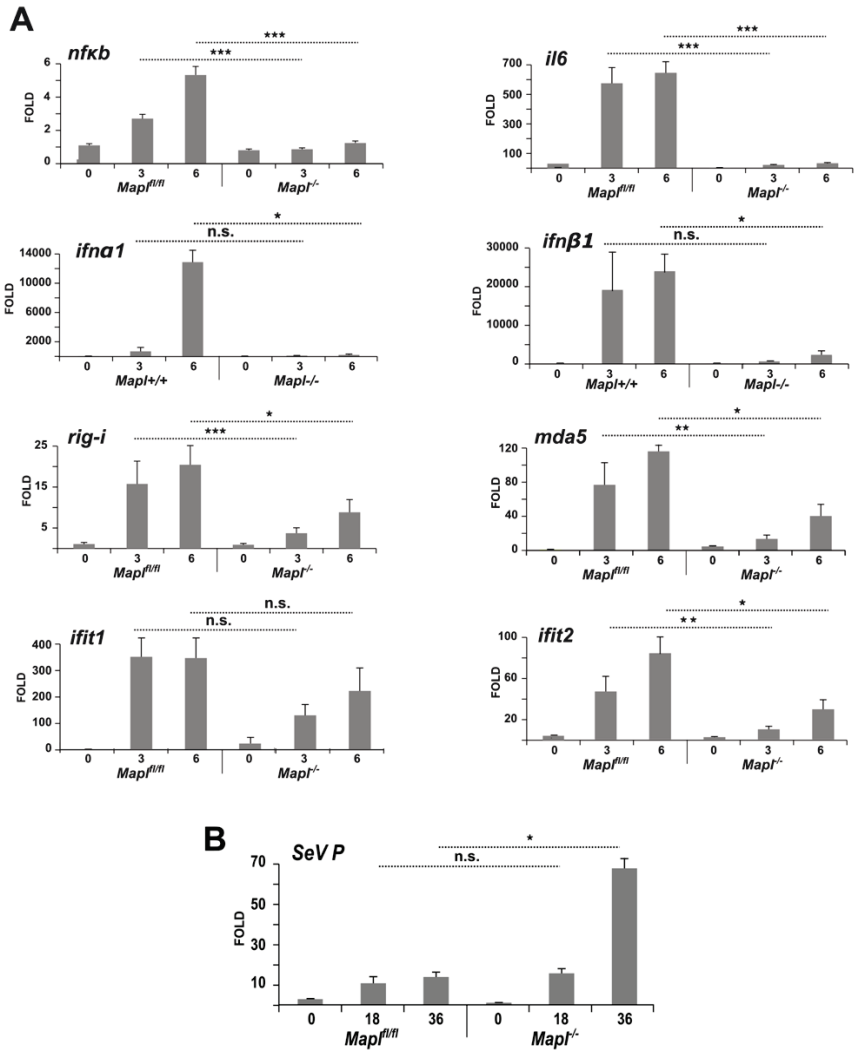

Figure 4.2. Impaired transcriptional response to viral infection with the loss of MAPL.

(A) *Mapl*$^{fl/fl}$ and *Mapl*$^{-/-}$ MEFs were left untreated or infected with Sendai virus (150 HAU/mL) for 3 or 6 hours, RNA was extracted, and NF-κB, IL6, IFNα1, IFNβ1, RIG-I, MDA5, IFIT1 and IFIT2 levels were measured by quantitative real-time RT-PCR (n=3). **(B)** MEFs were left untreated or infected with Sendai virus (150 HAU/mL) for 18 or 36 hours, RNA was extracted, and Sendai virus Protein P mRNA level was measured by quantitative real-time RT-PCR (n=3). Results are expressed as the mean induction, comparing *Mapl*$^{-/-}$ to *Mapl*$^{fl/fl}$. **P*<0.05, ***P*<0.01 and ****P*<0.001, n.s., nonsignificant.

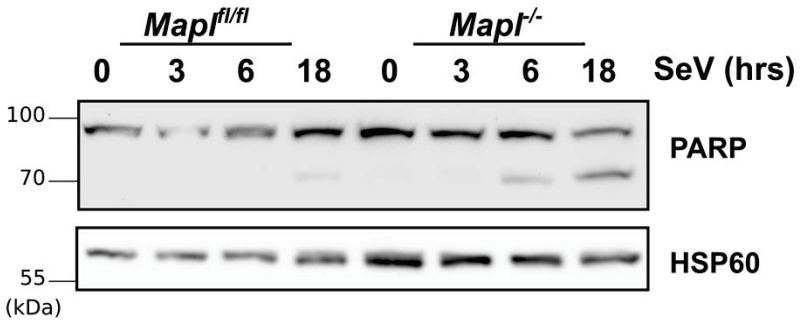

Figure 4.3. Earlier PARP cleavage in Mapl$^{-/-}$ following SeV infection.
Mapl$^{fl/fl}$ and *Mapl$^{-/-}$* MEFs were left untreated or infected with Sendai virus (150HAU/mL) over a time course of 18hours. Cells were lysed, ran on SDS-PAGE and immunoblotted as indicated.

4.1.4 Molecular events occurring during Sendai virus without MAPL

We next investigated the role of MAPL in the molecular events happening during SeV infection. We observe the expected increase in RIG-I protein levels at 6 hours post-infection in control cells but not in *Mapl$^{-/-}$* cells (**Fig. 4.4A**). Consistent with this, we observe a delay in the phosphorylation and the dimerization of IRF3, which are hallmarks of its activation (**Fig. 4.4A, B**). Although we observe a dramatic inhibition at the transcription level of antiviral genes (**Fig. 4.2**), IRF3 phosphorylation and dimerization are not completely blocked in *Mapl$^{-/-}$* MEFs (**Fig. 4.4A, B**). We also observe a reduction in the phosphorylation of IκBα, and consequently a lower level of activation of NF-κB over 24 hours of SeV infection in *Mapl$^{-/-}$* MEFs (**Fig. 4.4C**). Also, consistent with qRT-PCR data, the protein expression of interferon induced IFIT2 involved in downstream inhibition of viral assembly factors (Fensterl & Sen 2015; Reynaud et al. 2015), is also inhibited in the absence of MAPL.

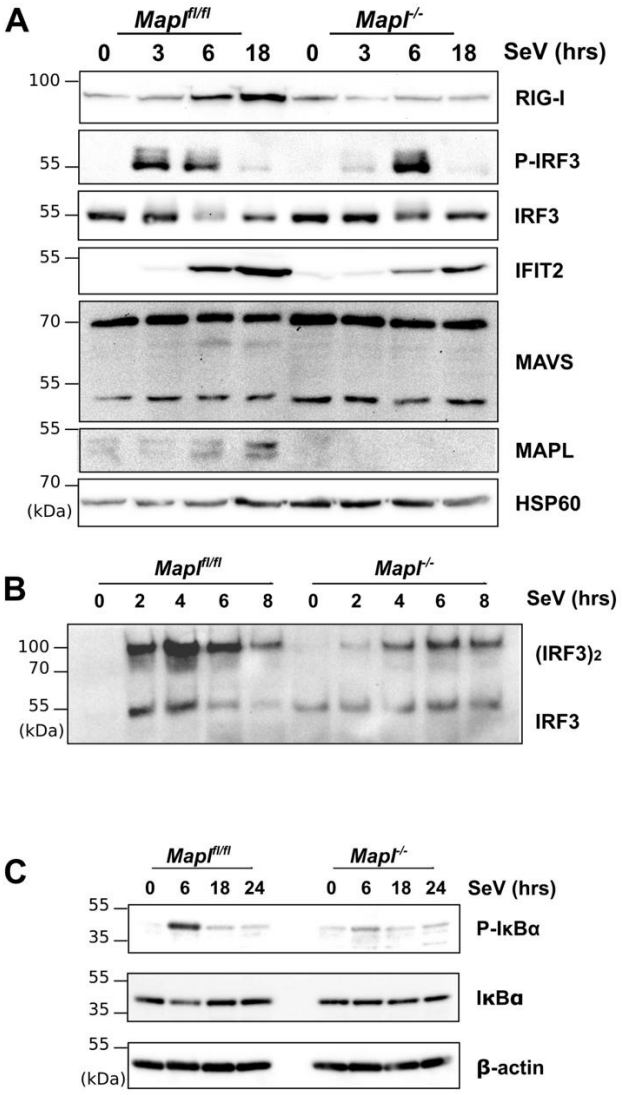

Figure 4.4. MAPL is required for early steps of immune response to Sendai virus infection.
(A) *Mapl*$^{fl/fl}$ and *Mapl*$^{-/-}$ MEFs were left untreated or infected with Sendai virus (150 HAU/mL) for up to 18 hours and lysates were immunoblotted with indicated antibodies. **(B)** IRF3 dimerization assay. Cells were infected with Sendai virus (150 HAU/mL) for the indicated periods, lysed, ran on a native gel and immunoblotted. **(C)** NF-κB activation assay through phosphorylation of IκBα. Cells were left untreated or infected with Sendai virus (150 HAU/mL) for up to 24 hours and lysates were immunoblotted.

4.1.5 Biotin identification (BioID) of MAPL interactome

With the aim of identifying direct MAPL binding partners and substrates related to the assembly of this signaling complex, and unique to SeV infection, we performed an unbiased protein interactome screen. Because MAPL is a catalytic enzyme, it can be challenging to isolate MAPL targets using simple immunoprecipitation approaches. In addition, since MAPL is a membrane-anchored protein and MAVS assembles into prion-like filamentous complexes, we decided to avoid the use of detergents and centrifugation steps in performing this assay. We consequently turned to a well-established proximity-dependent biotinylation screening method termed BioID (Roux et al. 2012; Roux et al. 2013; Roux et al. 2018). BioID involves a mutant form of the ~35 kDa E. coli BirA biotin ligase (BirA* R118G) which is fused to the RING-domain containing C-terminal tail of MAPL (Roux et al. 2013). The abortive BirA* mutant protein efficiently activates biotin but is unable to bind the activated product, and thereby releasing highly reactive biotinoyl-AMP. Proximal amines (including epsilon amine groups of nearby lysine residues) are thereby covalently labeled with biotin. This approach to generate high-resolution information on the complex and dynamic protein interactions in cell biological processes have now been used in numerous studies, most notably for the events at the centrosome/cilia (Gupta et al. 2015). In a side-by-side comparison of the same "bait" protein under different conditions, changes in the number of peptides identified for a given interactor implies altered residence time of the interaction throughout the time course of biotin incubation.

Stable HEK293 Tet-inducible Flp-In cell lines carrying either Flag-BirA or MAPL-Flag-BirA were generated. MAPL expression was induced for 9 hours with tetracycline, and biotin was added to the culture media in both untreated control and SeV infected cells for 15 more hours, totalizing 24 hours, to induce biotinylation of MAPL-proximal proteins. Biotinylated proteins

were isolated in fully denaturing conditions using streptavidin beads, and identified by mass spectrometry (**Fig. 4.5A**). In the control cells, MAPL is found to interact with expected targets such as DRP1 (Braschi et al. 2009; Prudent et al. 2015), and a multitude of mitochondrial fission proteins, including AKAP1 (Merrill et al. 2011; Dickey & Strack 2011; Kim et al. 2011), INF2 (Korobova et al. 2013; Ji et al. 2015), Mff (Gandre-Babbe & van der Bliek 2008; Otera et al. 2010; R. Liu & Chan 2015), and MTFR1 (Monticone et al. 2010). These data are consistent with the already well-established role of MAPL in stabilizing DRP1-mediated mitochondria-ER contacts during division (Braschi et al. 2009; Prudent et al. 2015), and validate the BioID approach for studying interactions at the mitochondria. While mitochondria-ER contacts have been previously involved in the RIG-I/MAVS signaling pathway (Castanier et al. 2010; West et al. 2011; Jacobs et al. 2014), the number of peptides identified from the fission machinery were unaltered upon infection (**Fig. 4.5A**).

Interestingly, a number of MAPL proximal interactions were significantly altered upon SeV infection (**Fig. 4.5A**). MAVS was found as a MAPL partner in uninfected cells, and this interaction was reduced during infection. Notably, we also identified a series of biotinylated proteins only in SeV infected cells, including the cytosolic receptor RIG-I and its enhancer, the IFN-inducible oligoadenylate synthetase-like OASL (Zhu et al. 2014), the interferon stimulated genes IFIT1 and IFIT2 (Reynaud et al. 2015), HERC5, an E3 ligase mediating the conjugation of the ubiquitin-like protein ISG15 (Wong et al. 2006; Dastur et al. 2006), and STAT1, a transcription factor responsive to cytokines (Yu et al. 2009) (**Fig. 4.5A**).

A

Gene ID	Symbol	MAPL-Ctrl Total	MAPL-SeV Total	log2 fold change	
3434	IFIT1		80	6.3	
55967	NDUFA12		13	3.8	
23586	**RIG-I**		**13**	**3.8**	
85461	TANC1		11	3.6	
51191	HERC5		8	3.2	
6945	MLX		8	3.2	
9100	USP10		7	3.0	
56267	CCBL2		7	3.0	
3433	IFIT2		7	3.0	
118881	COMTD1		7	3.0	**Up-regulated**
8638	OASL		7	3.0	
5879	RAC1		6	2.8	
10558	SPTLC1		6	2.8	
4191	MDH2		6	2.8	
54471	SMCR7L		6	2.8	
3157	HMGCS1		6	2.8	
5194	PEX13		5	2.6	
6905	TBCE		5	2.6	
10802	SEC24A		5	2.6	
6772	STAT1	2	15	2.4	
10059	DRP1	12	18	0.5	
9650	MTFR1	28	31	0.1	**Unchanged**
56947	MFF	97	92	-0.1	
64423	INF2	147	134	-0.1	
8165	AKAP1	310	287	-0.1	
57506	MAVS	173	84	-1.0	**Down-regulated**

B

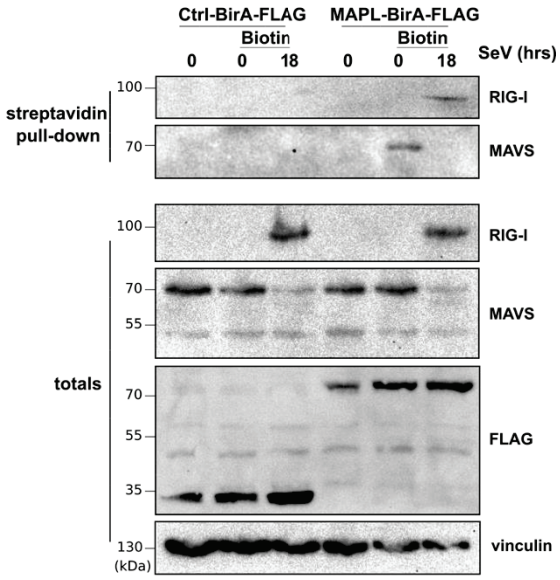

Figure 4.5. Biotin-labeled interaction landscape identifies RIG-I as a MAPL substrate upon SeV infection.

(A) HEK293 cells stably expressing an inducible Tet-ON fusion construct MAPL-BirA-FLAG or Ctrl-BirA-FLAG were induced with tetracycline for 9 hours, and infected (or not) with Sendai virus in the presence of excess biotin within the media for a further 15 hours. Biotinylated proteins were isolated and sequenced by mass spectrometry. Shown are total peptide counts observed for the indicated proteins. Proteins showing a greater than 2-fold change in the presence of Sendai virus are shown, along with the top MAPL binding partners related to mitochondrial fission as control **(B)** Cells were infected with Sendai virus for 18 hours and tagged proteins were isolated on streptavidin-sepharose and immunoblotted.

4.1.6 Validation of the BioID data

We then sought to validate this intriguing dual interaction of MAPL with MAVS in uninfected cells and then with RIG-I under infection conditions. We used the same system of HEK293 Flip-In cells, in which we induced expression of either Flag-BirA control or MAPL-Flag-BirA in cells. Cells were either left untreated or infected with SeV in the presence of biotin over a period of 18 hours, and then biotinylated proteins were isolated on streptavidin beads. We were able to confirm the interaction of MAPL with MAVS in control cells, which is lost upon SeV infection (**Fig. 4.5B**). We also validate that under infection conditions only RIG-I is biotinylated in a MAPL-dependent manner, corroborating the mass spectrometry analysis.

4.1.7 MAPL-dependent SUMOylation of RIG-I

With regard to the interaction of MAPL with both MAVS and RIG-I, we next tested whether MAVS or RIG-I are SUMO substrates of MAPL. To investigate this, we stably expressed His6-SUMO1 in control *Mapl*$^{fl/fl}$ and *Mapl*$^{-/-}$ MEFs. We infected the cells with SeV for a period of 18 hours and then isolated His6-SUMOylated proteins under high stringency conditions. Although we could not detect RIG-I in the *Mapl*$^{-/-}$ MEFs because it is not upregulated in absence of MAPL, we observe a MAPL-dependent SUMOylation of RIG-I upon SeV infection in the control cells. We also observe that MAVS, although it is a binding partner, does not appear to be a SUMO substrate for MAPL in either control or SeV infected MEFs (**Fig. 4.6**).

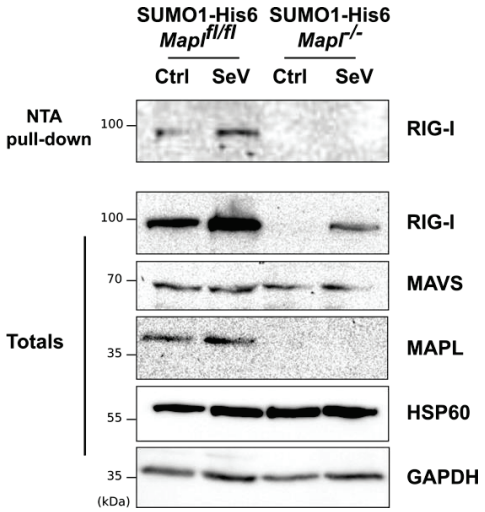

Figure 4.6. MAPL-dependent SUMOylation of RIG-I during Sendai virus infection.
Stable His6-SUMO1 *Mapl*$^{fl/fl}$ and *Mapl*$^{-/-}$ MEFs were infected with Sendai virus for 18 hours, lysed, and SUMOylated proteins were isolated on Ni-NTA beads and immunoblotted with indicated antibodies.

4.1.8 *In vitro* SUMOylation of RIG-I by MAPL E3 ligase

In order to determine whether MAPL could directly SUMOylate recombinant RIG-I, we used a cell free assay system (Braschi et al. 2009). Full-length recombinant RIG-I or a biotinylated SUMO consensus peptide as the positive control were incubated with His6-SUMO1, SUMO E1 heterodimer, the E2 ligase Ubc9 and the recombinant RING domain of MAPL as the E3 ligase. Following an incubation of 90 minutes in the presence of ATP, SUMOylated proteins or peptides were isolated using NTA-agarose beads. This *in vitro* SUMOylation assay confirms that the RING domain of MAPL can directly SUMOylate both RIG-I and the biotinylated consensus peptide, in an energy and temperature dependent manner. We also observe a certain SUMOylation activity of Ubc9 alone as previously established, mainly for the conjugation to the peptide containing the SUMO conjugation motif (**Fig. 4.7A, lane 1 vs. lane 3**).

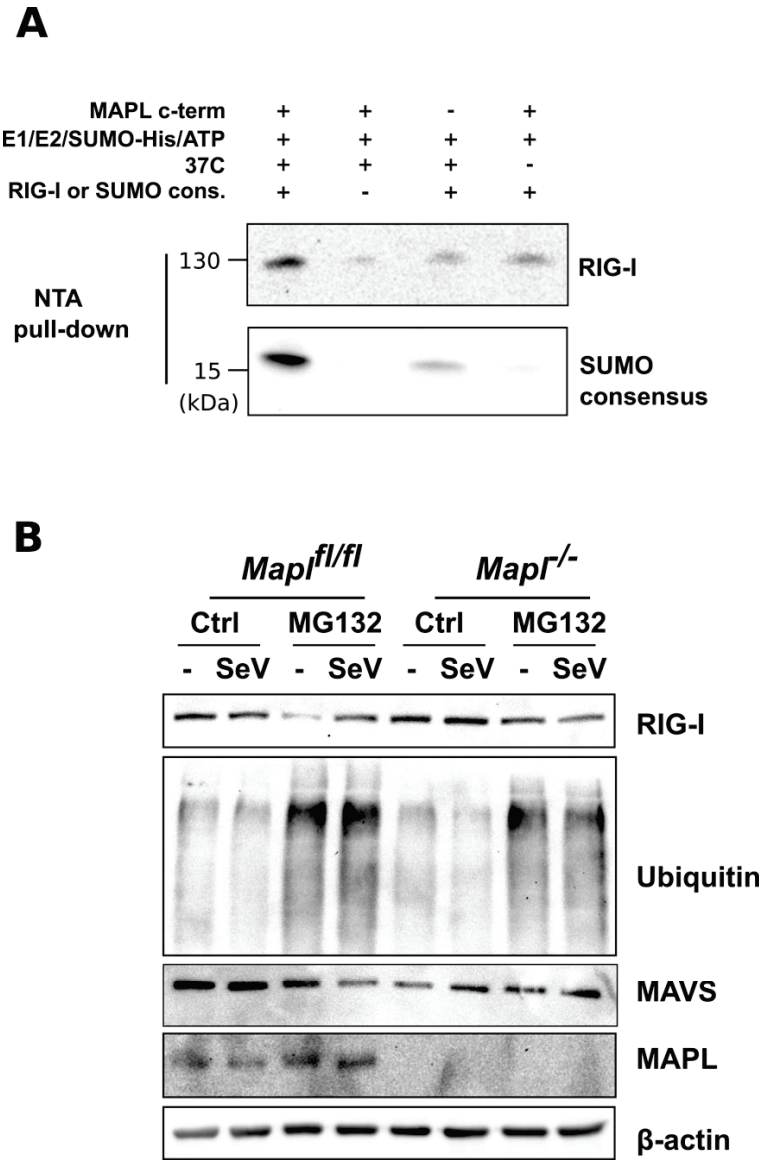

Figure 4.7. MAPL-dependent SUMOylation of RIG-I.

(A) *In vitro* SUMOylation assay. Recombinant RIG-I protein or SUMO consensus peptide were incubated in the indicated conditions. After the reaction, SUMO-conjugated proteins/peptides were isolated and immunoblotted. **(B)** *Mapl*$^{fl/fl}$ and *Mapl*$^{-/-}$ MEFs were incubated with MG132 (10μM) and infected with SeV for 6hrs then lysates were run on SDS-PAGE and immunoblotted with indicated antibodies.

4.1.9 SUMOylation of RIG-I does not increase its stability

SUMOylation in often coupled to ubiquitination events, where SUMOylation leads to stabilization of proteins against proteasomal degradation. Consequently, we sought to determine whether MAPL SUMOylation of RIG-I is required to stabilize it. To do this, we incubated both control and SeV infected cells in the presence of MG132, a proteasome inhibitor, over a period of 6 hours (**Fig. 4.7B**). We observe that the addition of MG132 leads to a dramatic accumulation of global ubiquitin conjugates in both *Map*$^{fl/fl}$ and *Mapl*$^{-/-}$ MEFs, and this is not affected upon SeV infection. Since the total protein levels of RIG-I and MAVS are not affected by the loss of MAPL, we conclude that SUMOylation of RIG-I does not interfere with its stability.

4.1.10 MAPL-dependent SUMOylation of RIG-I is required for RIG-I activation

SUMOylation of RIG-I has previously been shown to enhance type I IFN production and facilitate RIG-I interaction with its adaptor MAVS (Mi et al. 2010). This prompted us to test whether a constitutively active form of RIG-I containing only the CARD domains (ΔRIG-I) (Yoneyama et al. 2004) may override the requirement of MAPL in prompting the downstream transcriptional response. To do this, we used luciferase reporter assays in osteosarcoma U2OS cells, which drive expression of luciferase through the activation of both IFNβ and ISRE promoters, downstream of MAVS signaling at mitochondria. U2OS cells were silenced for either MAVS or MAPL and transfected with ΔRIG-I (**Fig. 4.8A, B**). In the control cells and those transfected with a non-targeting siRNA, the transfection of ΔRIG-I leads to a robust expression of luciferase driven by both reporter constructs (**Fig. 4.8**). Since MAVS is required at mitochondria in order to signal downstream of RIG-I activation, its silencing leads to an ablation of luciferase expression. However, silencing of MAPL has no effect on the activation of either IFNβ or ISRE

promoter driven luciferase in presence of ΔRIG-I. Since transfecting the constitutively active form of RIG-I shows no impairment in signaling in absence of MAPL, this suggests a requirement for MAPL SUMOylation of RIG-I in inducing a conformational change required to activate RIG-I itself.

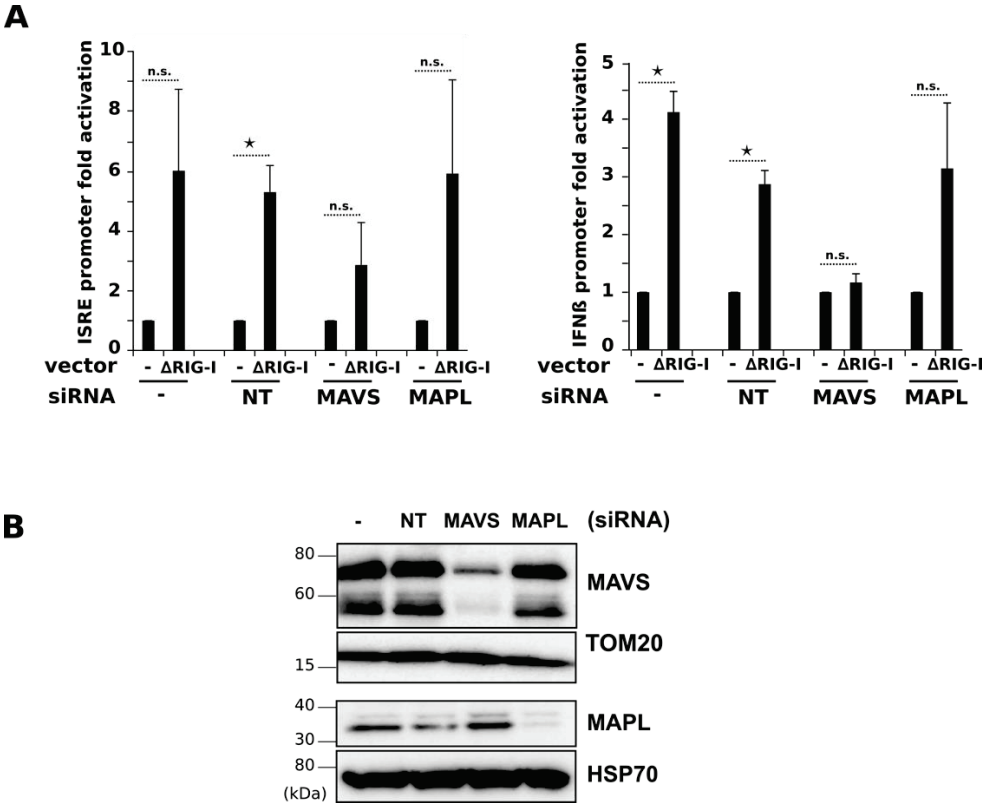

Figure 4.8. MAPL SUMOylation of RIG-I is required for RIG-I activation

(A) IFNβ- and ISRE-luciferase reporter assays. U2OS cells were transfected with indicated siRNA for 48 hours then with pIFNβ-luc or pISRE-luc reporter plasmid and pE-CFP (1μg each) together with 1μg of myc-ΔRIG-I (constitutively active form of RIG-I). Measures of luciferase activity and CFP were performed 21 hours post transfection. Data represents 2 different experiments done each time in triplicate. Values are reported as mean ± SD. **P*<0.05, ***P*<0.01 and ****P*<0.001, n.s., nonsignificant. (B) Western blot controls for knockdowns of *MAVS*, *TOMM20* and *MAPL (MUL1)*.

4.2 Hypothesis 2: mtDNA is released as a MDV cargo under certain conditions, and may drive an innate immune response.

Using immunofluorescence and gene silencing approaches, mtDNA release into the cytosol via MDVs was investigated. The innate immune response following mtDNA release was also examined.

4.2.1 Visualization of mtDNA by immunofluorescence

Since a wide variety of cargoes have been identified as incorporated within MDVs depending on the cell type and the stimulus (Neuspiel et al. 2008; Soubannier, Rippstein, et al. 2012; Matheoud et al. 2016), one of the possibilities would be that mtDNA might be a cargo under certain conditions.

There is emerging evidence of mtDNA release which leads to activation of the innate immune system, however no mechanism or regulation of this process has been documented. It was shown that during apoptosis, mtDNA is released through BAK/BAX channels forming in the outer membrane of mitochondria and herniation of the inner membrane (McArthur et al. 2018). It is unclear how mtDNA gets released under other physiological conditions not involving cell death.

To investigate whether mtDNA is released through MDVs, human osteosarcoma 143B or human fibroblasts were treated with a mild shortwave ultraviolet (UV) dose, to induce DNA damage. After one hour recovery time, mtDNA was visualized by immunofluorescence staining. Using a DNA antibody, a very clear staining of the nucleoids inside mitochondria is observed in both cell types. Upon UV exposure, vesicle-like structures, containing DNA are detected (**Fig. 4.9A, B**). These structures do not contain other mitochondrial proteins like TOMM20, indicating that the cargoes incorporated within the vesicles are highly selected (**Fig. 4.9A, B**). The release of

these vesicle-like structures is UV dose-dependent since a higher dose leads to a higher number of DNA containing vesicles (**Fig. 4.9C**). Interestingly, TFAM positive structures can also be detected outside the mitochondrial network (**Fig. 4.9B**). Although in some cases the TFAM-positive vesicle-like structures are also positive for DNA, most of the detected TFAM-positive vesicle-like structures are negative for DNA (**Fig. 4.9B**). It is possible that these TFAM-positive vesicle-like structures might contain oxidized DNA in the form of 8-oxo-7,8-dihydroguanine (8-oxoG), which is induced by UV light, and which is not detected by the DNA antibody. Although we tested an anti-8-oxoG antibody in these conditions, the background was too high to make reliable conclusions (data not shown).

In sum, these data indicate that mtDNA is released in vesicle-like structures upon UV treatment in human osteosarcoma 143B cells and human fibroblasts.

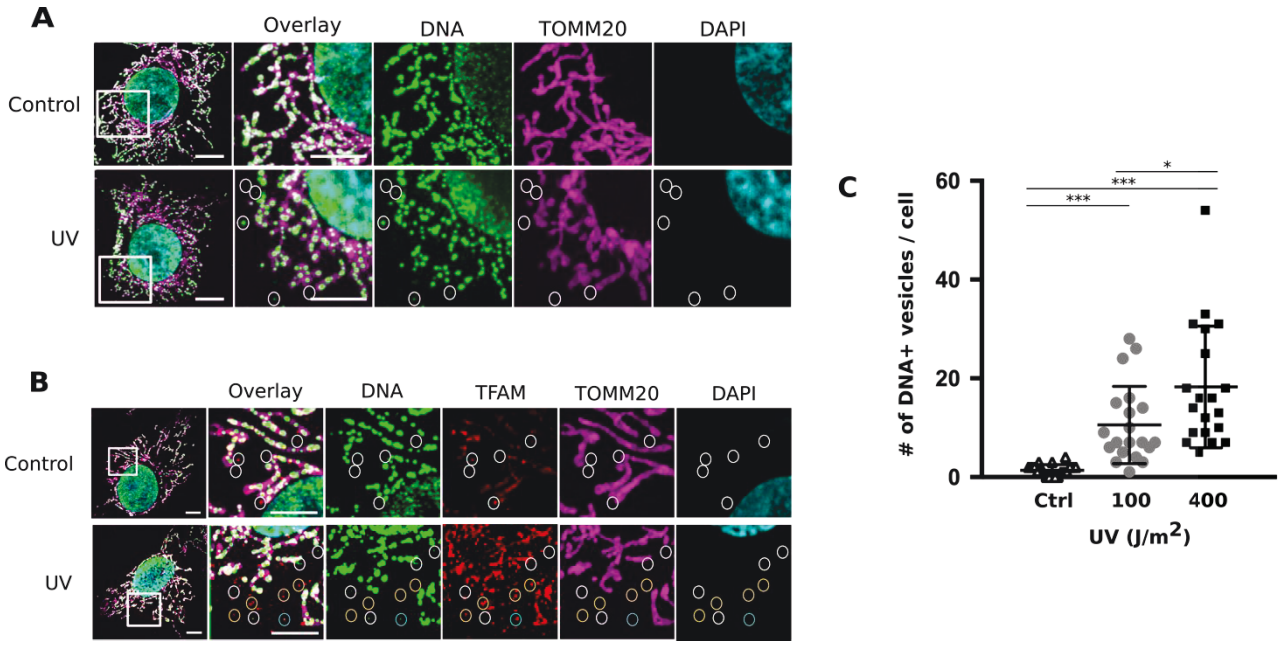

Figure 4.9. UV induces the release of vesicle-like structures in 143B and human fibroblasts cells.

(A) 143B cells were left untreated or exposed to 400J/m^2 UV, and left to recover for 1 hour. Cells were fixed and immune-stained as indicated. White circles represent mtDNA+ vesicles. **(B)** Human fibroblasts were left untreated or exposed to 400J/m^2 UV, and left to recover for 1 hour. Cells were fixed and immune-stained as indicated. White circles represent mtDNA+, TFAM- vesicles; blue circles represent mtDNA+, TFAM+ vesicles; and orange circles represent mtDNA-, TFAM+ vesicles. Scale bars: first column 5µm, second column 10µm. **(C)** 143B cells were exposed to different doses of UV as indicated, fixed, immune-stained, and mtDNA+ vesicles were counted. Bars represent mean ± SD, n = 25 cells per condition. *P < 0.05, and ***P < 0.001.

4.2.2 mtDNA-positive vesicle-like structures are independent of DRP1

One important characteristic of MDVs is that their formation is independent of the mitochondrial fission protein DRP1 (Neuspiel et al. 2008). To test if the vesicle structures seen in

Figure 4.9 are MDVs, *DRP1* was silenced in human fibroblasts. The number of mtDNA-positive vesicle-like structures detected upon UV treatment is not affected following *DRP1* silencing (**Fig. 4.10A, B**). This confirms that the observed mtDNA-positive vesicle-like structures are MDVs.

Another important characteristic of some subclasses of MDVs is that MDV formation is dependent on the molecular MDV machinery component SNX9 (Matheoud et al. 2016). Consistent with the role of SNX9 in MDV formation, silencing of *SNX9* leads to a decreased number of mtDNA-positive MDVs in human fibroblasts cells upon UV light exposure (**Fig. 4.11A, B**).

Together, that these mtDNA-positive vesicle-like structures do not require DRP1, show evidence of cargo selectivity, and are dependent on SNX9, demonstrates that these structures are MDVs.

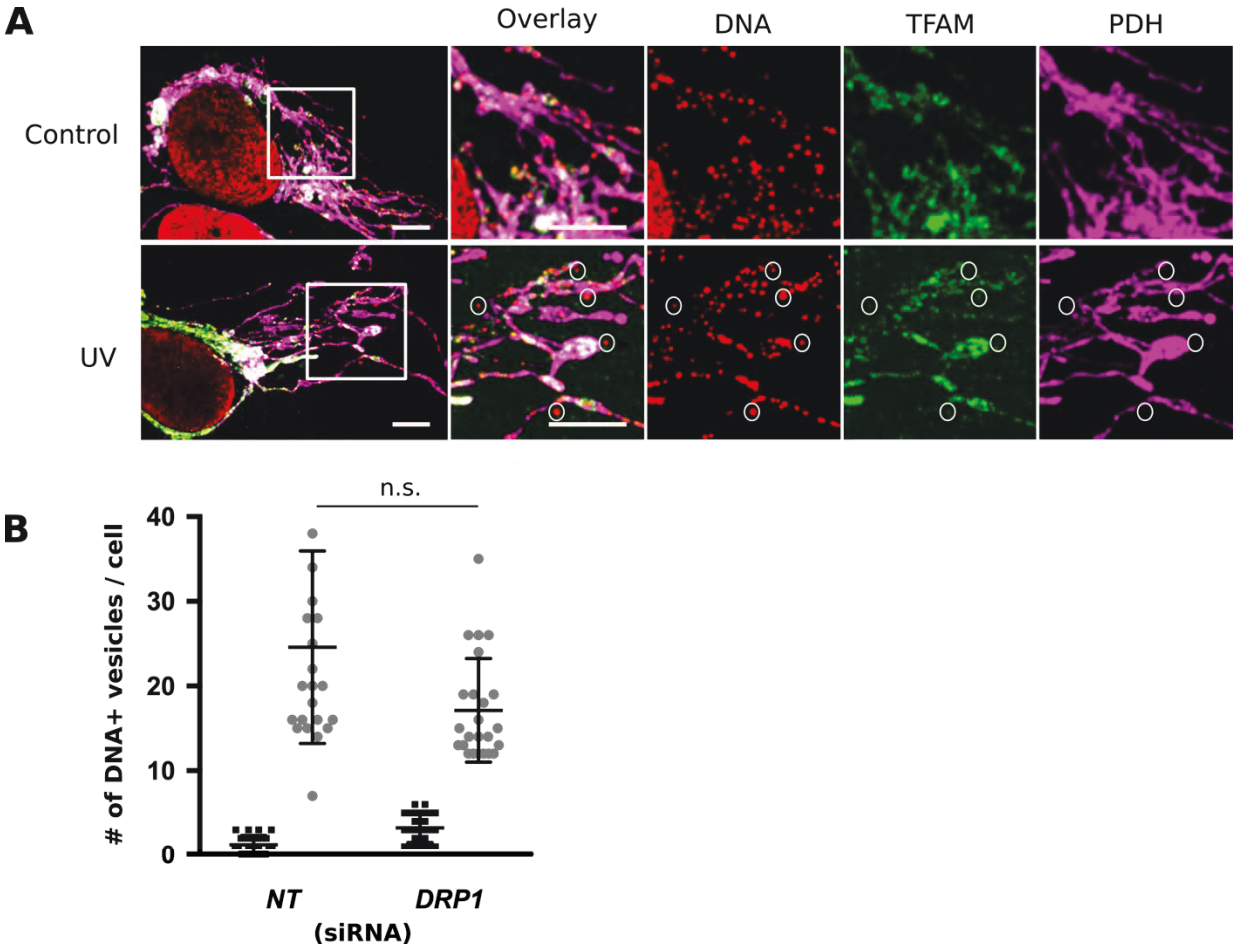

Figure 4.10. UV-induced vesicles are independent of DRP1

(A) Human fibroblasts were transfected twice with DRP1 siRNA over 3 days, cells were plated on coverslips, untreated or exposed to 400 J/m^2 UV, and left for recovery for 1 hour. Cells were fixed and immune-stained as indicated. Scale bars: first column 5µm, second column 10µm. **(B)** Vesicle count after *DRP1* (*DNM1L*) knock-down compared to non-targeting siRNA (*NT*) and UV exposure. Black squares: non-treated, Grey circles: UV-exposed. Bars represent mean ± SD (*n* = 25 cells per condition in 2 experiments). n.s., nonsignificant.

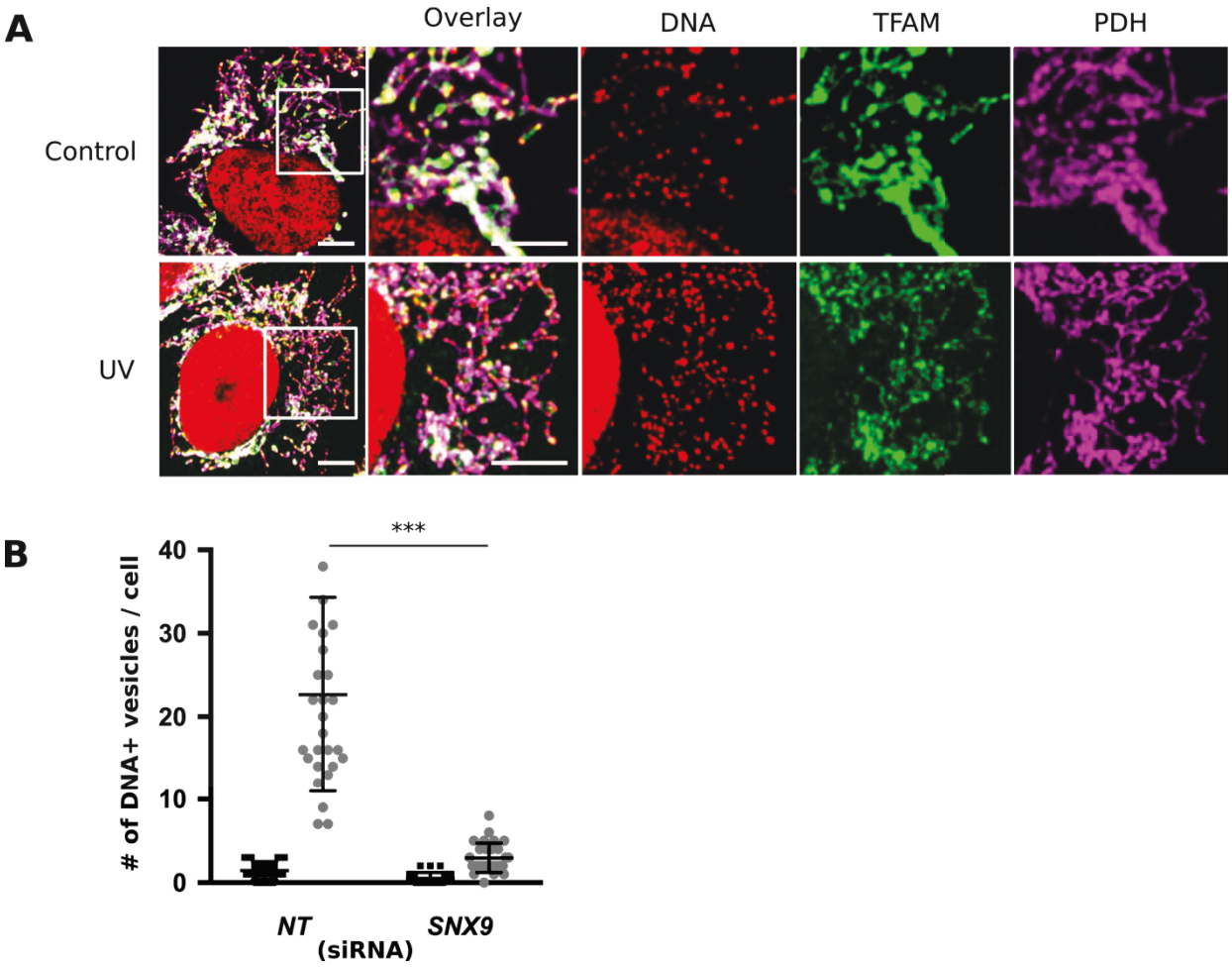

Figure 4.11. SNX9 is part of the machinery for UV-induced mtDNA containing MDVs

(A) Human fibroblasts were transfected twice with SNX9 siRNA over 3 days, cells were plated on coverslips, untreated or exposed to 400 J/m^2 UV, and left for recovery for 1 hour. Cells were fixed and immune-stained as indicated. Scale bars: first column 5µm, second column 10µm. **(B)** Vesicle count after *SNX9* knock-down compared to non-targeting siRNA (*NT*) followed by UV exposure. Black squares: non-treated, Grey circles: UV-exposed. Bars represent mean ± SD (n = 34 cells per condition in 2 experiments). ***P < 0.001.

4.2.3 Floatation of MDVs

To examine other cargoes that may be incorporated into MDVs in the context of UV treatment, MDVs were isolated by differential centrifugation and floated on a sucrose density gradient by centrifugation. This method allows to separate vesicles from any broken structures, which remain at the bottom of the gradient (Soubannier, Rippstein, et al. 2012). Human osteosarcoma 143B cells were left untreated or were treated with 400J/m^2 UV, harvested and broken with a dounce homogenizer. First, vesicles were separated from nuclei, intact mitochondria and other intracellular organelles by differential centrifugation. Then, the MDV-containing supernatant was adjusted to 50% sucrose and loaded at the bottom of a discontinuous sucrose step-gradient. Lysosomal-associated membrane protein 1 (LAMP1), which has been shown to be present in vesicles of the endo-lysosomal pathway (Szymanski et al. 2011; Humphries et al. 2011), as well as clathrin heavy chain (CHC), playing a major role in the formation of the coated vesicles involved in vesicular transport between organelles in the post-Golgi network connecting the trans-Golgi network, endosomes, lysosomes and the cell membrane (Robinson 2015), were used as positive controls for the fractionation of vesicles. Indeed, we detect LAMP1- and CHC-positive vesicles in the untreated cells, as well as in the UV-exposed cells where they get enriched and peak at 20% and the 20-30% interface respectively. Interestingly, the amount of LAMP1- and CHC-positive vesicles is increased after UV treatment, suggesting a general increase of the cellular vesicular transport under stress (**Fig. 4.12**).

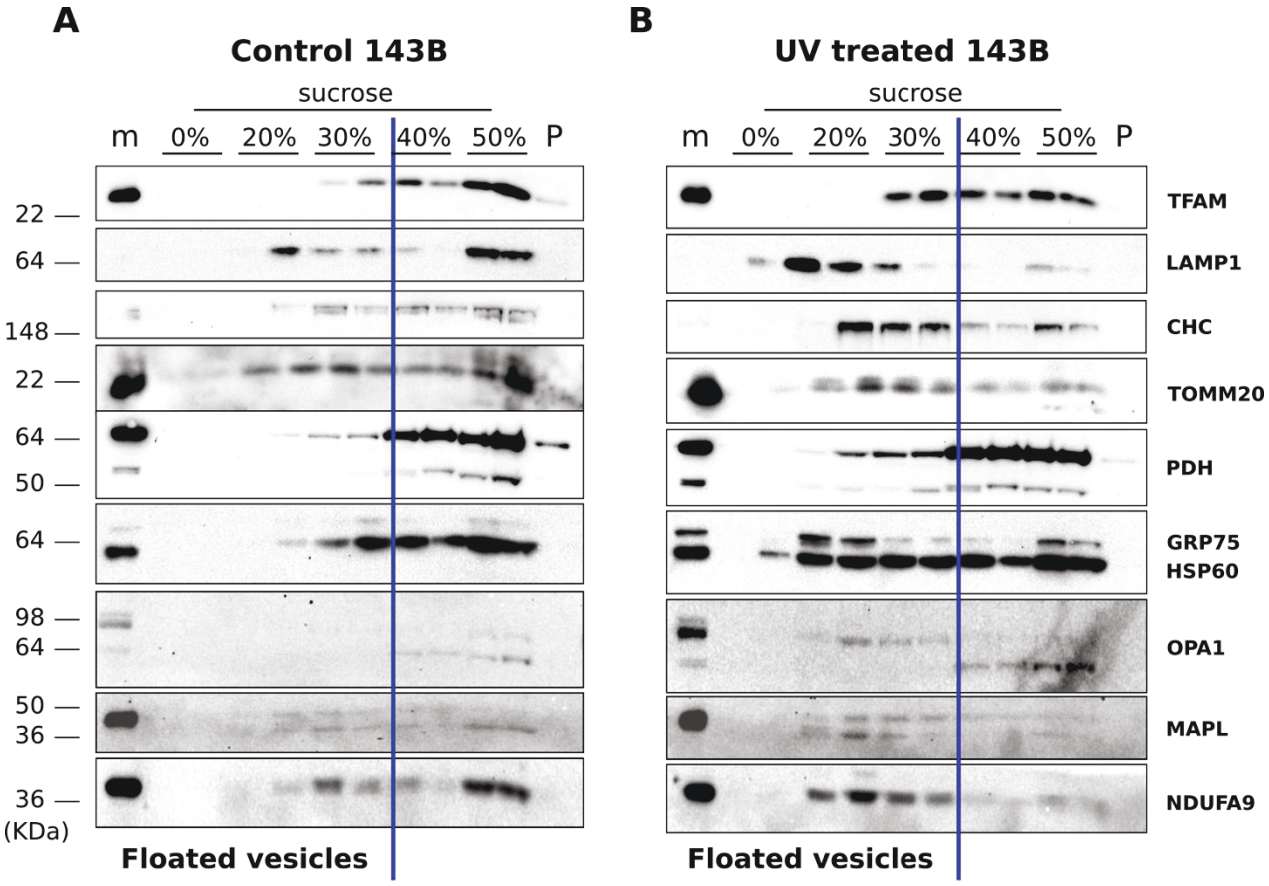

Figure 4.12. Numerous types of vesicles released upon UV exposure

143B cells were left untreated **(A)** or exposed to 400 J/m2 UV **(B)** and left to recover for 1 hour. Cells were scraped, broken using a homogenizer and spun at different speeds to remove unbroken cells, nuclei and debris, mitochondria and other intracellular organelles. Supernatants were loaded at the bottom of a discontinuous sucrose gradient and spun at 100 000 g for 6 hours. Fractions were collected, ran on SDS-PAGE and immunoblotted as indicated. m: mitochondria, P: pellet.

We observe that several types of mitochondria-derived vesicles are released in untreated cells (**Fig. 4.12A**). For example, the outer mitochondrial membrane TOMM20, which had been described previously as a cargo for MDVs (Soubannier, Rippstein, et al. 2012), is observed in the untreated but also in the UV-treated fractions, peaking around the 20-30% interface. Other

mitochondrial proteins such as TFAM, HSP60, MAPL and complex I NDUFA9 are also observed at low levels in the 30% fractions of untreated cells (**Fig. 4.12A**). In the UV-exposed cells, we observe an enrichment and shifting of TFAM towards the 20-30% interface, consistent with the immunofluorescence experiments (**Fig. 4.9B, 4.12B**). Other mitochondrial proteins including PDH, GRP75, HSP60, the higher form of the fusion protein OPA1, MAPL and complex I NDUFA9 are enriched in the lighter fractions (**Fig. 4.12B)**. Altogether, these data suggest that UV treatment leads to the release of a wide variety of MDVs with different cargoes.

4.2.4 Detection of mtDNA in the cytosol by PCR

Quantitative PCR has been used previously to detect the release of mtDNA in the cytosol, showing specificity for the D-loop region of the mitochondrial genome (West et al. 2015); however, other studies did not see any specific enrichment for mtDNA sequences in the cytosol (White et al. 2014; Rongvaux et al. 2014). To unravel if mtDNA can be detected in floated MDV fractions, portion of each fraction from the flotation experiment shown in **Figure 4.12** were used to isolate DNA and the presence of mtDNA was analyzed by performing PCR using primer pairs for different mitochondrial genes including the *D-loop* region (2 different sets of primers), the complex I NADH dehydrogenase subunit 4 (*ND4*) and Cytochrome b (*CYTB*). Surprisingly, PCR detects each of the mitochondrial genes tested in all fractions, in both untreated and UV treated cells (**Fig. 4.13**). These data indicate that PCR has to be used very carefully in assessing the release of mtDNA in the cytosol, since any break of cells at any step of the procedure will lead to the release of mitochondrial content in the supernatant.

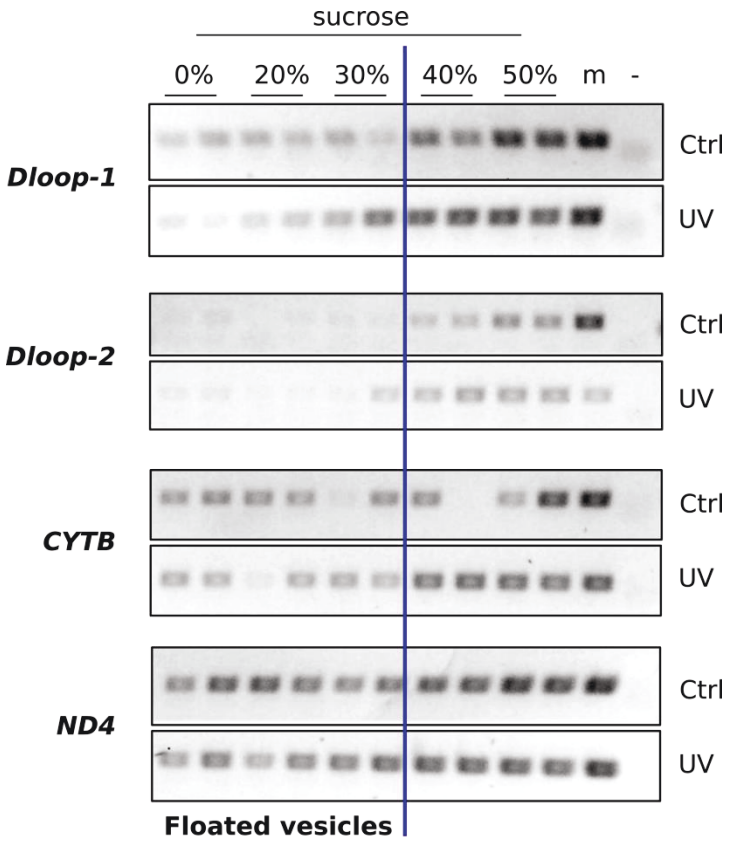

Figure 4.13. mtDNA detection by PCR

A portion of the fractions obtained in Figure 4.9 were used to extract DNA using QIAGEN DNA isolation kit. PCR was used to assess the presence of mtDNA. Four sets of primers were used for different mitochondrial genes including the *D-loop* region (2 different sets of primers), the complex I NADH dehydrogenase subunit 4 (*ND4*) and Cytochrome B (*CYTB*). m: mitochondria, -: PCR negative control.

4.2.5 Innate immune activation upon UV is dependent on SNX9 and mtDNA

UV light induces a wide spectrum of DNA damages, including cyclobutane pyrimidine dimers (CPDs), 8-oxo-7,8-dihydroguanine (8-oxoG), 6-4 photoproducts and single-strand breaks (Roy 2017). UV treatment has been shown to induce bulky CPD lesions in mtDNA (Pascucci et

al. 1997). In addition, UV light is well known to activate an inflammatory response through different pathways, including p38 MAPK, Jun N-terminal kinase, and NF-κB in skin cells (Clydesdale et al. 2001; Muthusamy & Piva 2010), and one study suggested that UV could potentiate the STING pathway (Kemp et al. 2015). The cGAS-STING signaling pathway participates in the sensing and activation of an immune response to mtDNA (West et al. 2015; White et al. 2014; Rongvaux et al. 2014). We therefore wanted to investigate whether UV exposure leads to activation of the cGAS-STING pathway through the release of mtDNA. To do this, human fibroblasts were exposed to UV light and the release of IL6 was measured by ELISA. A high induction of the cytokine IL6 is observed in control (*NT*) cells after UV treatment (**Fig. 4.14**). Silencing of *DRP1* or *MAVS* does not significantly affect the release of IL6 after UV treatment in comparison with IL6 released in UV-exposed *NT.* Since VPS35, a component of the retromer complex essential for the endosomal protein sorting machinery (Seaman et al. 1998), has been shown to mediate MDV transport (Braschi et al. 2010), we tested if its knock-down affected the release of IL6 following UV exposure. Although silencing of *VPS35* already leads to a significant decrease of IL6 in the non-treated cells (*VPS35* ctrl), the decrease in IL6 obtained upon UV exposure does not reach significance compared to UV-exposed *NT*. However, silencing of *SNX9* leads to a significant reduction of the IL6 released after UV treatment, compared with the UV-exposed *NT*, reinforcing a role for MDVs in this innate immune activation (**Fig. 4.14**).

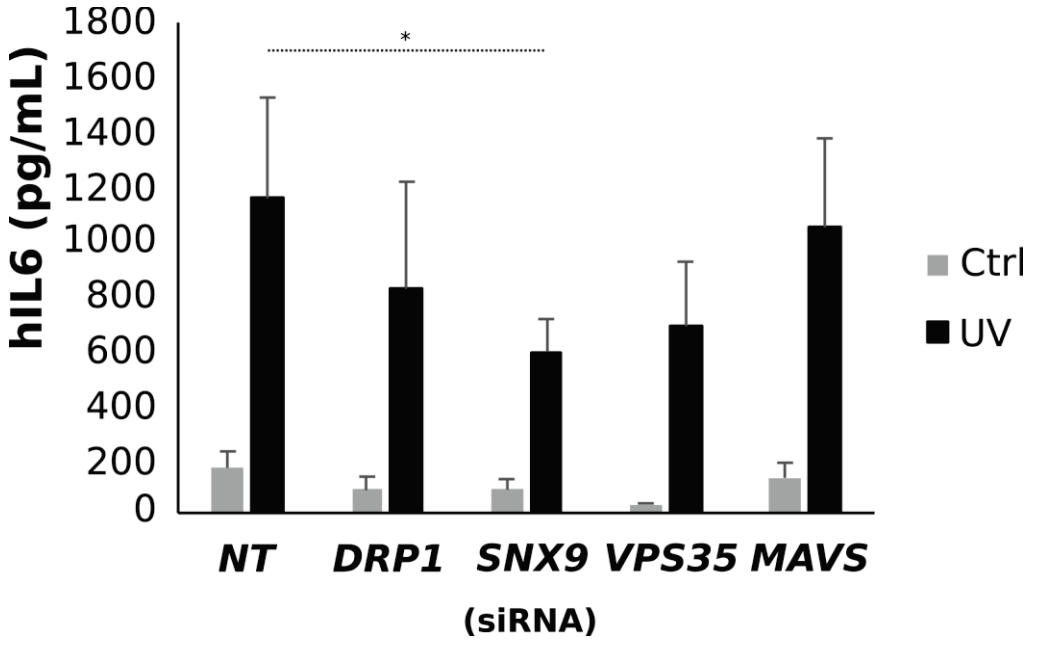

Figure 4.14. UV-induced immune response in human fibroblasts

Human fibroblasts were transfected twice with siRNA for *DRP1 (DNM1L)*, *SNX9*, *VPS35* and *MAVS* over 3 days. Cells were plated in 96 well plates, treated or not with 400 J/m^2 UV and supernatants were collected after 18 hours. hIL6 production was measured by ELISA. Values are reported as mean ± SD. **P*<0.05

In order to test if this immune response is dependent on mtDNA, we used 143B Rho0 cells, devoid of mitochondrial DNA (King & Attardi 1989), and exposed them to UV light. The 143B parental cell line was used as a positive control. We observe very low levels of released IL6 in Rho0 cells following UV treatment, suggesting a requirement for mtDNA in the activation of the innate response to UV (**Fig. 4.15**).

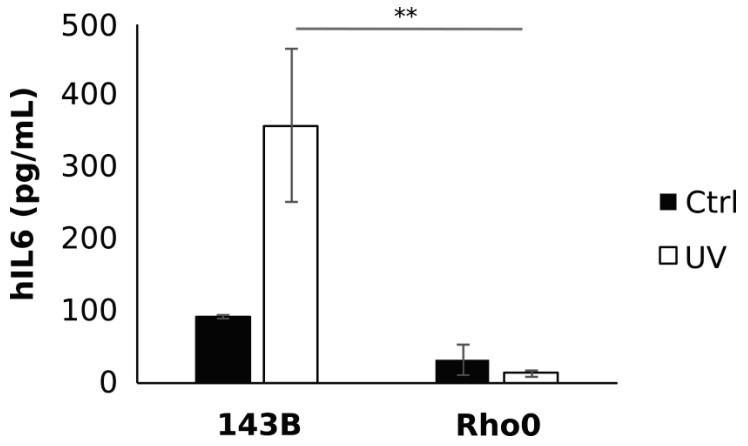

Figure 4.15. hIL6 release is dependent on mtDNA

Parental line 143B and Rho0 cells were left untreated or exposed to 400 J/m^2 UV. Supernatants were collected after 18 hours and hIL6 was measured by ELISA. Values are reported as mean ± SD. $^{**}P<0.01$.

4.2.6 cGAS is activated by UV exposure

To test whether this immune response is due to the activation of the cGAS pathway, *cGAS* was silenced by siRNA in human fibroblasts. After UV treatment, an ELISA assay was performed on supernatants to detect the release of IL6 and IFNβ. Knock down of *cGAS* results in an almost complete block of both IL6 and IFNβ release (**Fig. 4.16A, B**). In agreement with the role of cGAS in the activation of innate immunity to DNA, we also note a decreased production of both IL6 and IFNβ in untreated cells after knock-down of *cGAS*. Although MAPL has been shown to be required for regulating the dsDNA-induced STING-dependent innate immune response (Ni et al. 2017), silencing of MAPL does not impair the innate immune response following UV treatment (**Fig. 4.16A, B**). Altogether, these data demonstrate that UV light exposure leads to the release of mtDNA through MDVs and subsequently to the activation of the cGAS innate immune pathway.

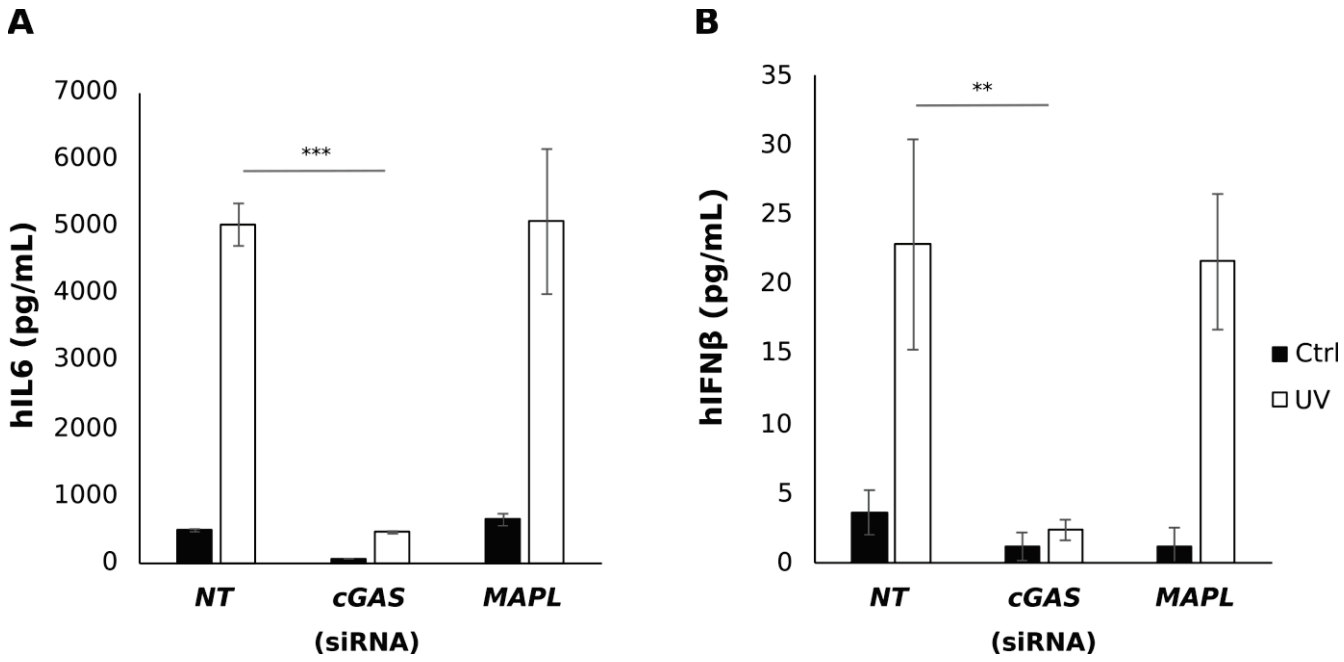

Figure 4.16. The UV-induced immune response is dependent on cGAS activation

Human fibroblasts were transfected twice with siRNA for *cGAS* (*MB21D1*) or *MAPL* (*MUL1*) over 3 days. Cells were plated in 96 wells, exposed or not with 400 J/m^2 UV and supernatants were collected after 18 hours. hIL6 and hIFNβ were measured in supernatants by ELISA. Values are reported as mean ± SD. **P<0.01 and ***P < 0.001.

Chapter 5: Discussion and Future Directions

5.1 MAPL is the SUMO E3 ligase for RIG-I and is required for the antiviral response to dsRNA virus

Recent evidences position mitochondria at the heart of immunity, as key intracellular signaling platforms regulating innate immune and inflammatory responses. Numerous mitochondrial proteins as well as mtROS have emerged as crucial actors orchestrating the innate immune response to pathogens and danger signals. Accordingly, mitochondria have been involved in the innate immune signaling of different classes of PRRs such as TLR, NLR and RLR (**Fig. 1.1**).

RIG-I is a cytosolic receptor of the RLR family, essential for the sensing of dsRNA viruses (Wu & Chen 2014). In the cytosol, RIG-I is in a closed auto-repressed conformation (Kowalinski et al. 2011). Upon sensing of dsRNA, RIG-I goes through a change of conformation exposing the CARD domains required to bind the adaptor MAVS at mitochondria, leading to MAVS assembly into prion-like aggregates (Hou et al. 2011) and signaling for the activation of IRF3/7 and NF-κB, resulting in the production of type I interferons and inflammatory cytokines respectively (Goubau et al. 2013; Ramos & Gale 2011).

The activation of the RIG-I signaling pathway is known to involve a multitude of post-translational modifications, including phosphorylation, ubiquitination and SUMOylation. We identify a requirement for the mitochondrial SUMO E3 ligase MAPL in the activation of RIG-I. The absence of MAPL prevents the activation of the antiviral transcriptional response, leading to an enhanced viral growth, and an increased susceptibility to Sendai virus infection.

It was suggested that RLR signaling requires mitochondrial fusion to be efficient, and induction of mitochondrial hyperfusion itself was shown to activate NF-κB, in a MAPL (MUL1)-dependent manner (Zemirli et al. 2014). The hyperfusion of the mitochondrial network would then

facilitate mitochondria-ER contacts required for signal transduction (Castanier et al. 2010; Ishikawa & Barber 2008; B. Zhong et al. 2008). Whether there may be functions in addition to the binding of MAVS and STING at the mitochondria-ER interface remains enigmatic, as is the functional contribution of mitochondrial hyperfusion. Contact sites may reflect a requirement for a rapid change in lipid composition within the outer membrane to help stabilize a signalling platform, or perhaps transient calcium pulses may help remodel the cristae to alter metabolism in some way. However, these contacts do not appear to drive mitochondrial division since the general morphology remains hyperfused during infection. Fused mitochondria are resistant to cell death, and this aspect of the response to infection may be mediated by the virus to ensure host survival.

Related to these potential functions of mitochondria-ER contact sites, MAPL was previously shown to stabilize mitochondria-ER contact sites through SUMOylation of DRP1 during apoptosis (Prudent et al. 2015). In cell death, the stabilized contacts were essential for sustained calcium flux and cristae remodelling required to release cytochrome c from the intercristal spaces. The ultimate fragmentation observed during cell death appeared to be a secondary consequence of the stabilized DRP1-mediated mitochondria-ER contact sites.

5.1.1 BioID for the investigation of the functional role of MAPL during antiviral response

Given the roles of MAPL in regulating mitochondrial dynamics, we had perhaps expected the viral-induced changes in MAPL interactors to include the fission or fusion machinery. Although the BioID results confirm a direct relationship between MAPL and other fission machinery proteins, these interactions are unaffected upon Sendai virus infection, suggesting that the contribution of MAPL to the anti-viral response is not related to morphological transitions.

In uninfected cells, MAPL interacts with MAVS, however this interaction decreases during Sendai virus infection, when we rather observe an interaction of MAPL with RIG-I. The interaction of MAPL with MAVS at steady-state may be required simply for MAPL to be available in close proximity in case of viral insult which requires RIG-I activation and its subsequent binding to MAVS. We did not detect any SUMOylation of MAVS by MAPL in the early phase of infection, but it is still possible that MAPL, and MAVS, are involved in the regulation at a later stage of the antiviral signaling.

In fact, the BioID experiment identifies a series of unexpected MAPL targets which act later in the antiviral response, particularly in the inhibition of viral assembly. IFIT1 and IFIT2 have been shown to play roles in binding viral mRNA and interfering with the translation of viral proteins (Reynaud et al. 2015), and IFIT1 is the strongest hit upon Sendai virus infection in the BioID. A previous study suggested that mitochondria may surround sites of viral replication (Onoguchi et al. 2010), and our data suggest a role for MAPL in the downstream events of the innate immune response as well. It is unknown whether MAVS acts in the late phase of viral infection, but it is tempting to speculate that both MAPL and MAVS might have a role to play in this late phase. Other antiviral response proteins are also identified such as the IFN-inducible oligoadenylate synthetase-like OASL (Zhu et al. 2014), HERC5, an E3 ligase mediating the conjugation of the ubiquitin-like protein ISG15 (Wong et al. 2006; Dastur et al. 2006), and STAT1, a transcription factor responsive to cytokines (Yu et al. 2009), highlighting a broader role for MAPL SUMOylation in the innate antiviral signaling.

However, since the loss of MAPL blocks the antiviral immune response at the level of RIG-I, it would be challenging to evaluate the functional requirements for MAPL in the downstream events. Future work will focus on the contribution of MAPL SUMOylation in the

antiviral activities of the additional interacting proteins identified with the BioID approach. We have currently opened the way for a systematic analysis of the interaction landscape that will provide important insights into the dynamic events accompanying the antiviral response.

5.1.2 MAPL SUMOylation of RIG-I

In cells expressing MAPL, we demonstrate that RIG-I is SUMOylated in a MAPL-dependent manner during Sendai virus infection. This is in agreement with the Sendai virus-specific interaction of MAPL with RIG-I, and consistent with a previous study showing RIG-I SUMOylation during infection (Mi et al. 2010; Hu et al. 2017). The fact that we do not observe any change in RIG-I protein stability in the absence of MAPL suggests that this modification is not involved in the regulation of protein stability or turnover. Plus, we show that MAPL is not required for signaling from a constitutively active form of RIG-I (ΔRIG-I). Altogether, these data indicate a role for SUMOylation in the conformational changes of RIG-I, leading to the exposition of the 2 CARD domains, which is required for binding the adaptor MAVS at the mitochondria (Feng et al. 2013) (**Fig. 5.1**). A sequence analysis of RIG-I reveals two conserved SUMO consensus sites, one within the helicase domain (mouse K626) and another in the C-terminus RNA binding domain (mouse K889). Conjugation at these sites may be involved in the generation of the "open" conformation of RIG-I and/or recognition of the dsRNA. Moreover, these sites lie outside of the CARD domains, consistent with the MAPL-independent activation of MAVS upon transfection of the constitutively active form of RIG-I.

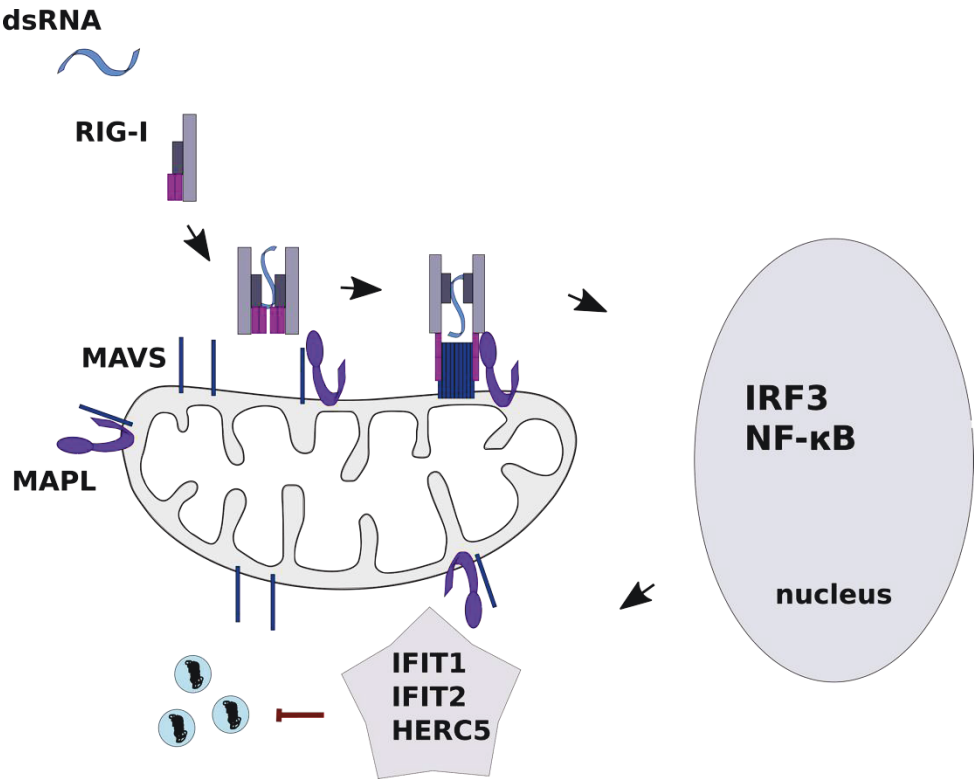

Figure 5.1 Model for RIG-I SUMOylation by MAPL and signaling at mitochondria.
Upon dsRNA recognition, RIG-I is SUMOylated by MAPL, changes its conformation and binds MAVS at mitochondria. MAVS assembles into prion-like aggregates and signals for IRF3 and NF-κB signaling.

Since the interaction between MAPL and MAVS is decreased upon infection with Sendai virus, MAPL is unlikely to be part of the MAVS signaling complex during the infection. As stated above, the steady-state interaction between MAPL and MAVS remains enigmatic and its function is unknown. Although the major role for MAVS is as a key mediator of the innate immune response upon viral infections, it has been shown to play a critical role during inflammasome activation (Subramanian et al. 2013), anti-bacterial responses (Buss et al. 2010), in the maintenance of intestinal homeostasis through sensing of commensal bacteria (X.-D. Li et al. 2011) and during apoptosis (Maadidi et al. 2014; Huang et al. 2014). Clearly MAVS acts upon various stresses, and

its binding to MAPL in uninfected cells might reflect a novel aspect of its many actions which requires further investigation.

Nonetheless, MAPL rather acts upstream of the assembly of the MAVS signalosome, and this is consistent with the previous evidence that SUMOylated RIG-I showed enhanced ubiquitination and interaction with the downstream adaptor MAVS (Mi et al. 2010). Interestingly MAPL is also targeted to peroxisomes in vesicular carriers from the mitochondria (Neuspiel et al. 2008; Braschi et al. 2010) and MAVS is also located on peroxisomes, where it is involved in an earlier antiviral cellular state (Dixit et al. 2010; Odendall et al. 2014). Although we have not dissected the specific contribution of MAPL within mitochondria and peroxisomes, we would speculate that its role is similar in both organelles.

We show that MAPL is required for the innate immune response, that it interacts and SUMOylates RIG-I upon infection, and that MAPL SUMOylation of RIG-I is required for the activation of RIG-I which leads to its interaction with MAVS and downstream signaling.

5.2 mtDNA is released via MDVs.

Recent evidence revealed that mtDNA is released in the cytosol and activates the innate immune response through the cGAS-STING signaling pathway (West et al. 2015; White et al. 2014; Rongvaux et al. 2014). However, it is still unclear how is mtDNA released in the cytosol. We demonstrate for the first time that mtDNA is released from mitochondria via MDVs.

5.2.1 UV exposure-induced DNA damage leads to mtDNA release via MDVs.

Accurate mtDNA maintenance is crucial for cell viability, but it is unclear how the cell deals with mtDNA damage. We demonstrate that mtDNA is released via vesicle-like structures in response to DNA damage triggered by exposure to UV. A previous study suggested that none of the known mitochondrial nucleases are involved in the degradation of damaged mtDNA, and that the DNA loss observed is not due to mitophagy, autophagy or apoptosis (Moretton et al. 2017). Our findings might represent a new pathway for the targeted degradation of mtDNA, which may be damaged or simply used as a signaling molecule, in a mitophagy and autophagy-independent manner. That mtDNA may act as a central signaling molecule in the immune response may have very long evolutionary origins (McBride 2018). As a proteobacteria, the earliest "mitochondria" may have shed their DNA in vesicles to deliver them within the colony, as seen in some of the vesicles derived from gram negative (and most gram positive) bacteria today. The use of DNA as a signaling molecule may therefore be at least one of the evolutionary driving forces for the current mitochondria to have retained their genomes rather than lose everything to the nucleus.

We show that these UV-induced vesicles are selective for their cargo, and that their formation is independent of the fission protein DRP1, which are the defining features of MDVs. We also identify a dependence for SNX9 in the formation of these MDVs, as previously published

for heat stress, LPS and oxidative stress-induced MDVs (Matheoud et al. 2016), thus identifying a piece of the machinery for our UV-induced DNA-positive MDVs. The presence of DNA-negative, TFAM-positive MDVs might reflect the fact that in these cases the DNA which is released is oxidized and impossible to detect with the DNA antibody used.

We show that UV not only induces the release of DNA-positive MDVs but also the release of numerous types of MDVs carrying different mitochondrial cargoes, as well as LAMP1- and CHC-positive vesicles, suggesting a broader cellular trafficking in response to the damage done by UV.

Along with immunofluorescence, quantitative PCR is the other technique used to assess mtDNA release in the cytosol (West et al. 2015; White et al. 2014; Rongvaux et al. 2014), one study suggesting an enrichment of mtDNA fragments containing the D-loop structure (origin of mtDNA replication) (West et al. 2015). We demonstrate that the use of PCR proves to be unsuitable for this purpose, since we detect every mitochondrial gene tested in all the fractions obtained, whether or not the cells are exposed to UV or not. We determine that it is extremely challenging to prevent and control for mitochondrial breakage during the fractionation process.

5.2.2 UV exposure and the immune response

UV exposure is known to activate the immune response, and we show that mtDNA is released via MDVs under this condition. We also demonstrate that UV exposure leads to immune activation through the production of IL6 and IFNβ, and that this response is dependent on the cytosolic DNA sensor cGAS. The DNA that activates cGAS appears to be derived from mitochondria since Rho0 cells do not elicit an immune response. One caveat to this may be that Rho0 cells are metabolically deficient, and a previous study has suggested that RLR antiviral

innate immunity requires oxidative phosphorylation activity (Yoshizumi et al. 2017). Overall these data suggest that either 1) the mtDNA observed within MDVs ultimately ends up in the cytosol, or 2) there are additional channels within mitochondria that may be competent to export mtDNA, either fragmented or whole.

There are a number of arguments that support the requirement for mtDNA within MDVs as a central intermediate in cGAS activation. First, we show that silencing *DRP1* has no effect on the number of DNA+ MDVs or IL6 production. However, silencing *SNX9* leads to the release of less DNA+ MDVs and also to a decreased production in IL6, hinting for an immune activation triggered by the release of mtDNA via MDVs.

5.2.3 A mechanism for the release of mtDNA from MDVs.

A crucial question remains: How is mtDNA released from MDVs to the cytosol where it can activate the cGAS pathway? One of the possibilities is that mtDNA containing MDVs would be delivered into a late endosome/multivesicular body which offers the possibility of back-fusion (Abrami et al. 2004) (**Fig. 5.2**). This would directly release the mtDNA into the cytosol where it could be recognized by cGAS (Wu & Chen 2014). Another possibility is that mtDNA may be released via the action of a pore-forming protein such as Gasdermin D (GSDMD) or Mixed Lineage Kinase domain-like protein (MLKL), which could form pores into MDV membranes to release their content in the cytosol (**Fig. 5.2**). A confounding factor in this model is that there would still be two membranes to cross before the mtDNA could get out of the vesicle. Therefore, it is also possible that the pores may form within the late endosome/lysosome after fusion of the MDV with these organelles. Permeabilization of the lysosome was recently seen as a mechanism for peptides to exit the lysosome transport into the ER for presentation on MHC-I (Ziegler et al.

2018). Perhaps this "permeabilization" could be mediated by cardiolipin (CL) specific pore forming proteins upon delivery of MDVs.

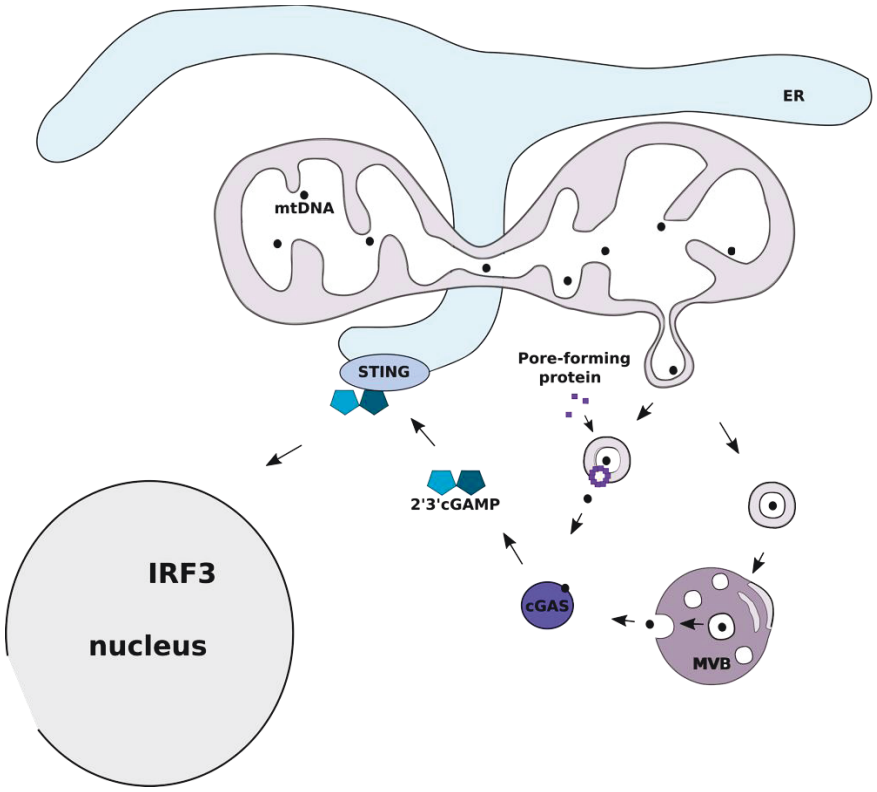

Figure 5.2 Model for the release of mtDNA from MDVs.

One possibility is that mtDNA containing MDVs might be delivered into a late endosome/multivesicular body (MVB) which offers the possibility of back-fusion. A second possibility is that mtDNA may be released via the action of a pore-forming protein. mtDNA released into cytosol can bind cGAS and activate the following signaling cascade.

Gasdermin D (GSDMD) exhibits a bactericidal activity, where its binding to CL leads to the formation of pores in bacterial membranes. GSDMD is also known to be responsible for the extracellular release of IL1β upon inflammasome activation, by forming pores in the cell plasma membrane (X. Liu et al. 2016). In this case, Gasdermin D is cleaved by caspase-1 into an amino-terminal pore-forming domain which inserts into the cellular membrane where it oligomerizes to form pores, resulting in the release of IL1β and a rapid lytic cell death named pyroptosis (J. Shi et al. 2015; X. Liu et al. 2016). MLKL forms a necrosis signaling complex named necrosome with RIP1 and RIP3 kinases (L. Sun et al. 2012). Phosphorylation of MLKL by RIP3 leads to the formation of MLKL oligomers which bind phosphatidylinositol lipids and CL, allowing its translocation to the plasma and intracellular membranes, where it directly disrupts membrane integrity, resulting in necroptosis (H. Wang et al. 2014). Interestingly, both of these pore-forming proteins have an affinity for CL. In mammalian cells, CL is almost exclusively found in the mitochondrial inner membrane. It would be very interesting to test whether mtDNA containing MDVs are enriched in CL and whether either of these pore-forming proteins might be involved in the release of mtDNA in the cytosol.

Altogether we demonstrate that mtDNA is released via MDVs upon DNA damage induction by UV exposure, and that this leads to an innate immune activation which is independent of DRP1, but dependent on SNX9 and cGAS.

5.3 Conclusion

Firstly, this thesis demonstrates a crucial role of SUMOylation by MAPL in the antiviral signaling pathway, as an essential mitochondrial protein for the innate immune response to dsRNA virus infection. In addition, the BioID approach establishes a systematic analysis of the interaction landscape of MAPL, providing important insights into the dynamic events occurring at the surface of mitochondria during the antiviral response.

Secondly, this thesis demonstrates for the first time mtDNA as a cargo of MDVs and underlines the importance of this pathway in the activation of the innate immune DNA sensor. The mtDNA release observed uses core proteins previously identified for the generation of vesicles, and leads to the activation of innate cGAS-STING pathway.

In conclusion, this thesis highlights two distinct contributions of mitochondria to innate immunity; as a signaling platform for the signaling of the RIG-I/MAVS pathway, and as a direct activator of the cytosolic DNA sensor cGAS.

Bibliography

Aanen, D.K., Spelbrink, J.N. & Beekman, M., 2014. What cost mitochondria? The maintenance of functional mitochondrial DNA within and across generations. *Philosophical transactions of the Royal Society of London. Series B, Biological sciences*, 369(1646), p.20130438.

Abrami, L. et al., 2004. Membrane insertion of anthrax protective antigen and cytoplasmic delivery of lethal factor occur at different stages of the endocytic pathway. *The Journal of Cell Biology*, 166(5), pp.645–651.

Agostini, L. et al., 2004. NALP3 forms an IL-1beta-processing inflammasome with increased activity in Muckle-Wells autoinflammatory disorder. *Immunity*, 20(3), pp.319–325.

Aguirre, S. & Fernandez-Sesma, A., 2017. Collateral Damage during Dengue Virus Infection: Making Sense of DNA by cGAS. M. U. Gack, ed. *Journal of Virology*, 91(14), pp.e01081–16.

Akira, S., Uematsu, S. & Takeuchi, O., 2006. Pathogen Recognition and Innate Immunity. *Cell*, 124(4), pp.783–801.

Alexeyev, M. et al., 2013. The Maintenance of Mitochondrial DNA Integrity--Critical Analysis and Update. *Cold Spring Harbor Perspectives in Biology*, 5(5), pp.a012641–a012641.

Archibald, J.M., 2015. Endosymbiosis and Eukaryotic Cell Evolution. *Current biology : CB*, 25(19), pp.R911–21.

Baker, P.J. et al., 2017. Posttranslational Modification as a Critical Determinant of Cytoplasmic Innate Immune Recognition. *Physiological reviews*, 97(3), pp.1165–1209.

Beltrao, P. et al., 2013. Evolution and functional cross-talk of protein post-translational modifications. *Molecular systems biology*, 9, p.714.

Boyapati, R.K. et al., 2017. Advances in the understanding of mitochondrial DNA as a pathogenic factor in inflammatory diseases. *F1000Research*, 6, p.169.

Braschi, Emelie & McBride, H.M., 2010. Mitochondria and the culture of the Borg: understanding the integration of mitochondrial function within the reticulum, the cell, and the organism. *BioEssays*, 32(11), pp.958–966.

Braschi, Emelie et al., 2010. Vps35 Mediates Vesicle Transport between the Mitochondriaand Peroxisomes. *Current Biology*, 20(14), pp.1310–1315.

Braschi, Emelie, Zunino, R. & McBride, H.M., 2009. MAPL is a new mitochondrial SUMO E3 ligase that regulates mitochondrial fission. *EMBO reports*, 10(7), pp.748–754.

Bruderer, R. et al., 2011. Purification and identification of endogenous polySUMO conjugates. *EMBO reports*, 12(2), pp.142–148.

Buss, C. et al., 2010. Essential role of mitochondrial antiviral signaling, IFN regulatory factor (IRF)3, and IRF7 in Chlamydophila pneumoniae-mediated IFN-beta response and control of bacterial replication in human endothelial cells. *Journal of immunology (Baltimore, Md. : 1950)*, 184(6), pp.3072–3078.

Caielli, S. et al., 2016. Oxidized mitochondrial nucleoids released by neutrophils drive type I interferon production in human lupus. *The Journal of Experimental Medicine*, 213(5), pp.697–713.

Castanier, C. et al., 2010. Mitochondrial dynamics regulate the RIG-I-like receptor antiviral pathway. *EMBO reports*, 11(2), pp.133–138.

Cha, M.-Y., Kim, D.K. & Mook-Jung, I., 2015. The role of mitochondrial DNA mutation on neurodegenerative diseases. *Experimental & Molecular Medicine*, 47(3), pp.e150–8.

Chakrabarty, S. et al., 2014. Upregulation of TFAM and mitochondria copy number in human lymphoblastoid cells. *Mitochondrion*, 15(C), pp.52–58.

Clydesdale, G.J., Dandie, G.W. & Muller, H.K., 2001. Ultraviolet light induced injury: immunological and inflammatory effects. *Immunology and cell biology*, 79(6), pp.547–568.

Coyaud, E. et al., 2015. BioID-based Identification of Skp Cullin F-box (SCF)beta-TrCP1/2 E3 Ligase Substrates. *Molecular & cellular proteomics: MCP*, 14(7), pp.1781–1795.

Dahlgren, C. et al., 2016. Basic characteristics of the neutrophil receptors that recognize formylated peptides, a danger-associated molecular pattern generated by bacteria and mitochondria. *Biochemical Pharmacology*, 114(C), pp.22–39.

Dastur, A. et al., 2006. Herc5, an interferon-induced HECT E3 enzyme, is required for conjugation of ISG15 in human cells. *Journal of Biological Chemistry*, 281(7), pp.4334–4338.

Deretic, V. & Levine, B., 2018. Autophagy balances inflammation in innate immunity. *Autophagy*, 14(2), pp.243–251.

Deribe, Y.L., Pawson, T. & Dikic, I., 2010. Post-translational modifications in signal integration. *Nature structural & molecular biology*, 17(6), pp.666–672.

Dickey, A.S. & Strack, S., 2011. PKA/AKAP1 and PP2A/Bbeta2 regulate neuronal morphogenesis via Drp1 phosphorylation and mitochondrial bioenergetics. *The Journal of neuroscience: the official journal of the Society for Neuroscience*, 31(44), pp.15716–15726.

Dixit, E. et al., 2010. Peroxisomes are signaling platforms for antiviral innate immunity. *Cell*, 141(4), pp.668–681.

Ekstrand, M.I., 2004. Mitochondrial transcription factor A regulates mtDNA copy number in mammals. *Human Molecular Genetics*, 13(9), pp.935–944.

Elliott, E.I. et al., 2018. Cutting Edge: Mitochondrial Assembly of the NLRP3 Inflammasome Complex Is Initiated at Priming. *The Journal of Immunology*, pp.3047–3052.

Feng, M. et al., 2013. Structural and biochemical studies of RIG-I antiviral signaling. *Protein & cell*, 4(2), pp.142–154.

Fensterl, V. & Sen, G.C., 2015. Interferon-induced Ifit proteins: their role in viral pathogenesis. *Journal of Virology*, 89(5), pp.2462–2468.

Flotho, A. & Melchior, F., 2013. Sumoylation: a regulatory protein modification in health and disease. *Annual review of biochemistry*, 82, pp.357–385.

Forrester, S.J. et al., 2018. Reactive Oxygen Species in Metabolic and Inflammatory Signaling. *Circulation research*, 122(6), pp.877–902.

Fu, J. et al., 2011. MDA5 is SUMOylated by PIAS2beta in the upregulation of type I interferon signaling. *Molecular immunology*, 48(4), pp.415–422.

Gandre-Babbe, S. & van der Bliek, A.M., 2008. The novel tail-anchored membrane protein Mff controls mitochondrial and peroxisomal fission in mammalian cells. *Molecular biology of the cell*, 19(6), pp.2402–2412.

Georgieva, E. et al., 2017. Mitochondrial Dysfunction and Redox Imbalance as a Diagnostic Marker of "Free Radical Diseases." *Anticancer Research*, 37(10), pp.1–9.

Gilkerson, R.W., 2009. Mitochondrial DNA nucleoids determine mitochondrial genetics and dysfunction. *The International Journal of Biochemistry & Cell Biology*, 41(10), pp.1899–1906.

Goubau, D., Deddouche, S. & Sousa, C.R.E., 2013. Cytosolic Sensing of Viruses. *Immunity*, 38(5), pp.855–869.

Granatiero, V., De Stefani, D. & Rizzuto, R., 2017. Mitochondrial Calcium Handling in Physiology and Disease. *Advances in experimental medicine and biology*, 982, pp.25–47.

Grazioli, S. & Pugin, J., 2018. Mitochondrial Damage-Associated Molecular Patterns: From Inflammatory Signaling to Human Diseases. *Frontiers in Immunology*, 9, pp.301–17.

Gringhuis, S.I. et al., 2017. HIV-1 blocks the signaling adaptor MAVS to evade antiviral host defense after sensing of abortive HIV-1 RNA by the host helicase DDX3. *Nature Immunology*, 18(2), pp.225–235.

Gupta, G.D. et al., 2015. A Dynamic Protein Interaction Landscape of the Human Centrosome-Cilium Interface. *Cell*, 163(6), pp.1484–1499.

Hay, R.T., 2013. Decoding the SUMO signal. *Biochemical Society transactions*, 41(2), pp.463–473.

Hemmi, H. et al., 2000. A Toll-like receptor recognizes bacterial DNA. *Nature*, 408(6813), pp.740–745.

Hickey, C.M., Wilson, N.R. & Hochstrasser, M., 2012. Function and regulation of SUMO proteases. *Nature Reviews Molecular Cell Biology*, 13(12), pp.755–766.

Hou, F. et al., 2011. MAVS forms functional prion-like aggregates to activate and propagate antiviral innate immune response. *Cell*, 146(3), pp.448–461.

Hu, M.-M. et al., 2017. Innate immunity to RNA virus is regulated by temporal and reversible sumoylation of RIG-I and MDA5. *The Journal of Experimental Medicine*, 214(4), pp.973–989.

Huang, Y. et al., 2014. MAVS-MKK7-JNK2 defines a novel apoptotic signaling pathway during viral infection. *PLOS Pathogens*, 10(3), p.e1004020.

Humphries, W.H.4., Szymanski, C.J. & Payne, C.K., 2011. Endo-lysosomal vesicles positive for Rab7 and LAMP1 are terminal vesicles for the transport of dextran. S. H. Caplan, ed. *PLoS ONE*, 6(10), p.e26626.

Hunter, T., 2007. The age of crosstalk: phosphorylation, ubiquitination, and beyond. *Molecular Cell*, 28(5), pp.730–738.

Ikeda, M. et al., 2015. Overexpression of TFAM or Twinkle Increases mtDNA Copy Number and Facilitates Cardioprotection Associated with Limited Mitochondrial Oxidative Stress J. Sadoshima, ed. *PLoS ONE*, 10(3), pp.e0119687–19.

Ingelsson, B. et al., 2018. Lymphocytes eject interferogenic mitochondrial DNA webs in response to CpG and non-CpG oligodeoxynucleotides of class C. *Proceedings of the National Academy of Sciences*, 115(3), pp.E478–E487.

Ishikawa, H. & Barber, G.N., 2008. STING is an endoplasmic reticulum adaptor that facilitates innate immune signalling. *Nature*, 455(7213), pp.674–678.

Iwamura, T. et al., 2001. Induction of IRF-3/-7 kinase and NF-kappaB in response to double-stranded RNA and virus infection: common and unique pathways. *Genes to cells : devoted to molecular & cellular mechanisms*, 6(4), pp.375–388.

Iyer, S.S. et al., 2013. Mitochondrial Cardiolipin Is Required for Nlrp3 Inflammasome Activation. *Immunity*, 39(2), pp.311–323.

Jacobs, J.L. et al., 2014. Regulation of mitochondrial antiviral signaling (MAVS) expression and signaling by the mitochondria-associated endoplasmic reticulum membrane (MAM) protein Gp78. *Journal of Biological Chemistry*, 289(3), pp.1604–1616.

Jenkins, K. et al., 2013. Mitochondrially localised MUL1 is a novel modulator of antiviral signaling. *Immunology and cell biology*, 91(4), pp.321–330.

Ji, W.-K. et al., 2015. Actin filaments target the oligomeric maturation of the dynamin GTPase Drp1 to mitochondrial fission sites. *eLife*, 4, p.e11553.

Kato, H. et al., 2005. Cell type-specific involvement of RIG-I in antiviral response. *Immunity*, 23(1), pp.19–28.

Kawai, T. & Akira, S., 2009. The roles of TLRs, RLRs and NLRs in pathogen recognition. *International Immunology*, 21(4), pp.317–337.

Kawai, T. et al., 2005. IPS-1, an adaptor triggering RIG-I- and Mda5-mediated type I interferon induction. *Nature Immunology*, 6(10), pp.981–988.

Kemp, M.G., Lindsey-Boltz, L.A. & Sancar, A., 2015. UV Light Potentiates STING (Stimulator of Interferon Genes)-dependent Innate Immune Signaling through Deregulation of ULK1 (Unc51-like Kinase 1). *Journal of Biological Chemistry*, 290(19), pp.12184–12194.

Kim, H. et al., 2011. Fine-tuning of Drp1/Fis1 availability by AKAP121/Siah2 regulates mitochondrial adaptation to hypoxia. *Molecular Cell*, 44(4), pp.532–544.

King, M.P. & Attardi, G., 1989. Human cells lacking mtDNA: repopulation with exogenous mitochondria by complementation. *Science*, 246(4929), pp.500–503.

Korobova, F., Ramabhadran, V. & Higgs, H.N., 2013. An actin-dependent step in mitochondrial fission mediated by the ER-associated formin INF2. *Science*, 339(6118), pp.464–467.

Kowalinski, E. et al., 2011. Structural basis for the activation of innate immune pattern-recognition receptor RIG-I by viral RNA. *Cell*, 147(2), pp.423–435.

Krysko, D.V. et al., 2011. Emerging role of damage-associated molecular patterns derived from mitochondria in inflammation. *Trends in Immunology*, 32(4), pp.157–164.

Kubota, T. et al., 2008. Virus infection triggers SUMOylation of IRF3 and IRF7, leading to the negative regulation of type I interferon gene expression. *Journal of Biological Chemistry*, 283(37), pp.25660–25670.

Kukat, C. & Larsson, N.-G., 2013. mtDNA makes a U-turn for the mitochondrial nucleoid. *Trends in cell biology*, 23(9), pp.457–463.

Kukat, C. et al., 2015. Cross-strand binding of TFAM to a single mtDNA molecule forms the mitochondrial nucleoid. *Proceedings of the National Academy of Sciences of the United States of America*, 112(36), pp.11288–11293.

Lamoliatte, F. et al., 2014. Large-scale analysis of lysine SUMOylation by SUMO remnant immunoaffinity profiling. *Nature communications*, 5, p.5409.

Lamoliatte, F. et al., 2013. Targeted identification of SUMOylation sites in human proteins using affinity enrichment and paralog-specific reporter ions. *Molecular & cellular proteomics : MCP*, 12(9), pp.2536–2550.

Lamoliatte, F. et al., 2017. Uncovering the SUMOylation and ubiquitylation crosstalk in human cells using sequential peptide immunopurification. *Nature communications*, 8, p.14109.

Landrigan, A., Wong, M.T. & Utz, P.J., 2011. CpG and non-CpG oligodeoxynucleotides directly costimulate mouse and human CD4+ T cells through a TLR9- and MyD88-independent mechanism. *Journal of immunology (Baltimore, Md. : 1950)*, 187(6), pp.3033–3043.

Larsson, N.G. et al., 1998. Mitochondrial transcription factor A is necessary for mtDNA maintenance and embryogenesis in mice. *Nature genetics*, 18(3), pp.231–236.

Li, W. et al., 2008. Genome-Wide and Functional Annotation of Human E3 Ubiquitin Ligases Identifies MULAN, a Mitochondrial E3 that Regulates the Organelle's Dynamics and Signaling. pp.1–14.

Li, X.-D. et al., 2011. Mitochondrial antiviral signaling protein (MAVS) monitors commensal bacteria and induces an immune response that prevents experimental colitis. *Proceedings of the National Academy of Sciences of the United States of America*, 108(42), pp.17390–17395.

Liang, C., Ahmad, K. & Sue, C.M., 2014. The broadening spectrum of mitochondrial disease: Shifts in the diagnostic paradigm. *BBA - General Subjects*, 1840(4), pp.1360–1367.

Liu, J., Qian, C. & Cao, X., 2016. Post-Translational Modification Control of Innate Immunity. *Immunity*, 45(1), pp.15–30.

Liu, R. & Chan, D.C., 2015. The mitochondrial fission receptor Mff selectively recruits oligomerized Drp1. *Molecular biology of the cell*, 26(24), pp.4466–4477.

Liu, X. et al., 2016. Inflammasome-activated gasdermin D causes pyroptosis by forming membrane pores. *Nature*, 535(7610), pp.153–158.

Lochmuller, H., Johns, T. & Shoubridge, E.A., 1999. Expression of the E6 and E7 genes of human papillomavirus (HPV16) extends the life span of human myoblasts. *Experimental cell research*, 248(1), pp.186–193.

Lundmark, R. & Carlsson, S.R., 2009. SNX9 - a prelude to vesicle release. *Journal of cell science*, 122(Pt 1), pp.5–11.

Maadidi, El, S. et al., 2014. A novel mitochondrial MAVS/Caspase-8 platform links RNA virus-induced innate antiviral signaling to Bax/Bak-independent apoptosis. *Journal of immunology (Baltimore, Md. : 1950)*, 192(3), pp.1171–1183.

Maharaj, N.P. et al., 2012. Conventional protein kinase C-alpha (PKC-alpha) and PKC-beta negatively regulate RIG-I antiviral signal transduction. *Journal of Virology*, 86(3), pp.1358–1371.

Martijn, J. et al., 2018. Deep mitochondrial origin outside the sampled alphaproteobacteria. *Nature*, 557(7703), pp.101–105.

Matheoud, D. et al., 2016. Parkinson's Disease-Related Proteins PINK1 and Parkin Repress Mitochondrial Antigen Presentation. *Cell*, 166(2), pp.314–327.

Matsuda, A. et al., 2003. Large-scale identification and characterization of human genes that activate NF-kappaB and MAPK signaling pathways. *Oncogene*, 22(21), pp.3307–3318.

McArthur, K. et al., 2018. BAK/BAX macropores facilitate mitochondrial herniation and mtDNA efflux during apoptosis. *Science*, 359(6378), p.eaao6047.

McBride, H.M., 2018. Mitochondria and endomembrane origins. *Current biology : CB*, 28(8), pp.R367–R372.

McCrow, J.P. et al., 2015. Spectrum of mitochondrial genomic variation and associated clinical presentation of prostate cancer in South African men. *The Prostate*, 76(4), pp.349–358.

McInerney, J., Pisani, D. & O'Connell, M.J., 2015. The ring of life hypothesis for eukaryote origins is supported by multiple kinds of data. *Philosophical transactions of the Royal Society of London. Series B, Biological sciences*, 370(1678), p.20140323.

McLelland, G.-L. et al., 2014. Parkin and PINK1 function in a vesicular trafficking pathway regulating mitochondrial quality control. *The EMBO Journal*, 280(Pt 2), pp.e201385902–n/a.

McLelland, G.-L. et al., 2016. Syntaxin-17 delivers PINK1/parkin-dependent mitochondrial vesicles to the endolysosomal system. *The Journal of Cell Biology*, 214(3), pp.275–291.

McManus, F.P., Lamoliatte, F. & Thibault, P., 2017. Identification of cross talk between SUMOylation and ubiquitylation using a sequential peptide immunopurification approach. *Nature protocols*, 12(11), pp.2342–2358.

Merrill, R.A. et al., 2011. Mechanism of neuroprotective mitochondrial remodeling by PKA/AKAP1. *PLoS biology*, 9(4), p.e1000612.

Meylan, E. et al., 2005. Cardif is an adaptor protein in the RIG-I antiviral pathway and is targeted by hepatitis C virus. *Nature*, 437(7062), pp.1167–1172.

Mi, Z. et al., 2010. SUMOylation of RIG-I positively regulates the type I interferon signaling. *Protein & cell*, 1(3), pp.275–283.

Monticone, M. et al., 2010. The nuclear genes Mtfr1 and Dufd1 regulate mitochondrial dynamic and cellular respiration. *Journal of cellular physiology*, 225(3), pp.767–776.

Moretton, A. et al., 2017. Selective mitochondrial DNA degradation following double-strand breaks M. Sola, ed. *PLoS ONE*, 12(4), pp.e0176795–17.

Mowen, K.A. & David, M., 2014. Unconventional post-translational modifications in immunological signaling. *Nature Immunology*, 15(6), pp.512–520.

Muthusamy, V. & Piva, T.J., 2010. The UV response of the skin: a review of the MAPK,

NFkappaB and TNFalpha signal transduction pathways. *Archives of dermatological research*, 302(1), pp.5–17.

Nakahira, K. et al., 2010. Autophagy proteins regulate innate immune responses by inhibiting the release of mitochondrial DNA mediated by the NALP3 inflammasome. *Nature Immunology*, 12(3), pp.222–230.

Neuspiel, M. et al., 2008. Cargo-Selected Transport from the Mitochondria to Peroxisomes Is Mediated by Vesicular Carriers. *Current Biology*, 18(2), pp.102–108.

Ni, G., Konno, H. & Barber, G.N., 2017. Ubiquitination of STING at lysine 224 controls IRF3 activation. *Science immunology*, 2(11), p.eaah7119.

Nie, M. & Boddy, M.N., 2016. Cooperativity of the SUMO and Ubiquitin Pathways in Genome Stability. *Biomolecules*, 6(1), p.14.

Nour, A.M. & Modis, Y., 2014. Endosomal vesicles as vehicles for viral genomes. *Trends in cell biology*, 24(8), pp.449–454.

Odendall, C. et al., 2014. Diverse intracellular pathogens activate type III interferon expression from peroxisomes. *Nature Immunology*, 15(8), pp.717–726.

Onoguchi, K. et al., 2010. Virus-infection or 5'ppp-RNA activates antiviral signal through redistribution of IPS-1 mediated by MFN1. *PLOS Pathogens*, 6(7), p.e1001012.

Osman, C., Voelker, D.R. & Langer, T., 2011. Making heads or tails of phospholipids in mitochondria. *The Journal of Cell Biology*, 192(1), pp.7–16.

Otera, H. et al., 2010. Mff is an essential factor for mitochondrial recruitment of Drp1 during mitochondrial fission in mammalian cells. *The Journal of Cell Biology*, 191(6), pp.1141–1158.

Pascucci, B. et al., 1997. DNA repair of UV photoproducts and mutagenesis in human mitochondrial DNA. *Journal of Molecular Biology*, 273(2), pp.417–427.

Patel, M.N. et al., 2017. Inflammasome Priming in Sterile Inflammatory Disease. *Trends in molecular medicine*, 23(2), pp.165–180.

Peeva, V. et al., 2018. Linear mitochondrial DNA is rapidly degraded by components of the replication machinery. *Nature communications*, 9(1), p.1727.

Prudent, J. et al., 2015. MAPL SUMOylation of Drp1 Stabilizes an ER/ Mitochondrial Platform Required for Cell Death. *Molecular Cell*, 59(6), pp.941–955.

Ramos, H.J. & Gale, M., Jr., 2011. RIG-I like receptors and their signaling crosstalk in the regulation of antiviral immunity. *Current Opinion in Virology*, 1(3), pp.167–176.

Ran, Y. et al., 2011. SENP2 negatively regulates cellular antiviral response by deSUMOylating IRF3 and conditioning it for ubiquitination and degradation. *Journal of molecular cell biology*, 3(5), pp.283–292.

Reynaud, J.M. et al., 2015. IFIT1 Differentially Interferes with Translation and Replication of Alphavirus Genomes and Promotes Induction of Type I Interferon. *PLOS Pathogens*, 11(4), p.e1004863.

Riley, J.S. et al., 2018. Mitochondrial inner membrane permeabilisation enables mtDNA release during apoptosis. *The EMBO Journal*, pp.e99238–16.

Robinson, M.S., 2015. Forty Years of Clathrin-coated Vesicles. *Traffic (Copenhagen, Denmark)*, 16(12), pp.1210–1238.

Rongvaux, A., 2018. Mitochondrion. *Mitochondrion*, pp.1–0.

Rongvaux, A. et al., 2014. Apoptotic Caspases Preventthe Induction of Type I Interferons by Mitochondrial DNA. *Cell*, 159(7), pp.1563–1577.

Roux, K.J. et al., 2012. A promiscuous biotin ligase fusion protein identifies proximal and interacting proteins in mammalian cells. *The Journal of Cell Biology*, 196(6), pp.801–810.

Roux, K.J. et al., 2018. BioID: A Screen for Protein-Protein Interactions. *Current protocols in protein science*, 91, pp.19.23.1–19.23.15.

Roux, K.J., Kim, D.I. & Burke, B., 2013. BioID: a screen for protein-protein interactions. *Current protocols in protein science*, 74, p.Unit 19.23.

Roy, S., 2017. Impact of UV Radiation on Genome Stability and Human Health. *Advances in experimental medicine and biology*, 996, pp.207–219.

Sagan, L., 1967. On the origin of mitosing cells. *Journal of theoretical biology*, 14(3), pp.255–274.

Schneider, W.M., Chevillotte, M.D. & Rice, C.M., 2014. Interferon-stimulated genes: a complex web of host defenses. *Annual Review of Immunology*, 32, pp.513–545.

Schoggins, J.W. et al., 2014. Pan-viral specificity of IFN-induced genes reveals new roles for cGAS in innate immunity. *Nature*, 505(7485), pp.691–695.

Schroder, K. & Tschopp, J., 2010. The Inflammasomes. *Cell*, 140(6), pp.821–832.

Seaman, M.N., McCaffery, J.M. & Emr, S.D., 1998. A membrane coat complex essential for endosome-to-Golgi retrograde transport in yeast. *The Journal of Cell Biology*, 142(3), pp.665–681.

Seth, R.B. et al., 2005. Identification and Characterization of MAVS, a Mitochondrial Antiviral Signaling Protein that Activates NF-κB and IRF3. *Cell*, 122(5), pp.669–682.

Shadel, G.S. & Clayton, D.A., 1997. Mitochondrial DNA maintenance in vertebrates. *Annual review of biochemistry*, 66, pp.409–435.

Shi, J. et al., 2015. Cleavage of GSDMD by inflammatory caspases determines pyroptotic cell death. *Nature*, 526(7575), pp.660–665.

Shi, Y. et al., 2012. Mammalian transcription factor A is a core component of the mitochondrial transcription machinery. *Proceedings of the National Academy of Sciences of the United States of America*, 109(41), pp.16510–16515.

Shimada, K. et al., 2012. Oxidized Mitochondrial DNA Activatesthe NLRP3 Inflammasome during Apoptosis. *Immunity*, 36(3), pp.401–414.

Soubannier, V., McLelland, G.-L., et al., 2012. A Vesicular Transport Pathway Shuttles Cargofrom Mitochondria to Lysosomes. *Current Biology*, 22(2), pp.135–141.

Soubannier, V., Rippstein, P., et al., 2012. Reconstitution of Mitochondria Derived Vesicle Formation Demonstrates Selective Enrichment of Oxidized Cargo O. S. Shirihai, ed. *PLoS ONE*, 7(12), p.e52830.

Srikumar, T. et al., 2013. Global analysis of SUMO chain function reveals multiple roles in chromatin regulation. *The Journal of Cell Biology*, 201(1), pp.145–163.

Stehling, O., Wilbrecht, C. & Lill, R., 2014. Mitochondrial iron-sulfur protein biogenesis and human disease. *Biochimie*, 100, pp.61–77.

Subramanian, N. et al., 2013. The adaptor MAVS promotes NLRP3 mitochondrial localization and inflammasome activation. *Cell*, 153(2), pp.348–361.

Sugiura, A. et al., 2014. A new pathway for mitochondrial quality control: mitochondrial-derived vesicles. *The EMBO Journal*, 33(19), pp.2142–2156.

Sugiura, A. et al., 2017. Newly born peroxisomes are a hybrid ofmitochondrial and ER-derived pre-peroxisomes. *Nature Publishing Group*, 542(7640), pp.251–254.

Sun, B. et al., 2017. Dengue virus activates cGAS through the release of mitochondrial DNA. *Scientific Reports*, 7(1), p.1148.

Sun, L. et al., 2013. Cyclic GMP-AMP synthase is a cytosolic DNA sensor that activates the type I interferon pathway. *Science*, 339(6121), pp.786–791.

Sun, L. et al., 2012. Mixed lineage kinase domain-like protein mediates necrosis signaling downstream of RIP3 kinase. *Cell*, 148(1-2), pp.213–227.

Sun, Z. et al., 2011. Phosphorylation of RIG-I by casein kinase II inhibits its antiviral response. *Journal of Virology*, 85(2), pp.1036–1047.

Szymanski, C.J., Humphries, W.H.4. & Payne, C.K., 2011. Single particle tracking as a method to resolve differences in highly colocalized proteins. *The Analyst*, 136(17), pp.3527–3533.

Taanman, J.W., 1999. The mitochondrial genome: structure, transcription, translation and replication. *Biochimica et biophysica acta*, 1410(2), pp.103–123.

Takamatsu, C. et al., 2002. Regulation of mitochondrial D-loops by transcription factor A and single-stranded DNA-binding protein. *EMBO reports*, 3(5), pp.451–456.

Takeda, K. & Akira, S., 2004. Microbial recognition by Toll-like receptors. *Journal of dermatological science*, 34(2), pp.73–82.

Takeuchi, O. & Akira, S., 2010. Pattern Recognition Receptors and Inflammation. *Cell*, 140(6), pp.805–820.

Unterholzner, L. & Bowie, A.G., 2008. The interplay between viruses and innate immune signaling: recent insights and therapeutic opportunities. *Biochemical Pharmacology*, 75(3), pp.589–602.

Vakifahmetoglu-Norberg, H., Ouchida, A.T. & Norberg, E., 2017. The role of mitochondria in metabolism and cell death. *Biochemical and biophysical research communications*, 482(3), pp.426–431.

Wang, H. et al., 2014. Mixed lineage kinase domain-like protein MLKL causes necrotic membrane disruption upon phosphorylation by RIP3. *Molecular Cell*, 54(1), pp.133–146.

Wang, W. et al., 2016. Parkinson's disease-associated mutant VPS35 causes mitochondrial dysfunction by recycling DLP1 complexes. *Nature medicine*, 22(1), pp.54–63.

Wei, X. et al., 2015. Cationic nanocarriers induce cell necrosis through impairment of Na. *Nature Publishing Group*, 25(2), pp.237–253.

West, A.P. et al., 2015. Mitochondrial DNA stress primes the antiviral innate immune response. *Nature*, 520(7548), pp.553–557.

West, A.P., Shadel, G.S. & Ghosh, S., 2011. Mitochondria in innate immune responses. *Nature Reviews Immunology*, 11(6), pp.389–402.

White, M.J. et al., 2014. Apoptotic Caspases Suppress mtDNA-Induced STING-Mediated Type I IFN Production. *Cell*, 159(7), pp.1549–1562.

Wies, E. et al., 2013. Dephosphorylation of the RNA sensors RIG-I and MDA5 by the phosphatase PP1 is essential for innate immune signaling. *Immunity*, 38(3), pp.437–449.

Wong, J.J.Y. et al., 2006. HERC5 is an IFN-induced HECT-type E3 protein ligase that mediates type I IFN-induced ISGylation of protein targets. *Proceedings of the National Academy of Sciences of the United States of America*, 103(28), pp.10735–10740.

Woo, D.K. et al., 2012. Mitochondrial genome instability and ROS enhance intestinal tumorigenesis in APC(Min/+) mice. *The American journal of pathology*, 180(1), pp.24–31.

Wu, J. & Chen, Z.J., 2014. Innate Immune Sensing and Signaling of Cytosolic Nucleic Acids. *Annual Review of Immunology*, 32(1), pp.461–488.

Xu, L.-G. et al., 2005. VISA Is an Adapter Protein Required for Virus-Triggered IFN-β Signaling. *Molecular Cell*, 19(6), pp.727–740.

Yoneyama, M. et al., 2004. The RNA helicase RIG-I has an essential function in double-stranded RNA-induced innate antiviral responses. *Nature Immunology*, 5(7), pp.730–737.

Yoshizumi, T. et al., 2017. RLR-mediated antiviral innate immunity requires oxidative phosphorylation activity. *Scientific Reports*, 7(1), p.1313.

Yu, H., Pardoll, D. & Jove, R., 2009. STATs in cancer inflammation and immunity: a leading role for STAT3. *Nature reviews. Cancer*, 9(11), pp.798–809.

Zemirli, N. et al., 2014. Mitochondrial hyperfusion promotes NF-κB activation via the mitochondrial E3 ligase MULAN. *The FEBS Journal*, 281(14), pp.3095–3112.

Zhang, Q. et al., 2010. Circulating mitochondrial DAMPs cause inflammatory responses to injury. *Nature*, 464(7285), pp.104–107.

Zhong, B. et al., 2008. The adaptor protein MITA links virus-sensing receptors to IRF3 transcription factor activation. *Immunity*, 29(4), pp.538–550.

Zhong, Z. et al., 2018. New mitochondrial DNA synthesis enables NLRP3 inflammasome activation. *Nature*, pp.1–26.

Zhong, Z. et al., 2016. NF-kB Restricts Inflammasome Activation via Elimination of Damaged Mitochondria. *Cell*, 164(5), pp.896–910.

Zhu, J. et al., 2014. Antiviral activity of human OASL protein is mediated by enhancing signaling of the RIG-I RNA sensor. *Immunity*, 40(6), pp.936–948.

Ziegler, P.K. et al., 2018. Mitophagy in Intestinal Epithelial Cells Triggers Adaptive Immunity during Tumorigenesis. *Cell*, 174(1), pp.88–101.e16.